Faculties of Engineering, Science and Medicine
Study Board of Industry and Global Business Development
Fibigerstraede 16
DK - 9220 Aalborg East
Phone +45 99 40 93 09
www.industri.aau.dk

AALBORG UNIVERSITET

Validation study of real gas models

Applied on a wide range of temperatures and pressures

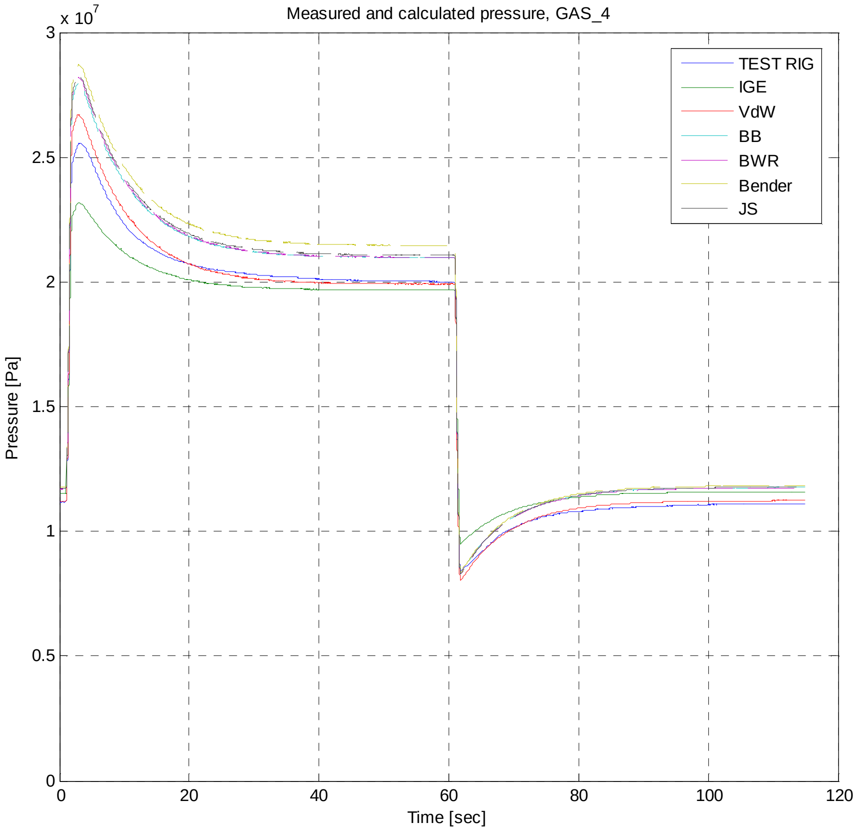

Master Thesis
Aalborg Universitet
Handed in: February 8th, 2010

Aalborg University
Faculties of Engineering, Science and Medicine

Study Board of Industry and Global Business Development
Fibigerstraede 16
DK - 9220 Aalborg East
Phone +45 99 40 93 09
www.industri.aau.dk

TITLE:
Validation study of real gas models - Applied on a wide range of temperatures and pressures

PROJECT PERIOD:
October, 15th 2009
- February, 8th 2010

SEMESTER:
10.

Author:
Jeppe Mulvad Larsen

Supervisor:
Torben O. Andersen
Professor

Henrik C. Pedersen
Associate Professor

NUMBER PRINTED:
6

NUMBER OF PAGES, REPORT:
66

NUMBER OF PAGES, APPENDIX:
61

NUMBER OF PAGES; TOTAL:
127

SYNOPSIS:

The objectives of the project has been to investigate the correlation between complexity and accuracy when calculating the gas pressure and temperature in a hydraulic accumulator using a number of different real gas models. A literature survey has been carried out to identify suitable models. Five models was identified together with the ideal gas equation. The models was ranging in complexity from 4 constants to 32 constants. The models was validated in two test rigs with varying accumulator sizes.
No clear conclusions could be drawn for the gas temperature due to insufficient measuring equipment. Nor could any clear conclusions regarding pressure be made for the large accumulator as problems occur during the test runs. But for the small accumulator a clear tendency could be observe. Based on this it is recommended to use Van der Waals equation of state for normal and warm ambient temperatures. For cold ambient temperatures it is recommended to use Beattie-Bridgeman equation of state. The both shows very very accurate results with differences of some few percent.

Preface

This report documents the Master Thesis written by Jeppe Mulvad Larsen. The project followings the study regulations for 10th semester in Electro-Mechanical Systems Design at Aalborg University. The project is titled Validation study of real gas models.

The purpose of the project is to study a number of different models to calculate the pressure and temperature in a gas and to compare them with data measured in a test rig.

The project is devised by instructions of Professor Torben O. Andernsen and Associate Professor Henrik C. Pedersen.

The author would like thank Peter Windfeld Rasmussen, Fritz Schur Energy for outstanding support and guidance throughout the project.

Cite references are made by the Harvard method with [Author year, page reference]. More detailed information about the sources are located in the reference list of literature placed at the back of the report.

The project is documented through a main report and a set of appendices. The main report can be read as a self-contained work, but is supported by appendices containing more derivations, describtion of the test rig and experimental reports. Enclosed in the main report is a CD containing main report, data sheets, to the extend they have been available, program code, SIMULINK models and additional information.

Jeppe Mulvad Larsen
Aalborg University
February 8th, 2010

Table of contents

List of Symbols

A	Area	$\left[m^2\right]$
A_0	Orifice area	$\left[m^2\right]$
A_w	Effective wall area	$\left[m^2\right]$
A_{gas}	Area of accumulator piston on gas side	$\left[m^2\right]$
A_{oil}	Area of accumulator piston on oil side	$\left[m^2\right]$
C_d	Discharge coefficient	$[-]$
C_v	Specific heat capacity of the gas	$\left[\frac{J}{kgK}\right]$
Cyl_{length}	Internal length of cylinder	$[m]$
F_{fric}	Friction on accumulator piston	$\left[\frac{N \cdot sec}{m}\right]$
F_{gas}	Force on accumulator piston produced by gas pressure	$[N]$
F_{oil}	Force on accumulator piston produced by oil pressure	$[N]$
M	Molar mass	$\left[\frac{kg}{mol}\right]$
N	Mole number	$[mole]$
$P_{gas,precharge}$	Precharge pressure of the gas	$[Pa]$
Q_{leak}	Leakage flow in accumulator	$\left[\frac{m^3}{sec}\right]$
Q_{nom}	Nominal flow	$\left[\frac{m^3}{sec}\right]$
Q_{oil}	Oil flow in accumulator	$\left[\frac{m^3}{sec}\right]$
R	Gas constant	$\left[\frac{m^3 \cdot Pa}{K \cdot kg}\right]$
R_u	Universal gas constant	$\left[\frac{m^3 \cdot Pa}{K \cdot mol}\right]$
T	Temperature of the gas	$[K]$
T_R	Reduced temperature	$[-]$
T_a	Ambient temperature	$[K]$
T_{cr}	Critical temperature	$[K]$
U	Voltage	$[V]$
U_v	Voltage after transfer function	$[V]$
U_{nom}	Nominal voltage	$[V]$
V	Volume	$\left[m^3\right]$
V_{hose}	Volume of hoses	$\left[m^3\right]$
Z	Compressibility factor	$[-]$
$\bar{v}$	Specific molar volume	$\left[\frac{m^3}{mol}\right]$
$\ddot{x}$	Acceleration of accumulator piston	$\left[\frac{m}{s^2}\right]$
$\dot{U}$	Change in internal energy	$[J]$
$\dot{W}$	Work done by the piston	$[J]$
$\dot{Q}_{conv}$	Rate of heat transfer by convection	$[J]$
$\dot{x}$	Speed of accumulator piston	$\left[\frac{m}{s}\right]$
ρ	Density	$\left[\frac{kg}{m^3}\right]$
ρ_{cr}	Critical density	$\left[\frac{kg}{m^3}\right]$
τ	Thermal-time constant	$[sec]$
ζ	Damping	$[-]$
h	Convection heat transfer coefficient	$\left[\frac{W}{m^2K}\right]$
k	Spring constant	$\left[\frac{N}{m}\right]$
m_1	Mass of accumulator piston	$[kg]$
m_2	Mass of position transducer rod	$[kg]$
m_g	Mass of the gas	$[kg]$
p	Pressure	$[Bar]$
p_R	Reduced pressure	$[-]$
p_s	Supply pressure	$[Bar]$
p_{cr}	Critical pressure	$[Bar]$
p_{gas}	Pressure in accumulator on gas side	$[Bar]$
p_{nom}	Nominal pressure	$[Bar]$
p_{oil}	Pressure in accumulator on oil side	$[Bar]$
p_{tank}	Tank pressure	$[Bar]$
v	Specific volume	$\left[\frac{m^3}{kg}\right]$
x	Position of accumulator piston	$[m]$
$x_{initial}$	The initial position of the piston	$[m]$

Executive Summary

1

The objectives of the project have been to investigate the correlation between complexity and accuracy when calculating the gas pressure and gas temperature in a hydraulic accumulator for a number of real gas models. The problem thesis of the project is *What mathematical model describes the gas pressure during a cycle in a hydraulic accumulator most precisely, when comparing accuracy with complexity* and this will be studied throughout the report which the following chapters. The project have been performed in cooperation with Fritz Schur Energy.

In the first chapter of the project the results of a literature survey are presented. This survey have been carried out to identify which real gas models that should be used in the project. In total five real gas models was selected together with the ideal gas model. The five real gas models are; Van der Waals, Beattie-Bridgeman, Benedicte-Webb-Rubin, Jacobsen & Stewart and Bender equation of state. They range in complexity with three, six, nine, 20 and 33 constants respectively where the ideal gas model only have one.

To validate the models two test rig where developed and modeled. The difference between the two test rigs was the size of the accumulator. The next five chapters in the report are presenting the models. In total four models was presented, namely a mechanical, a hydraulic, a gas pressure and a gas temperature model. The first two was not of big interest of the project which is why they have only been given little focus. The third model, the gas pressure model, was based on the literature survey. The last model, the gas temperature model, was based on an energy balance for the gas side of the accumulator. It turned out that this balance was a function of among others the pressure of the gas, which his way in total six sub models was produced.

Above part is followed by two chapter dealing with test variables and the test schedule. A discussion about what variable should be working as the reference is presented. For the small accumulator the position should work as the reference signal. In this way there will be total control of the volume of the accumulator, which is beneficial due to some sub experiments that should be performed. Furthermore the chapter describe at what temperatures the test runs should be performed. Three temperatures was chosen, namely 260 Kelvin, 300 Kelvin and 350 Kelvin. The latter chapter presents a full test schedule to be followed during the test runs.

Finally four chapters presents the outcome from a number of validations. Firstly the test rig itself are validated to determine the variability. This gives an picture of how reliable the measure data is. The conclusion was that the test rig has a very low variability. Secondly the result from the experiment for determining the thermal time constant was presented. The thermal time constant is a measure for how fast the pressure drops when the accumulator is exposed to a step change is volume. The pressure drops because the temperature drops as it interacts with the surround air. Finally two chapters presents the outcome from the validation of the models found in the literature survey.

Some problems with the test rig has unfortunately resulted in problems with drawing clear conclusions for the temperature models and the large accumulator. But for the small accumulator it is clear to see, that the Van der Waals equation of state is the most precise for normal and warm ambient temperature ranging from 300 Kelvin to 350 Kelvin. No significant differences was to be found when comparing pressures. Furthermore it turned out that for cold ambient temperatures, the Van der Waals equation of state was not the best equation to use. In this case the Beattie-Bridgeman equation of state was recommended. It should be mentioned that the large accumulator showed a tendency that supports the conclusion that the same is valed for the large accumulator as for the small. Finally although no clear conclusions can be made for the temperature model, it is also assumed that the same conclusions are valid for this as well. This is assumed as the temperature and pressure models are closely linked and that the approach for calculating the temperature are supported by other sources.

The project has therefore shown that it is not necessary to use very complex models to obtain accurate results when calculating the pressure in a hydraulic accumulator. The opposite has actually shown to be the case, namely that the least complex real gas models resulted in the most accurate results. The above is valid for temperatures ranges from 260 Kelvin to 350 Kelvin, precharge pressures from 50 bar to 150 bar, maximum pressures of 250 bar and minimum pressures of 40 bar.

Introduction

2

Today hydraulic accumulators are used in a vast number of hydraulic systems such as in the landing gear of an aeroplane, in the pitch control system of a wind turbine, in hydraulic cranes, in suspension systems of vehicles and much more. The accumulator can work either as a safety device engaging when the pressure in the system is not sufficient (e.g. when the power pack is malfunctioning) or it can smoothen out any pressure peaks or drops that may occur in a hydraulic system. The accumulator works as an energy storing device (like a battery) where hydraulic fluid is stored under pressure. The energy is supplied to the system when the oil pressure drops to below the pressure of the accumulator. As the applications for hydraulic accumulators are diverse, the environments that the accumulator should work in are equally diverse meaning that an accumulator should work in temperatures ranging from e.g. -25$^\circ C$ to 60$^\circ C$ and also in off-shore conditions.[Rasmussen, 2009]

The accumulator consists of two sides, namely the oil side and the gas side. The two sides are separated from each other by either a piston, a bladder or diaphragm. The gas side acts as a spring on the oil side, storing and delivering energy to the hydraulic system when needed. In fact the gas side can also be fitted with a spring. The normal gas to use in a accumulator is nitrogen because it is cheap and inert. Other gas types like argon and helium can although also be used, but both of them have some disadvantages, e.g. a high price.[Pourmovahed, 1993]

When the accumulator is used as a safety device it is crucial that the engineer is able to size it correctly. Something that have caused many problems over time. Years ago the gas in the accumulator was assumed to be ideal, making it very easy to calculate the gas properties, but this have in many cases also shown to result in large errors[Pourmovahed and Otis, 1985]. In the next chapter a small example are made to shown the difference when using different models.

The project will deal with this problem, by presenting a number of mathematical models that describes a gas under pressure i.e. the gas side of the accumulator. The models will be identified through a comprehensive literature review. A hydraulic system involving a hydraulic accumulator of the piston-type will be modeled and simulated using the identified models. The results of the simulations will be evaluated against a full scale test setup, with multiple accumulator sizes and at different pressures and temperatures. The result will be presented and compared based on complexity and accuracy. Finally a user-friendly model adjustable for other sizes of piston type accumulators should be produced.

The above leads to the following problem statement

2.1 Problem statement

What mathematical model describes the gas pressure during a cycle in a hydraulic accumulator most precisely, when comparing accuracy with complexity.

The statement leads to the following sub questions, that all will be addressed in the report:

- Which models should be included in the comparison?
- How are the gas temperature calculated?
- At what gas temperature, ambient temperature and pressures are the models valid to use?
- Is the accuracy of a model proportional to the complexity?

Why this study?

3

As mentioned in the introduction it is often crucial to be able to calculate the right pressure when designing accumulators. The differences between using different approaches are shown in the following example.

Scope

Assuming that in a wind turbine five hydraulic accumulators each with a volume of 20 liters are installed for every wing. The accumulators are used when the emergency stop is engaged and should supply two hydraulic pistons ø125mm with enough oil so that the pistons are moved 600mm in 10 seconds witch is equal to 15 liters of oil. The accumulators each have a precharge pressure of 100 bar, the system have a maximum pressure of 200 bar and the final pressure should be minimum 150 bar. The temperature is 300 Kelvin and only the final pressures are of interest.

The process can be divided into three different parts, namely

1. Before pressurizing the system
   The volume of the gas is 20 liters and the pressure is 100 bar
2. During normal operation
   The pressure will be 200 bar and the volume is unknown
3. When emergency stop is engaged
   The pressure should be minimum 150 bar and the volume are increases with three liters per accumulator compared with normal operation

Isothermal

Using this approach the following equation should be used:

$$p_1V_1 = p_2V_2 \tag{3.1}$$

Ideal gas equation

The ideal gas equation are given with[Cengel and Turner, 2001, (3-9)]

$$pv = RT \tag{3.2}$$

Van der Waals

Finally a simple real gas model is used, namely the Van der Waals equation of state. This is given by[Cengel and Turner, 2001, (3-21)]

$$\left(p + \frac{a}{v^2}\right)(v - b) = RT \tag{3.3}$$

and

$$a = \frac{27R^2T_{cr}^2}{64p_{cr}} \qquad b = \frac{RT_{cr}}{8p_{cr}} \tag{3.4}$$

$$= \frac{27 \cdot \left(296.79 \left[\frac{Pa \cdot m^3}{kg \cdot K}\right]\right)^2 (126.2\,[K])^2}{64 \cdot 3.39 \cdot 10^6 [Pa]} \qquad = \frac{296.79 \left[\frac{Pa \cdot m^3}{kg \cdot K}\right] \cdot 126.2\,[K]}{8 \cdot 3.39 \cdot 10^6 [Pa]} \tag{3.5}$$

$$= 174.58 \left[\frac{Pa \cdot m^6}{kg^2}\right] \qquad = 1.38 \cdot 10^{-3} \left[\frac{m^3}{kg}\right] \tag{3.6}$$

Results

The results of the calculations are presented in Table 3.1

Model	Part 1		Part 2		Part 3	
	p [bar]	V [m^3]	p [bar]	V [m^3]	p [bar]	V [m^3]
Isothermal	100	0.0200	200	0.0100	154	0.0130
Ideal gas equation	100	0.0200	200	0.0076	138	0.0106
Van der Waals	100	0.0200	200	0.0076	142	0.0106

Table 3.1: *Results for three different pressure calculations*

As seen the result differs significant and for this case it also have quite an substantial effect on the final result. If the first calculation methods was used, the result would yield that a pressure of more then 150 bar was archived when the hydraulic pistons was moved 600mm. But using the more correct ideal gas equation the result yields only 138 bar. Finally the Van der Waals equation of state yield 142 bar, which must be considered to be the most accurate of the methods.

The above example shown the importens of using the right models when designing hydraulic accumulators. Otherwise essential pressure might not be reached.

Method

4

This chapter will explain how the writer has approached the project in relation to gaining information about the topic. A combination of different methods to obtain knowledge has be used in the project. They will all be presented in the chapter. But first an explanation will be given for how the project has been approached holistically.

4.1 Using models to simulate the real world

The scope of the project is to come up with a number of mathematical models that describe hydraulic accumulators in some given conditions. Models are often used by engineers and scientists in the approach to understand the theory behind a given problem, although the usage of the models differ between the sciences.

There are basically two types of models; namely analytical models and empirical models. Empirical models can give an output based on an input, but it normally can not tell anything about the system in between. The analytical model on the other hand is based on mathematical models giving an insight in the system in all details (a scientific approach). The later model will be used in this project, even though a problem with this approach can be that some systems are very complex to describe mathematically. Therefore it is sometime useful to simplify the system, although this method will not be used initially in this project. Later the project analysis might show that some simplification is in order (a more engineering approach)[Thurén, 2006].

All analytical models are build using the hypothetical-deductive method where a hypothesis will be outlined and a deductive conclusion will be drawn. The hypothesis is then compared with the real system (the empirical model), meaning that the model of the system will be compared with the real system. Based on this inductive conclusions will be drawn and a final model will be presented.

4.2 Interviews

As an introduction to the project and the problems involved an interview was carried out with Peter Windfeld Rasmussen at Fritz Schur Teknik[Rasmussen, 2009]. Normally an interview is characterized by flexibility and no fixed rules are to be found although some guidelines are available. To structure at least the beginning of the interview a couple of questions were prepared. The intention with the questions was simply to make sure that a thorough introduction to the project was given. Another reason for asking the questions was to ensure the objectives the company and the writer had to the project were aligned. The questions are stated below with a short explanation.

- What the company is producing and to whom
  The question is not essential to the project, but will give a good insight in the products.
- Where the component in question (hydraulic accumulator) are used and for what purpose
  To get knowledge about the hydraulic accumulators in question and what performance is should deliver.
- What conditions the component is working under
  To get information about at what pressure and temperature the component should work under.

- What kind of test rig should be used for the project
  To get knowledge about any components in the system that should be included in the model.

The interview was, especially in the beginning, characterized by the interviewed person explaining about the project together with the company and thereby unintentional answering many of the questions. Not until the end of the interview the interviewer asked specific questions. Peter Windfeld Rasmussen will be used throughout the project for clarification and informal interviews.

4.3 Literature review

A comprehensive literature review has been performed with the objective to obtain a large degree of knowledge about the topic namely hydraulic accumulators and their behaviors together with any relevant topics. The literature review can be divide into two sources both listed below.

1. Text books
2. Scientific articles and ph.d. thesis

In the following it will be described how the objective of the literature review has been achieved, that is how to obtain a large degree of knowledge about the topic. The following sections also presents the two sources more thoroughly including a description of actions to find the right information. A description of how the correctness of the information will be evaluated is also included.

4.3.1 Text books

Criteria for evaluation of correctness

Preferable only text books used in the teaching at Aalborg University will be used as these are all assumed reliable sources. If a text book not used for teaching, is used as a reference in the project, this will clearly be stated in the bibliography including a note explaining why this source is assumed reliable. Criteria for this evaluation could be recommendation from scientists, engineers or other persons with knowledge within the topic. Another criteria could be many references to the book in scientific articles or books.

Procedure for obtaining the literature

Text books are found either at Aalborg University Library or at the writers private book collection.

4.3.2 Scientific articles and ph.d. thesis

Criteria for evaluation of correctness

No fixed rules for how to evaluate the correctness of an article or thesis are used. But in general if an article is published in a journal, at a conference or similar the article is considered reliable. The reliability is supported if the article is cited in other articles or books. Alternatively the author of an article should have published a number of articles of which some of them could be considered high standing. The evaluation must be made on a case-by-case basis.

Procedure for obtaining the literature

The majority of the literature used in the project are scientific articles. The main database for searching information was the Digital Article Database Service (DADS) accessed via Aalborg University Library. The database contains both articles and journals within scientific fields as e.g. engineering. For the initial review about hydraulic accumulators, a number of text strings have been used for searching. They are all listed in Table 4.1. In the same table the number of articles in the search results are listed. To make sure that as many articles as possible were found, other databases were also used. That is Artikelbasen.dk (AB), Cambridge Scientific Abstracts (CSA) and Web of Science (WoS). They are all also accessed via Aalborg University Library.

Text string	Search result			
	(DADS)	(AB)	(CSA)	(WoS)
Hydraulic accumulator	121	0	15	115
Hydraulisk akkumulator (Danish)	0	1	0	0
Hydrospeicher (German)	21	0	0	0
Modelling hydraulic accumulator	0	0	0	7
Modellering hydraulisk akkumulator (Danish)	0	0	0	0
Modellierung hydrospeicher (German)	0	0	0	0
Hydropneumatic accumulators	27	0	0	4

Table 4.1: *Text strings used for searching for articles in a number of databases.*

Approximately 15 articles were selected for further studying. Only one was selected[Pourmovahed and Otis, 1990] from these. The rest was rejected mainly because they did not focus on modeling of hydraulic accumulators and the mathematics involved, but more on explaining what accumulators could be used for and the advantages and disadvantages with such. Thirdly some of them focused on implementing hydraulic accumulators in vehicles, without presenting useful mathematical information.

The references for the selected article were then studied and a number of articles were found and evaluated. One of these was of interest for the project[Pourmovahed and Otis, 1985]. In the reference of this article another article was found to be of interest[Otis, 1974].

Besides the scientific articles two ph.d. thesis' were at the writers disposal[Rupprecht, 1988] and [Rotthäuser, 1993]. The thesis' was provided by Peter Windfeld Rasmussen.

To give an overview of the literature found, a flowchart is shown in Figure 4.1. The chart shows the references between the articles and thesis together with a note of any citations of the article in other references. The arrows are pointing to the article/thesis that are referred to. For comparison a search has been performed on the Internet (www.google.com) on all the articles and thesis. The search result is also shown in Figure 4.1.

4.4 Summary

Based on the literature review some initial conclusions about hydraulic accumulators can be drawn. In many years when sizing accumulators it was assumed that the gas behaved ideally. (Please see Section 7.1.1 for an explanation and definition of an ideal gas). But with temperatures of some 200 K and pressures up to 200 bar, the gas is not suitable to be treated as an ideal gas. Doing so will result in large errors. Another problem occurs if the process is assumed to be a isothermal process. If the volume change is fast, the temperature in the gas will not have time to interact with the ambient temperature and the temperature will therefore change. This can be seen in Figure 4.2 which is a history of gas temperature, T_{gas}, volume, V, pressure, p

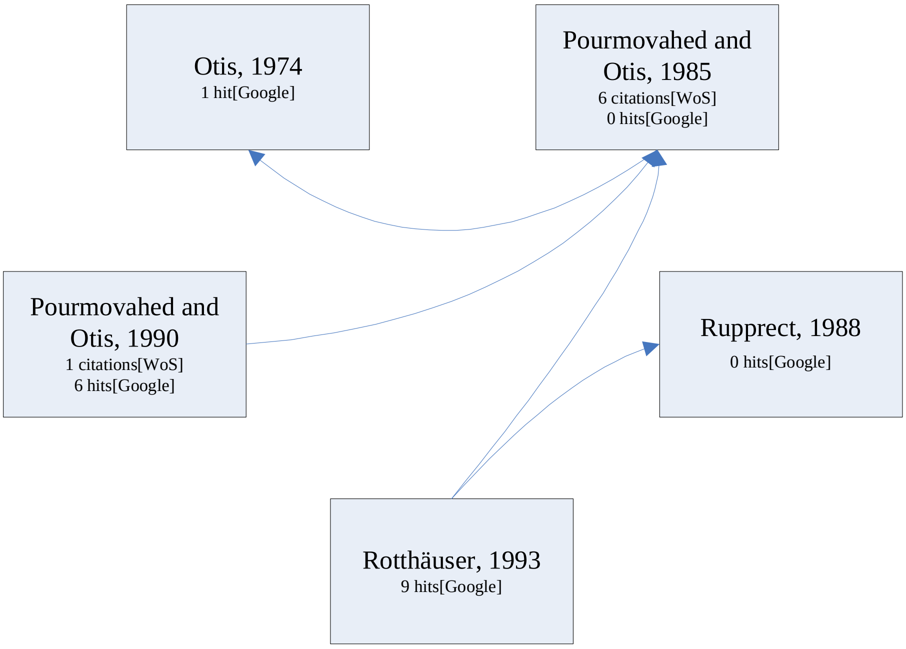

Figure 4.1: *Diagram showing the references between articles and thesis. Arrows pointing to the article/thesis that are referred to.*

and wall temperature, T_w, for a piston-type accumulator exposed to a fast volume change. Errors also occur if the process is assumed to be adiabatic or polytropic.

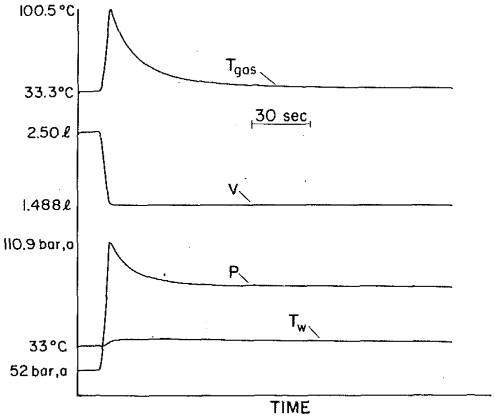

Figure 4.2: *Gas temperature, T_{gas}, volume, V, pressure, p and wall temperature, T_w history for piston-type accumulator exposed to a fast volume change[Pourmovahed and Otis, 1990].*

To calculate the pressure and temperature of a gas other approaches must be used. In Chapter 7 a number of equations are presented, of which some of them have shown very accurate results, also at high pressures and low temperatures. Focus in this project will therefore be to calculate the temperature and to find a suitable equation to calculate the pressure.

Nonlinear model

5

In this chapter the nonlinear model is presented. Firstly the structure of model will be described following by a brief note on assumptions. In the following chapters the actual equations will be presented. In Appendix B a description of how the equations are implemented in SIMULINK are to be found.

In Chapter A is a thorough description of the test rig that will be modeled in the following chapters. In Figure 5.1 is a sketch of the hydraulic system.

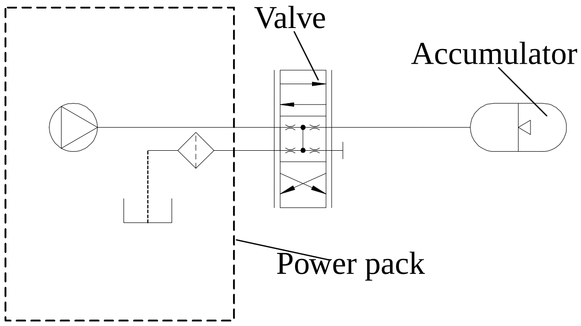

Figure 5.1: *The hydraulic diagram showing the components of the system*

5.1 The structure of the model

The model is structured as sketched in Figure 5.2. It consists of six blocks each representing one part of the system.

The hydraulic part of the model is fairly simple and is to be found in Chapter 6. The more interesting parts of the model, as regard to the objective of the project, is the calculation of the gas temperature and the gas pressure. The first one is elaborated in Chapter 8 and the latter in Chapter 7.

5.2 Assumptions

The following assumptions are used in building the model.

- **Constant supply pressure**
  The supply pressure, p_s, is maintained at a constant pressure.
- **Constant tank pressure**
  The pressure in the tank, p_{tank}, is maintained at a contact pressure, namely 1 atm.
- **Constant pressure drop in filter**
  The pressure drop in the filter, p_{filter}, is maintained at a constant value.
- **Using the orifice to model the valve**
  The valve is assumed to bed an orifice and is therefore modeled using the orifice equation.

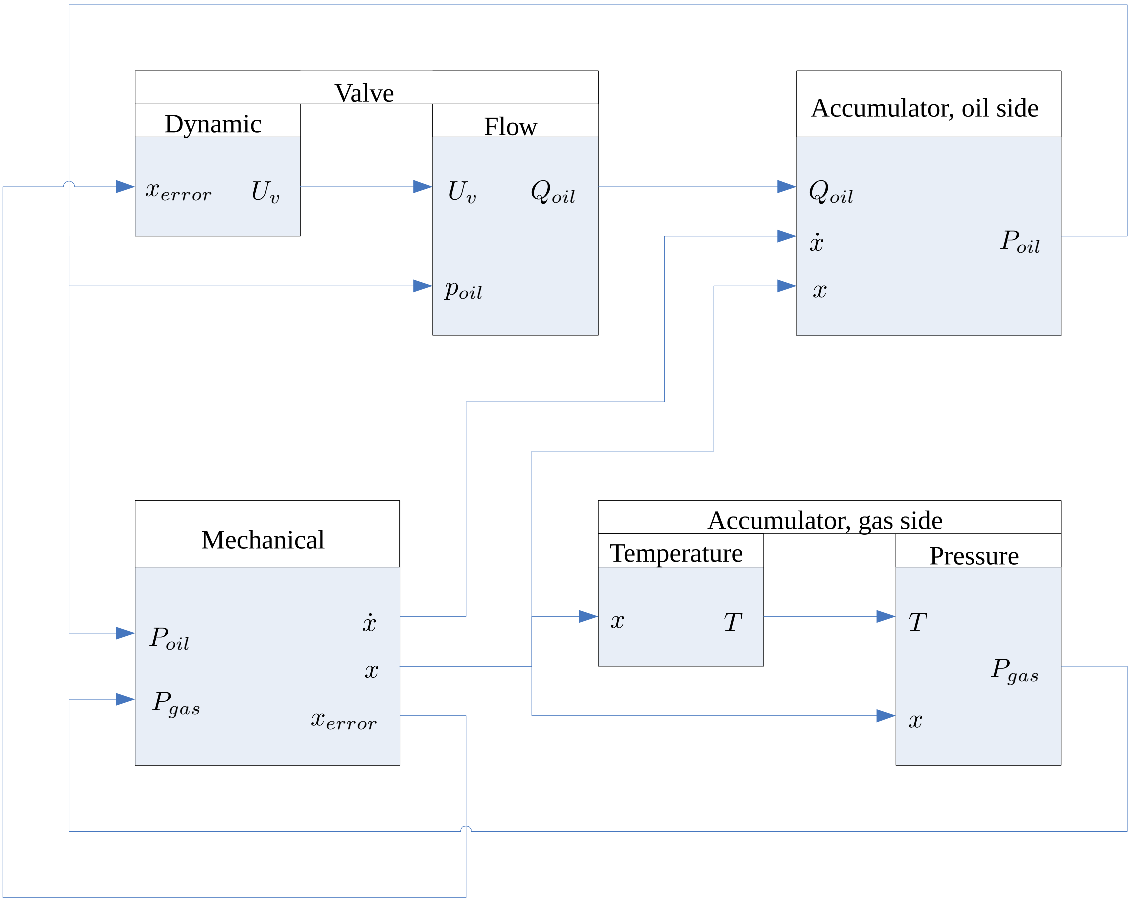

Figure 5.2: *Sketch of model to simulate the hydraulic system*

- **Bulk modulus is constant throughout the cylinders**
  Bulk modulus could be modeled as functions of the pressure, but the expected gain is considered insignificant.

All other constants and parameters are calculated and included in the project. Simulations and experiments although might show that some of them have very low influence on the system and that they may be neglected. If this is the case this will be mentioned later in the report.

Hydraulic and mechanical model

6

The chapter will deal with the hydraulic part of the model. The chapter is divided into two parts.

The first part of this chapter will present the equations describing the hydraulic part of the model. After this a section with a description of how the equations have been implemented in MATLAB/SIMULINK are to be found.

6.1 Equations

6.1.1 Mechanical

The only mechanical part of the system to be modeled is the hydraulic accumulator, more precisely the piston. In Figure 6.1 a free body diagram of the part is sketched. In the same figure some constants are shown on the accumulator.

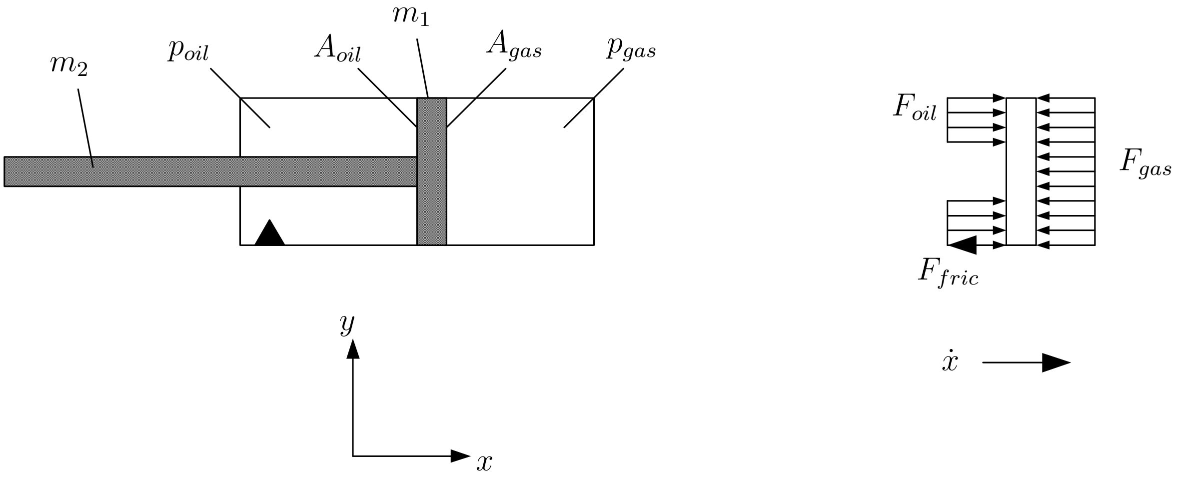

Figure 6.1: *LEFT: Some constants on the accumulator. RIGHT: Free body diagram of the hydraulic accumulator*

The mechanical part is modeled using Newtons 2. law, namely

$$\sum F = ma \tag{6.1}$$

Applying this on the system yields

$$F_{oil} - F_{gas} - F_{fric} = (m_1 + m_2)\ddot{x} \tag{6.2}$$

$$\ddot{x} = \frac{F_{oil} - F_{gas} - F_{fric}}{m_1 + m_2} \tag{6.3}$$

$$\dot{x} = \int \frac{F_{oil} - F_{gas} - F_{fric}}{m_1 + m_2} dt \tag{6.4}$$

$$x = \int\int \frac{F_{oil} - F_{gas} - F_{fric}}{m_1 + m_2} dtdt \tag{6.5}$$

where F_{oil} is the force produced by the oil pressure on the piston, F_{gas} is the force produced by the gas pressure on the piston, F_{fric} is the force produced by the friction between the piston and the accumulator walls, m_1 is the mass of the piston and m_2 is the mass of a small rod connected to the piston used for position measuring. The rod will not be present in a normal accumulator. The friction coefficient is assumed to be coulomb friction with a value of 1000.

6.1.2 Dynamic of the valve

Based on the frequency characteristics in the data sheet, see Appendix N.2, the dynamic of the valve can be modeled using a 2. order transfer function shown in (6.6)[Ogata, 2001, (5-9)]

$$U_v = \frac{1}{\frac{1}{\omega_n}s^2 + \frac{2\zeta}{\omega_n}s + 1}U \tag{6.6}$$

The frequency, ω_n, can be read in the frequency response curve in the data sheet at -90° phase lag and ±90% command signal to be 140 Hz. The damping, ζ, is calculated using the expression shown in (6.7) where ζ is isolated[Ogata, 2001].

$$\phi = -tan^{-1}\left(\frac{2\zeta\frac{\omega}{\omega_n}}{1-\left(\frac{\omega}{\omega_n}\right)^2}\right) \tag{6.7}$$

$$-tan\left(\phi\right) = \frac{2\zeta\frac{\omega}{\omega_n}}{1-\left(\frac{\omega}{\omega_n}\right)^2} \tag{6.8}$$

$$\zeta = \frac{tan\left(\phi\right)\left(\left(\frac{\omega}{\omega_n}\right)^2 - 1\right)}{2\frac{\omega}{\omega_n}} \tag{6.9}$$

Four values of ω and the corresponding phase lag are read in the frequency response curve and the damping is calculated. The values and the corresponding results for this are

$$\begin{aligned} \zeta_{\omega=50,\phi=-26} &= 0.596 \\ \zeta_{\omega=70,\phi=-44.5} &= 0.737 \\ \zeta_{\omega=100,\phi=-66} &= 0.770 \\ \overline{\zeta} &= 0.701 \end{aligned}$$

Applying the calculated values to (6.6) yields

$$U_v = \frac{1}{\frac{1}{350\cdot 2\pi\left[\frac{rad}{s}\right]}s^2 + \frac{2\cdot 0.701}{350\cdot 2\pi\left[\frac{rad}{s}\right]}s + 1}U \tag{6.10}$$

6.1.3 Flow through the valve

The flow through the valve in the system is modeled using the orifice equation[Andersen and Hansen, 2003, Eq. 2.34] as shown in (6.11).

$$Q = C_d A_0 \sqrt{\frac{2}{\rho}\left(\Delta p\right)} \tag{6.11}$$

which is rewritten to

$$Q = K\sqrt{\Delta p} \tag{6.12}$$

where K describes the flow as a function of the voltage. An expression for the flow should be made. As seen in the data sheet for the valve, the flow is not linear. A 4th degree polynomial curve has therefore been fitted to the flow curve. The expression for the polynomial curve is

$$Q(U_v) = c_1U_v^4 + c_2U_v^3 + c_3U_v^2 + c_4U_v^1 + c_5 \tag{6.13}$$

where

$$c_1 = 1.711 \cdot 10^{-8}; c_2 = -6.2408 \cdot 10^{-7}; c_3 = 4.7339 \cdot 10^{-6}; c_4 = 3.9433 \cdot 10^{-5}; c_5 = 0$$

The polynomial is divided by the square root of the nominal pressure, yielding

$$K = \frac{Q(U_v)}{\sqrt{p_{nom}}} \tag{6.14}$$

6.1.4 Oil pressure

The hydraulic side of the accumulator is modeled using the Flow continuity equation[Andersen and Hansen, 2003, Eq. 3.5] as shown in (6.15).

$$Q_{in} - Q_{out} = \frac{dV}{dt} + \frac{V}{\beta}\frac{dP}{dt} \tag{6.15}$$

Applying this on the system yields

$$\begin{aligned}
Q_{oil} &= A_{oil}\frac{dx}{dt} + \frac{V_{hose} + A_{oil} \cdot x}{\beta}\frac{dp}{dt} + Q_{leak} && (6.16)\\
&= A_{oil} \cdot \dot{x} + \frac{V_{hose} + A_{oil} \cdot x}{\beta}\dot{p} + Q_{leak} && (6.17)\\
\dot{p} &= \frac{(Q_{oil} - A_{oil} \cdot x - Q_{leak})\,\beta}{V_{hose} + A_{oil} \cdot x} && (6.18)\\
p_{oil} &= \int \frac{(Q_{oil} - A_{oil} \cdot x - Q_{leak})\,\beta}{V_{hose} + A_{oil} \cdot x}dt && (6.19)\\
& && (6.20)
\end{aligned}$$

6.2 Implementing in SIMULINK

Please refer to Appendix B.1 for description of how the equations are implemented in SIMULINK.

6.3 Summery

The chapter presented a model of the hydraulic and mechanical part of the test rig, namely the valve and the oil side of the accumulator including the accumulator piston. Basic modeling theory has been used and good accuracy is expected. The model will be validated against accumulator #1. Later in the project the model will be used to simulate accumulator #2.

7

Gas pressure model

This chapter will describe the different equations chosen to calculate the gas pressure in the model. In the end of the chapter a description of how the equations have been implemented in MATLAB/SIMULINK are to be found.

A number of different equations are chosen to calculate the gas pressure in the accumulator. The equations, that all relates pressure, temperature and specific volume, are also called "equations of state"[Cengel and Turner, 2001, page 96]. They range from very simple equations with few constants to very complex equations with a large number of constants. In the following they are all presented with an explanation of why they are included in the project and how they are implemented in SIMULINK. It is the scope of this project to study the accuracy of the equations. Some results are although already available. In Figure 7.1 is shown the percentage of error in specific volume for three different equations of state for nitrogen.

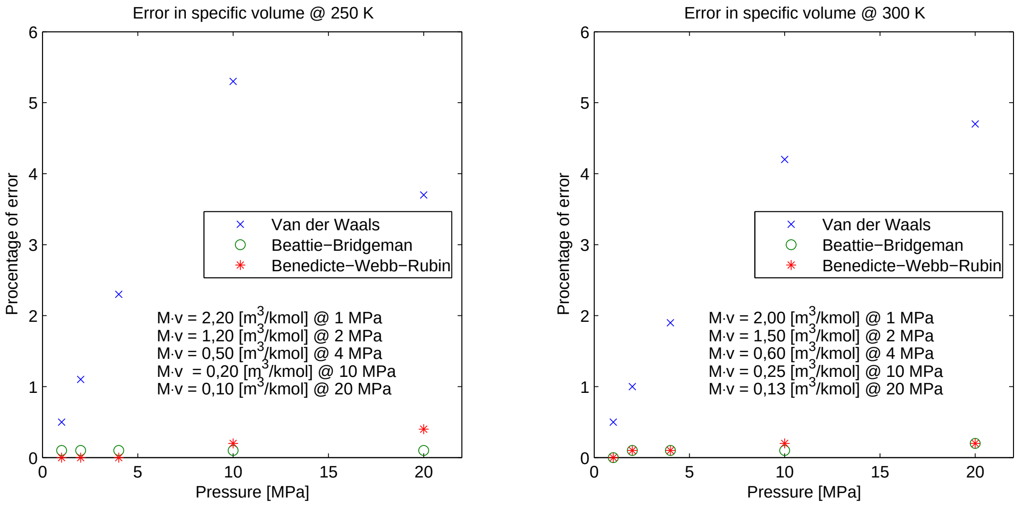

Figure 7.1: *Percentage of error in specific volume for various equations of state for nitrogen.* $M \cdot v = \bar{v} =$ *specific molar mass[Cengel and Turner, 2001, Figure 3-62].*

It is seen that in general the accuracy is decreasing as the pressure increases. It is also seen that the more complex equations of state (Beattie-Brigdeman and Benedicte-Webb-Rubin) are more accurate than the rather simple equations of state (Van der Waals). But an interesting observation is, that for 250 K (-23°C), Van der Waals equation of state has the highest inaccuracy at 10 MPa after which it becomes more accurate. But since this pressure is very low compared to normal pressure experience this will not be examined further.

In this chapter different properties for nitrogen gas have been used. They are, to give an overview, all listed in Table 7.1.

Name	Constant	Value	Unit	[Cengel and Turner, 2001]
Critical pressure	p_{cr}	33.9	$[Bar]$	Table A-1
Critical temperature	T_{cr}	126.2	$[Kelvin]$	Table A-1
Critical density	ρ_{cr}	311.60	$\left[\frac{kg}{m^3}\right]$	Table A-1
Molar mass	M	$28.013 \cdot 10^{-3}$	$\left[\frac{kg}{mol}\right]$	Table A-1
Universal gas constant	R_u	8.314	$\left[\frac{Pa \cdot m^3}{mol \cdot Kelvin}\right]$	(3-11)

Table 7.1: *Properties for nitrogen gas.*

7.1 Equations of state

7.1.1 Ideal gas equation (IGE)

The Ideal gas equation is a very simple equation of state using only one constant, namely the Gas constant. The Ideal gas equation was developed in 1802 by J. Charles and J. Gay-Lussac and is given by[Cengel and Turner, 2001, (3-9)]:

$$pv = RT \tag{7.1}$$

where p is the pressure, v is the specific volume, R is the Gas constant and T is the temperature. As the Gas constant is different for each gas, it can also be calculated by using[Cengel and Turner, 2001, (3-10)]:

$$R = \frac{R_u}{M} \tag{7.2}$$

where R_u is the universal gas constant and M is the molar mass which can be calculated by $M = \frac{N}{m_{gas}}$, where N is the mole number and m_{gas} is the mass of the gas. Applying (7.2) to (7.1) yields

$$pvM = R_u T \tag{7.3}$$

It is important to mention that the Ideal gas equation is only valid to use on ideal gases. For nitrogen to be an ideal gas, one of the following two statement should be satisfied[Cengel and Turner, 2001, page 100]:

- The gas should be at very low pressure regardless of temperature
- The gas should be at high temperature regardless pressure (except for very high pressures)

As long as the gas is an ideal gas, the Ideal gas equation relates p, v and T with an error of less then 1%[Cengel and Turner, 2001, page 97]. Since high temperature and low or high pressure is very different depending of the gas in question, two normalization expressions have been developed, namely[Cengel and Turner, 2001, (3-20)]

$$p_R = \frac{p}{p_{cr}} \qquad T_R = \frac{T}{T_{cr}} \tag{7.4}$$

where $_{cr}$ is the critical pressure and T_{cr} is the critical temperature. p_R and T_R is called the reduced pressure and reduced temperature respectively. Definition of very low pressure, very high pressure and high temperature is then given by[Cengel and Turner, 2001, page 100]

Vey low pressure: $p_R \ll 1$
Very high pressure: $p_R \gg 1$
High temperature: $T_R > 2$

With critical pressure and critical temperature as listed in Table 7.1 very low pressure, very high pressure and high temperature can be defined as

$$\frac{p}{p_{cr_{nitrogen}}} \ll 1 \qquad \frac{p}{p_{cr_{nitrogen}}} \gg 1 \qquad \frac{T}{T_{cr_{nitrogen}}} > 2$$
$$p \ll 33.9[bar] \qquad p \gg 33.9[bar] \qquad T > 252.4[K]$$

For this project temperatures below 250 Kelvin (at low pressures) are expected together with pressures well above 33.9 bar. To account for the effects of not complying to the definitions for an ideal gas a compressibility factor has been developed. This will be explained in Section 7.1.2. The Ideal gas equation, as stated in this section, will be used in the project, but no accurate results will be expected. The reason for including the equation in the project, is because of its simplicity making it very easy to do initial basic calculations on a system.

The derivatives of P

The derivatives of p with respect to temperature T is

$$\frac{\partial p}{\partial T} = \frac{R}{v} \tag{7.5}$$

7.1.2 Ideal gas equation including compressibility factor (IGEcomp)

The Ideal gas equation can be modified to take into account that the gas is not an ideal gas, but rather a real gas. This is done by multiplying the right side of (7.1) with the compressibility factor Z, yielding:

$$pv = ZRT \tag{7.6}$$
$$pvM = ZR_uT \tag{7.7}$$

The factor takes into account any deviations there must be if the gas is not an ideal gas. In Figure 7.2 is reproduced experimentally data for primarily nitrogen when this was possible[Cengel and Turner, 2001, Figure 5-56]. The Z factor deviates slightly for different gases, but in Figure 7.3 data is shown for Z factors valid for all gases with good accuracy[Alvarez, 2006, Figure 5.1.4-5].

The two figures are consistent with good accuracy. To use this equation of state one must read off the Z factor for every state that the gas may be in. This makes it very good to use for static calculations but very difficult to implement in a simulation as the Z factor will have to be described mathematically and only be applied when the gas is not ideal. Therefore the equal will not be used in the rest of the project. But it is still important to mention, that the model has shown good accuracy for static calculations.

The derivatives of p

The derivatives of p with respect to temperature T is

$$\frac{\partial p}{\partial T} = \frac{ZR}{v} \tag{7.8}$$

7.1.3 Van der Waals (VdW)

A second equation to determine the pressure is the Van der Waals equation of state which was proposed in 1873 and is given by[Cengel and Turner, 2001, (3-21)]:

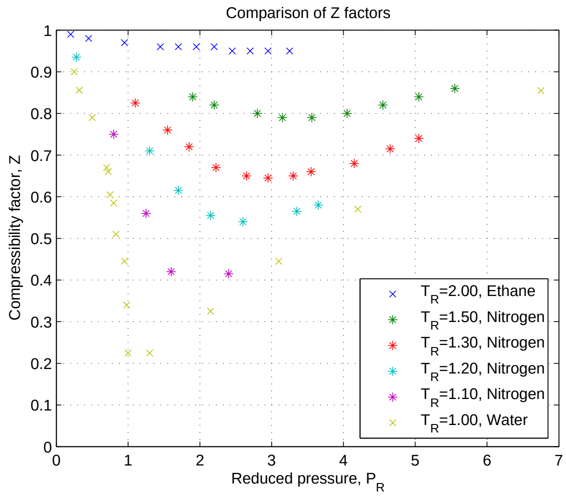

Figure 7.2: *Experimentally obtained Z factors for primarily nitrogen. For two reduced temperatures, namely $T_R = 2.00$ and $T_R = 1.00$, no data for nitrogen was available[Cengel and Turner, 2001, Figure 5-56].*

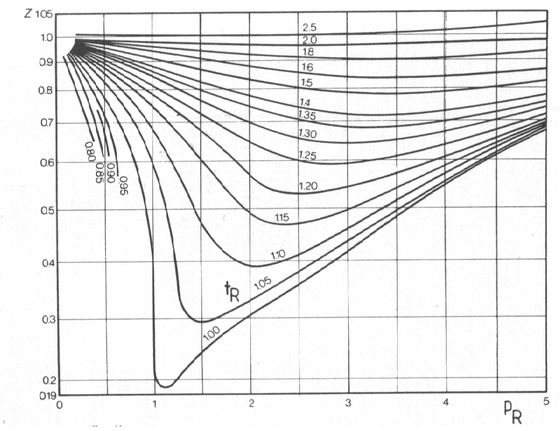

Figure 7.3: *Fitted Z factor curves applicable for all gases with good accuracy[Alvarez, 2006, Figure 5.1.4-5].*

$$\left(p + \frac{a}{v^2}\right)(v - b) = RT \tag{7.9}$$

The Van der Waals equation is with its three constants slightly more complex than the Ideal gas equation. The intention with the equation is to take into account two effects, namely the intermolecular attraction forces and the volume occupied by the molecules themselves. The two constants are being calculated using[Cengel and Turner, 2001, (3-23)]

$$a = \frac{27R^2T_{cr}^2}{64p_{cr}} \qquad b = \frac{RT_{cr}}{8p_{cr}} \tag{7.10}$$

Where R can be replaced by (7.2) and the critical temperature and pressure are given in Table 7.1. The universal gas constant, R_u, and the molar mass, M, for nitrogen are also given i Table 7.1. Inserting all properties in (7.10) yields the following result for nitrogen gas

$$a = \frac{27R^2T_{cr}^2}{64p_{cr}} \qquad b = \frac{RT_{cr}}{8p_{cr}} \tag{7.11}$$

$$= \frac{27 \cdot \left(296.79\left[\frac{Pa \cdot m^3}{kg \cdot K}\right]\right)^2 (126.2\,[K])^2}{64 \cdot 3.39 \cdot 10^6 [Pa]} \qquad = \frac{296.79\left[\frac{Pa \cdot m^3}{kg \cdot K}\right] \cdot 126.2\,[K]}{8 \cdot 3.39 \cdot 10^6 [Pa]} \tag{7.12}$$

$$= 174.58\left[\frac{Pa \cdot m^6}{kg^2}\right] \qquad = 1.38 \cdot 10^{-3}\left[\frac{m^3}{kg}\right] \tag{7.13}$$

The results are confirmed by [Sandri, 1973].

Based on Figure 7.1 no accurate results are expected when using the equation at high pressures. The equation is although still included in the project as it is still very simple and should give some accurate results at lower pressures.

The derivatives of p

The derivatives of p with respect to temperature T is

$$\frac{\partial p}{\partial T} = \frac{R}{v-b} \tag{7.14}$$

7.1.4 Beattie-Bridgeman (BB)

One of the first equations of state based on empirical data was the Beattie-Brigdeman equation. The equation was proposed in 1928 and is based on five experimentally constants and the universal gas constant. The equation is given by[Beattie and Bridgeman, 1928, (1)]

$$p = \frac{R_u T}{\bar{v}^2}\left(1 - \frac{c}{T^3\bar{v}}\right)(\bar{v}+B) - \frac{A}{\bar{v}^2} \tag{7.15}$$

where

$$A = A_0\left(1 - \frac{a}{\bar{v}}\right) \qquad\qquad B = B_0\left(1 - \frac{b}{\bar{v}}\right) \tag{7.16}$$

$\bar{v}$ is the specific molar mass calculated with $\bar{v} = \frac{V}{N}$ and the five constants, a, b, c, A_0 and B_0 is for nitrogen gas given by[Beattie and Bridgeman, 1928, Table 1]

$$a = 0.02617 \qquad b = -0.00691 \qquad c = 4.20 \cdot 10^4$$
$$A_0 = 136.2315 \qquad B_0 = 0.05046$$

The above is valid when p is in kPa, $\bar{v}$ is in $\frac{m^3}{kmol}$ and T is in Kelvin. The constants are verified by [Cengel and Turner, 2001, Table 3-4].

Despite that the equation is based on experimental constants, it is known to be reasonably accurate for densities up to about $0.8\rho_{cr}$, where ρ_{cr} is the critical density[Cengel and Turner, 2001, page 102].

The equation is included in the project as it is one of the most simple experimentally based equations of state. The equation can still to some extend be used for making initial calculations. Furthermore studies showns that the equation yields some quite accurate results with a deviation of some 0,2% at a temperature range of 250 K to 300 K and max pressures up to 20 MPa[Cengel and Turner, 2001, Figure 3-62]. Other studies shows an average deviation of 0,19% in a temperature range of 145 K to 673 K and a max pressure of 21.5 MPa[Beattie and Bridgeman, 1928].

The derivatives of p

The derivatives of p with respect to temperature T is

$$\frac{\partial p}{\partial T} = \frac{R_u\left(T^3\bar{v} + 2c\right)(\bar{v}+B)}{T^3\bar{v}^3} \tag{7.17}$$

7.1.5 Benedicte-Webb-Rubin (BWR)

In 1940 the Beattie-Bridgeman equation of state was extended by Benedicte, Webb and Rubin. They raised the number of constants to eight plus the Universal gas constant. The equation is given by[Cengel and Turner, 2001, (3-26) and page 102]

$$p = \frac{R_u T}{\bar{v}} + \frac{B_0 R_u T - A_0 - \frac{C_0}{T^2}}{\bar{v}^2} + \frac{bR_u T - a}{\bar{v}^3} + \frac{a\alpha}{\bar{v}^6} + \frac{c\left(1 + \frac{\gamma}{\bar{v}^2}\right)e^{-\frac{\gamma}{\bar{v}^2}}}{\bar{v}^3 T^2} \tag{7.18}$$

where the constants a, b, c, A_0, B_0, C_0, α and γ are given by[Cengel and Turner, 2001, Table 3-4]

$$\begin{aligned} a &= 2.54 & b &= 0.002328 & c &= 7.379 \cdot 10^4 \\ A_0 &= 106.73 & B_0 &= 0.04074 & C_0 &= 8.164 \cdot 10^5 \\ \alpha &= 1.272 \cdot 10^{-4} & \gamma &= 0.0053 \end{aligned}$$

The above i valid when p is in kPa, $\bar{v}$ is in $\frac{m^3}{kmol}$ and T is in Kelvin. It has not be possible to verify the constants from other sources. The equation can compute accurate results for densities up to $2.5\rho_{cr}$[Cengel and Turner, 2001, page 102].

The equation has been included in the project because studies shows, that despite its higher numbers of constants compared to the Beattie-Bridgemann equation of state, it is not more accurate at high pressures (and T $>$ 200 K). This behavior will be studied, as this is in fact the pressure range that the project will focus on, and the accuracy versus complexity is therefore of high interest.

The derivatives of p

The derivatives of p with respect to temperature T is

$$\frac{\partial p}{\partial T} = \frac{R_u}{\bar{v}} + \frac{\left(B_0 R_u + \frac{2C_0}{T^3}\right)}{\bar{v}^2} + \frac{bR_u}{\bar{v}^3} - \frac{2c\left(1 + \frac{\gamma}{\bar{v}^2}\right) e^{-\frac{\gamma}{\bar{v}^2}}}{\bar{v}^3 T^3} \tag{7.19}$$

7.1.6 Bender

The Bender equation of state was publish in 1970 on the 5th Symposium On Thermophysical Properties in New York and is given by[Ghazouani et al., 2005, (1) & (2)]

$$p = \rho T \left(R + B\rho + C\rho^2 + D\rho^3 + E\rho^4 + F\rho^5 + \left(G + H\rho^2\right)\rho^2 e^{-n_{20}\rho^2}\right) \tag{7.20}$$

where

$$\begin{aligned} B &= n_1 + \frac{n_2}{T} + \frac{n_3}{T^2} + \frac{n_4}{T^3} + \frac{n_5}{T^4} & C &= n_6 + \frac{n_7}{T} + \frac{n_8}{T^2} \\ D &= n_9 + \frac{n_{10}}{T} & E &= n_{11} + \frac{n_{12}}{T} \\ F &= \frac{n_{13}}{T} & G &= \frac{n_{14}}{T^3} + \frac{n_{15}}{T^4} + \frac{n_{16}}{T^5} \\ H &= \frac{n_{17}}{T^3} + \frac{n_{18}}{T^4} + \frac{n_{19}}{T^5} \end{aligned}$$

The coefficient a_{20} is usually predicted with $a_{20} = \frac{a}{\rho_{cr}}$. It could although yield some considerable improvements if this relation is adjusted [Polt and Maurer, 1992]. But using this assumption, (7.20) is a linear function of the 19 coefficients. The coefficients can be evaluated using numerical fitting[Ghazouani et al., 2005].

To make the coefficients dimensionless, two ratios are introduced namely[Rotthäuser, 1993, (4.23) & (4.24)]

$$\omega = \frac{v_{cr}}{v} = \frac{\rho}{\rho_{cr}} \qquad \gamma = \frac{T_{cr}}{T} \tag{7.21}$$

Using those (7.20) can be rewritten to[Rotthäuser, 1993, (4.25)]

$$p = \frac{RT}{v}\left[1 + \sum_{i=1}^{19} B_i Y_i\right] \tag{7.22}$$

Please see Appendix C for a complete list of all coefficients[Ghazouani et al., 2005] and how to calculate B_i and Y_i.

The Bender equation of state is included in the project as it shows very good accuracy for among others nitrogen gases in the temperature range of 64 - 2,000 K and pressure range of 0.08 bar - 1,000 bar, with an accuracy of 0.06%[Ghazouani et al., 2005].

The derivatives of p

The derivatives of p with respect to temperature T is

$$\frac{\partial p}{\partial T} = -\frac{R}{T^5 v}\Big(-T^5 - B_1\omega\, T^5 - B_6\omega^2 T^5 - B_9\omega^3 T^5 - B_{11}\omega^4 T^5 + 4\, B_{16}\omega^2 {T_{cr}}^5 e^{\alpha\,\omega^2} \tag{7.23}$$

$$+ 4\, B_{19}\omega^4 {T_{cr}}^5 e^{\alpha\,\omega^2} + B_3\omega\, {T_{cr}}^2 T^3 + 2\, B_4\omega\, {T_{cr}}^3 T^2 + 3\, B_5\omega\, {T_{cr}}^4 T \tag{7.24}$$

$$+ B_8\omega^2 {T_{cr}}^2 T^3 + 2\, B_{14}\omega^2 {T_{cr}}^3 e^{\alpha\omega^2} T^2 + 3B_{15}\omega^2 {T_{cr}}^4 e^{\alpha\omega^2} T \tag{7.25}$$

$$+2B_{17}\omega^4 {T_{cr}}^3 e^{\alpha\omega^2} T^2 + 3B_{18}\omega^4 {T_{cr}}^4 e^{\alpha\omega^2} T\Big) \tag{7.26}$$

7.1.7 Jacobsen & Stewart (JS)

The last equation of state to be used in the project is the Jacobsen & Stewart equation of state. The equation is very similar to the Bender equation of state, see Section 7.1.6. But the equation contains 32 coefficients plus the gas constant and is given by[Rupprecht, 1988, (5.8)] and [Stewart and Jacobsen, 1973, (6)]

$$p = \frac{RT}{v}\left[1 + \sum_{i=1}^{32} N_i X_i\right] \tag{7.27}$$

As seen the equation is of the same form as the Bender equation, but is contains 13 more coefficients. In Appendix D all coefficients are listed together with equations for how to calculate N_i and X_i. Stewart and Jacobsen have given a thorough explanation of how the coefficients were fitted with the property data for nitrogen[Stewart and Jacobsen, 1973].

The Jacobsen & Stewart equation of state is included in the project because of its very high degree accuracy. Accuracies of up to 0,05% for temperatures between 200 til 400 K and pressures up to 400 bar has been observed[Rupprecht, 1988] and [Stewart and Jacobsen, 1973].

The derivatives of p

The derivatives of p with respect to temperature T is

$$\frac{\partial p}{\partial T} = \frac{-0.5R}{\sqrt{\frac{T_{cr}}{T}}T^5 v}\left(-2N_6\omega^2T^5\sqrt{\frac{T_{cr}}{T}} - 2N_{10}\omega^3T^5\sqrt{\frac{T_{cr}}{T}} - N_2\omega T_{cr}T^4 - 2T^5\sqrt{\frac{T_{cr}}{T}}\right. \tag{7.28}$$

$$+ 2N_{14}\omega^5{T_{cr}}^2T^3\sqrt{\frac{T_{cr}}{T}} + 6N_{29}\omega^{10}{T_{cr}}^4e^{\alpha\omega^2}T\sqrt{\frac{T_{cr}}{T}} + 4N_{30}\omega^{12}{T_{cr}}^3e^{\alpha\omega^2}T^2\sqrt{\frac{T_{cr}}{T}} \tag{7.29}$$

$$+ 4N_{28}\omega^{10}{T_{cr}}^3e^{\alpha\omega^2}T^2\sqrt{\frac{T_{cr}}{T}} + 4N_{20}\omega^2{T_{cr}}^3e^{\alpha\omega^2}T^2\sqrt{\frac{T_{cr}}{T}} + 6N_{25}\omega^6{T_{cr}}^4e^{\alpha\omega^2}T\sqrt{\frac{T_{cr}}{T}} \tag{7.30}$$

$$+ 4N_{22}\omega^4{T_{cr}}^3e^{\alpha\omega^2}T^2\sqrt{\frac{T_{cr}}{T}} + 6N_{21}\omega^2{T_{cr}}^4e^{\alpha\omega^2}T\sqrt{\frac{T_{cr}}{T}} + 6N_{31}\omega^{12}{T_{cr}}^4e^{\alpha\omega^2}T\sqrt{\frac{T_{cr}}{T}} \tag{7.31}$$

$$+ 4N_{26}\omega^8{T_{cr}}^3e^{\alpha\omega^2}T^2\sqrt{\frac{T_{cr}}{T}} + 2N_{17}\omega^7{T_{cr}}^2T^3\sqrt{\frac{T_{cr}}{T}} + 2N_{12}\omega^3{T_{cr}}^2T^3\sqrt{\frac{T_{cr}}{T}} \tag{7.32}$$

$$+ 8N_{32}\omega^{12}{T_{cr}}^5e^{\alpha\omega^2}\sqrt{\frac{T_{cr}}{T}} + 8N_{23}\omega^4{T_{cr}}^5e^{\alpha\omega^2}\sqrt{\frac{T_{cr}}{T}} + 8N_{27}\omega^8{T_{cr}}^5e^{\alpha\omega^2}\sqrt{\frac{T_{cr}}{T}} \tag{7.33}$$

$$+ 4N_5\omega{T_{cr}}^3T^2\sqrt{\frac{T_{cr}}{T}} + 2N_8\omega^2{T_{cr}}^2T^3\sqrt{\frac{T_{cr}}{T}} + 4N_{24}\omega^6{T_{cr}}^3e^{\alpha\omega^2}T^2\sqrt{\frac{T_{cr}}{T}} \tag{7.34}$$

$$+ 4N_{15}\omega^5{T_{cr}}^3T^2\sqrt{\frac{T_{cr}}{T}} + 4N_9\omega^2{T_{cr}}^3T^2\sqrt{\frac{T_{cr}}{T}} + 2N_4\omega{T_{cr}}^2T^3\sqrt{\frac{T_{cr}}{T}} \tag{7.35}$$

$$+ 4N_{18}\omega^7{T_{cr}}^3T^2\sqrt{\frac{T_{cr}}{T}} + 2N_{16}\omega^6{T_{cr}}^2T^3\sqrt{\frac{T_{cr}}{T}} + 4N_{19}\omega^8{T_{cr}}^3T^2\sqrt{\frac{T_{cr}}{T}} \tag{7.36}$$

$$\left. -2N_1\omega T^5\sqrt{\frac{T_{cr}}{T}}\right) \tag{7.37}$$

7.2 Implementing in SIMULINK

Please refer to Appendix B.2 for description of how the equations are implemented in SIMULINK.

7.3 Summery

Six ways of calculation the pressure in a gas have been presented ranging from very simple equations with poor accuracy to very complex equations with high accuracy. A seventh equation was also introduced, namely the Ideal gas equation with compressibility factor. The equation takes into account the differences when a gas is not an ideal gas. The equation although is not included in the rest of the report, as the equation is only suitable for static calculations and not simulations with large and quick variations.

In Table 7.2 all the equations are listed with any limitations the equations may have and the accuracy that can be expected within the limitations. The high accuracy is especially found at low pressures regardless of temperature valid for all equations. But some larger deviations in the accuracy of the equations are expected for higher pressures. This is especially the case for lower temperatures (some 260 Kelvin).

The equations are all to be modeled in a computer software. Since more complex equations yield more calculation, it will take longer time to determine pressure and temperature. For short simulations this is not a problem, but for longer simulations (>2 min) the difference between e.g. Jacobsen & Stewart and the Ideal gas equation is noticeable. Another thing to have in mind is the equations ability to be used in a quick static calculation. Here especially the Ideal gas equation and Van der Waals equation of state distinguish them self as being easy-to-use and very simple. Above is why complexity will be a factor of comparison in the final conclusion.

A validation of all the models is to be found in Chapter 13.

Name	Number of constants	Accuracy	Limitations
IGE	1	Good within limitations, otherwise poor	Ideal gases
VdW	3	0.5% - 5.3%	p < 200 bar and T > 250 K
BB	6	0.0% - 0.2%	p < 215 bar, T > 145 K and $\rho \leq 0.8\rho_{cr}$
BWR	9	0.0% - 0.4%	p < 200 bar, T > 250 K and $\rho \leq 2.5\rho_{cr}$
Bender	20	0.06%	64K < T < 2,000K and 0.08 bar < p < 1,000 bar
JS	33	0.05%	200K < T < 400K and p < 400 bar

Table 7.2: *A list of all the equations of state presented in this chapter. Please see the individual section for details about the equations and references.*

Gas temperature model

8

The chapter will deal with calculating the temperature of the gas.

The ideal gas equation in Chapter 7.1.1 states that the temperature of the gas will increase when the pressure increases. Because a system always seeks to be in equilibrium with its surroundings a heat transfer will take place to obtain thermal equilibrium. Heat will be transferred from the high-temperature medium to the low-temperature medium. The heat transfer will stop when the the mediums have reached the same temperature[Cengel and Turner, 2001, page 604]. Heat transfer can occur in three different ways, namely by conduction, by convection and by radiation. In the following a short description of the three modes is given, which all occurs when there is a temperature difference.

8.1 Theory

8.1.1 Conduction

Conduction occurs when heat is transferred from more energetic particles to less energetic particles as a result of interaction between the particles. In gases and liquids the conduction is due to the collisions and diffusion of the molecules, while in solids it is due to the combination of vibrations of the molecules in a lattice and the energy transport by free electrons. For instance a cold canned soda places in room temperature will have the same temperature as the surroundings after some time because of heat transfer from the soda through the can to the air around it.

The rate of heat transferred by conduction is a function of the geometry of the medium, its thickness and the material of the medium together with the temperature difference across the medium. Studies have shown that the rate of heat transfer is proportional to the temperature differers and the wall area, but is inversely proportional to the thickness[Cengel and Turner, 2001, page 604]:

$$\textit{Rate of heat conduction} \propto \frac{\textit{Area} \cdot \textit{Temperature difference}}{\textit{Thickness}}$$

$$\dot{Q}_{cond} = kA\frac{\Delta T}{\Delta x} \tag{8.1}$$

where Δx is the wall thickness, A is the wall area, ΔT is the temperature differers and k is the thermal conductivity of the material, which is a measure of the ability of a material to conduct heat[Cengel and Turner, 2001, page 605].

8.1.2 Radiation

Radiation is the energy emitted by matter in the form of electromagnetic waves as a result of the changes in the electronic configurations of the atoms or molecules. Energy transfer by radiation does not need a medium and the transfer is infact fastest i vacuum. All solids, liquids and gases emit, absorb or transmit radiation to varying degrees. The maximum rate of radiation that can be emitted from a surface at an absolute temperature, T, is given by the Stefan-Boltzmann law[Cengel and Turner, 2001, (14-5) and page 613]:

$$\dot{Q}_{emit,max} = \sigma A T^4 \tag{8.2}$$

where $\sigma = 5.67 \cdot 10^{-8} \left[\frac{W}{m^2 \cdot K^4}\right]$ and A is the area. Only an idealized surface called a Blackbody radiates heat at this rate. Therefore (8.2) is multiplied by the emissivity, ϵ[Cengel and Turner, 2001, (14-6)]:

$$\dot{Q}_{emit} = \epsilon \sigma A T^4 \tag{8.3}$$

The emissivity varies from surface to surface. The Blackbody has an emissivity of $\epsilon = 1$.

8.1.3 Convection

The third and last mean of heat transfer is by convection and is energy transfer between a solid surface and the adjacent liquid or gas. The different between convection and conduction is that at convection the adjacent gas or liquid is in motion opposite to conduction. There are two types of convection, namely forced convection and natural convection. At forced convection the fluid or gas is forced to flow across the surface e.g. by using a fan or a pump. At natural convection, the liquid or gas flows freely across the surface and the motion is only caused by the fact that the gas or liquid will raise when it gets warmer and fall when it gets cooler[Cengel and Turner, 2001, page 611-612].

Observations have shown that the rate of heat transfer is proportional to the temperature difference and is expressed by Newton's law of cooling[Cengel and Turner, 2001, (14-4)]:

$$\dot{Q}_{conv} = hA\left(T_a - T\right) \tag{8.4}$$

where A is the area, T_a is the ambient temperature, T is the gas temperature and h is the convection heat transfer coefficient. The convection heat transfer coefficient is a parameter whose value depends on many variables such as surface geometry, the nature of fluid motion, the properties of the fluid etc. The coefficient can be calculated theoretically, but will in this project be determined experimentally. The coefficient will be determined in Appendix G. As it can be seen, convection heat transfer is basically conduction heat transfer with fluid motion, but of practical reasons this has been given its own name, namely convection[Cengel and Turner, 2001, page 612]. In the project it will be assumed that heat transfer only will occur by convection neglecting any radiation. Convection has been chosen since the gas in the accumulator is being forced to move when the piston is moving, so it can not be considered stagnant. When the piston is not moving than movement of the gas is still assumed. This is especially the case since the gas will change temperature resulting in a change in density, making some parts of the gas lighter or heavier then other parts of the gas. The difference in density will force the gas to move around. Regarding the surrounding air it is assumed that this also will not be stagnant as the air will be moved around by people moving, air entering the room via leaks or ducts and by varying temperatures and densities in the air caused by a fan heater placed in the room of the test rig. Please see Chapter A for more about the latter.

8.2 Equation

In the following an expression describing the temperature of the gas will be presented.

If the gas side of the accumulator is considered a closed system where no change in mass can occur but change in energy can occur and the first law of thermodynamics is applied, stating that energy neither can be created nor destroyed, but only change forms, an energy balance can be written[Cengel and Turner, 2001, (5-10)]. This procedure has been used in several other references[Rupprecht, 1988, (5.1)], [Rotthäuser, 1993, (6.1)] and [Pourmovahed and Otis, 1985, (1)].

$$\dot{Q}_{conv} - \dot{W} = \dot{U} \tag{8.5}$$

The balance states that the change in internal energy, $\dot{U}$, equals the output of heat, $\dot{Q}$, minus the work, $\dot{W}$. In 1843 Joule showed that for ideal gases, internal energy is a function of temperature only. He later showed that for real gases the internal energy is a function of not only the temperature[Cengel and Turner, 2001, page 107]. The internal energy for real gases can be calculated using (8.6)[Pourmovahed and Otis, 1990, (2)]. This has been verified[Rupprecht, 1988, (5.4)b].

$$\dot{U} = mC_v\frac{dT}{dt} + m\left(T\left(\frac{\partial p}{\partial T}\right)_v - p\right)\frac{dV}{dt} \tag{8.6}$$

Furthermore Q can be calculated using (8.4) and W can be calculated by[Cengel and Turner, 2001, (4-11)]

$$\dot{W} = p \cdot \frac{dV}{dt} \tag{8.7}$$

Applying (8.4), (8.6) and (8.7) to (8.5) yields

$$hA_w\left(T_a - T\right) - p \cdot \frac{dV}{dt} = m_{gas}C_v\frac{dT}{dt} + m_{gas}\left(T\left(\frac{\partial p_{gas}}{\partial T}\right)_v - p_{gas}\right)\frac{dv}{dt} \tag{8.8}$$

with some rearrangement yields

$$\begin{aligned}
hA_w\left(T_a - T\right) - p_{gas} \cdot \frac{dV}{dt} &= m_{gas}C_v\frac{dT}{dt} + \left(m_{gas}T\left(\frac{\partial p_{gas}}{\partial T}\right)_v - m_{gas}p_{gas}\right)\frac{dv}{dt} && (8.9)\\
hA_w\left(T_a - T\right) - p_{gas} \cdot \frac{dV}{dt} &= m_{gas}C_v\frac{dT}{dt} + m_{gas}T\left(\frac{\partial p_{gas}}{\partial T}\right)_v\frac{dv}{dt} - m_{gas}p_{gas}\frac{dv}{dt} && (8.10)\\
hA_w\left(T_a - T\right) - p_{gas} \cdot \frac{dV}{dt} &= m_{gas}C_v\frac{dT}{dt} + m_{gas}T\left(\frac{\partial p_{gas}}{\partial T}\right)_v\frac{dv}{dt} - p_{gas}\frac{dV}{dt} && (8.11)\\
hA_w\left(T_a - T\right) &= m_{gas}C_v\frac{dT}{dt} + m_{gas}T\left(\frac{\partial p_{gas}}{\partial T}\right)_v\frac{dv}{dt} && (8.12)\\
m_{gas}C_v\frac{dT}{dt} &= hA_w\left(T_a - T\right) - m_{gas}T\left(\frac{\partial p_{gas}}{\partial T}\right)_v\frac{dv}{dt} && (8.13)\\
\frac{dT}{dt} &= \frac{hA_w}{m_{gas}C_v}\left(T_a - T\right) - \frac{m_{gas}}{m_{gas}C_v}T\left(\frac{\partial p_{gas}}{\partial T}\right)_v\frac{dv}{dt} && (8.14)\\
\frac{dT}{dt} &= \frac{\left(T_a - T\right)}{\tau} - \frac{T}{C_v}\left(\frac{\partial p_{gas}}{\partial T}\right)_v\frac{dv}{dt} && (8.15)\\
T &= \frac{\left(T_a - T\right)}{\tau} - \frac{T}{C_v}\left(\frac{\partial p_{gas}}{\partial T}\right)_v\frac{dv}{dt}dt && (8.16)
\end{aligned}$$

where T_a is the ambient temperature, T is the gas temperature, C_v is the specific heat capacity of gas and τ is the thermal-time constant given by

$$\tau = \frac{m_{gas}C_v}{hA_w} \tag{8.17}$$

where m_{gas} is the mas of the gas, A_w is the effective wall area and h is the convection heat transfer coefficient. τ will be experimentally determined in Appendix G. τ is not the same value at all time, and will therefore be determined several times during the test runs. Above result is also to be found in other references[Rupprecht, 1988, (5.7)] and [Pourmovahed and Otis, 1985, (5)].

8.3 Implementing in SIMULINK

Please refer to Appendix B.3 for description of how the equations are implemented in SIMULINK.

8.4 Summery

The temperature of the gas is calculated assuming the gas side of the accumulator to be a closed system with no mass transfer but heat transfer with convection. The expression is valid also for reel gases and accurate results are therefore expected. It should be mentioned that although only one model is shown in this chapter, actually one model exists for each equation of state. This is because the derivative of the pressure with respect to the temperature should be calculated which is different for each equation of state. Therefore a validation of six temperature models will be produces. Please seeChapter 14 for the validation.

Selection of test variables

9

This chapter will discuses which variables that should be used during the validation. Furthermore a discussion about the values these variables should obtain to fully validate the equations of state mentioned in Chapter 7 is included.

9.1 Variables

A number of variables can be adjusted before and during a test run. Before the test run the supply pressure, P_s, and precharge pressure, $P_{gas,precharge}$, can be adjusted as desired to obtain any initial and final pressure. Furthermore the temperature of the surroundings will be tried adjusted to lower and higher temperatures than normal room temperature. During the test run the opening of the valve, A, can be adjusted by three ways, namely:

- By a open loop system with a voltage, U, that can either be constant or vary following a sinus curve, pulse curve, saw tooth curve, etc.
- By a closed loop system measuring the oil pressure, P_{oil} or gas pressure, P_{gas}.
- By a closed loop system measuring the position of the piston, x.

9.2 Value of variables

To be able to test and validate the equations of state, it is crucial to select the right values of the different variables. Some of the equations of state have limits with in which they are most accurate, see Table 7.2. The test runs will be used to challenge this limits and to see what accuracy that can be obtained when exceeding the limits.

As seen in Table 7.2 both the VdW equation of state and the BWR equation of state have lower temperature limits at around 250 Kelvin. Therefore a series of test runs at temperatures around that value should be performed. It is presumed that it is not possible to reach ambient temperatures much lower than 260 Kelvin and much higher than 330 Kelvin. This combined with expansion and compression will yield even lower and higher temperatures. This mean that some of the lower temperature limits of e.g. BB and JS equation of state also could be challenged. As regard to pressure, both VdW, BB and BWR equations of state have pressure limits of maximum 200 bar till 216 bar. This will be challenged by using the power packs maximum supply pressure, p_s, of 250 bar. Both the Bender and JS equations of state have too high pressure limits to reach with the power pack. As the precharge pressure, $p_{gas,precharge}$, has not been mentioned in any of the used articles so fare in the project, the precharge pressure will vary from some 1 bar to some 150 bar to see the effect of this.

As regard to adjusting the opening of the valve, A, is has been decided to control this by a closed loop system measuring the position of the piston. This setup has been selected based on two reasons:

1. Using the position of the piston makes it possible to use piston speed for controlling the valve opening, A. This is beneficial as the rate of pressure change in the gas, p_{gas}, then also can be controlled. In this way it is possible to verify if the rate of pressure change has an influence on the

accuracy of the equations of state. Something that has not been mentioned in any cited article so far in the project.

2. When verifying the thermal-time constant is it necessary to control the volume of the gas side. This can only be done by controlling the position of the piston.

Piston position will be adjusted during test runs to obtain the desired piston speed or gas pressure. This setup is only possible for accumulator #1 since this is the only one with position transducer. Accumulator #2 will therefore be controlled by the oil pressure. The hydraulic model will be used to simulate the accumulator with the position as feedback. The modeled oil pressure will then be used as reference signal in the test rig.

10

Test schedule

This chapter will present a test schedule. The test schedule describes what pressure, reference signal, etc, that should be used for each test run.

In this section a schedule for all test runs will be presented together with a description of why the different test methods have been chosen. All test runs will be given a name, which will be different for each test run. If more test runs are performed with the same setup, the name of each sample will be added a continuous number starting from 1.

Only the gas pressure and temperature models are validated. This because they are the objectives of the project and focus will therefore only be on them. When the test rig is simulated with the different models, the measured oil pressure will be used to simulate the hydraulic model. The reason for this is to ensure that when validating the gas and pressure models, the hydraulic and mechanical models dos not have any influence on the result. The position will in all test runs be used as the reference signal.

10.1 Validating the test rig

The test rig is validated to determine the variability, that is how similar the outputs are when the same input is used for several test runs. A ramp function will be used as the input. The ramp function will move from an initial position to an final position and back to the initial position. The temperature of the gas should reach the ambient temperature before returning to the initial position. It is important that all other variables are the same at each test run. In Table 10.1 are listed all properties for the test runs. Please see Chapter 11 for the result of the validation. The results of the validation will be used to decide how many times every test run should be repeated.

Name	TESTRIG_1	TESTRIG_2	TESTRIG_3	TESTRIG_4
Function	Ramp	Ramp	Ramp	Ramp
Supply pressure [Bar]	250			
Precharge pressure [Bar]	50	100	50	100
Initial position [m]	0.01			
Final position [m]	0.07	0.07	0.14	0.14
Slope of ramp [m/s]	0.20	0.25	0.20	0.25
Duration [sec]	115	115	115	115
Samples	10			

Table 10.1: *Properties for test runs used for validating the test rig.*

10.2 Validating the gas pressure and temperature models

The gas pressure and temperature models are validated to seen whether the correct gas pressure and temperature are calculated. As seen from (8.16) a large temperature change is among other things obtained by having a large change in pressure. Therefore it would be reasonable to use a step function as input for the validation. However a step function would yield that the regulator would go into saturation which is not a desirable situation during test runs as there are no more control of the valve. Therefore a steep ramp input is used. The slope of the ramp is adjusted from test run to test run to obtain the highest velocity, and thereby the highest temperature changes, without the regulator saturating. The hydraulic and mechanical models are used to adjust the slope of the ramp before the test run.

The initial gas pressures of interest in this project is 50 bars, 100 bars and 150 bars since these are normally found in accumulators. Regarding temperature both low and high temperatures are of interest. Therefore the ambient temperature will be raised as much as possible (in the test runs approximately 335 Kelvin). That combined with and compression of the gas would yield the highest possible temperature. Vice versa a low ambient temperature (in the test runs approximately 250 Kelvin) combined with an expansion of the gas would yield the lowest possible temperatures. Therefore all ramp functions should return to the initial position when the gas temperature has reached ambient temperature. Please refer to Appendix H for explanation of how low and high ambient temperatures have been archived. The piston in accumulator #1 will be moved 0.07 m and 0.14 meter respectively and 0.09 m and 0.17 m for accumulator #2.

In total 28 test runs were performed. In Appendix E are listed all properties for each test run. The properties are selected according to the above and to challenge the different pressure models as described in Chapter 7. Please note that no test run will be performed for a precharge pressure of 150 bar combined with an end position of 0.19 m. This is because this configuration causes the piston not to reach the end position as the gas pressure would have to exceed the supply pressure. Listed test runs will be repeated for both cold, normal and warm ambient temperature. Please see Chapter 13 and Chapter 14 for the result of the validation.

10.3 Measuring the thermal time constant

To simulate the accumulator is it necessary to measure the thermal time constant. The thermal time constant is defined as the time it takes the gas pressure to drop 63.2% from maximum pressure compared to the final equllibrium pressure when the system is exposed to a step change in the volume[Pourmovahed and Otis, 1990]. This is shown graphically in Figure 10.1.

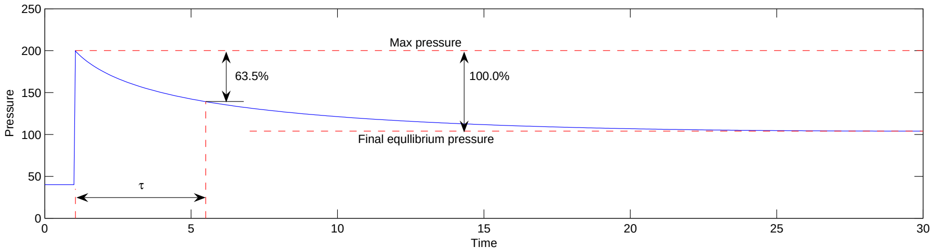

Figure 10.1: *Definition of thermal time constant, τ*

As described in Chapter 8, τ will be determined several times to make sure that the correct value is used in the simulation. As a minimum, τ should be determined every time the precharge pressure is changed or when the ambient temperature is changing. To validate the measured data, τ will be measured both before and after a test run.

The thermal time constant is determined by exposing the system to a step change in volume. No rules are to be found as regard to how big a step change that should be used. So in the test runs the same change as in the test run will be applied. A ramp function will be used with the same properties as described above. In Appendix G the experiments are described together with the results.

Validating test rig

11

This chapter will present the results from the experiment performed to validate the test rig. The aim of the experiment was to investigate the variability of the text rig.

A report of this experiment can be found in Appendix F. The experiment was performed to investigate the variability of the test rig, that is how similar the results was for the same setup. Four different setups has been used. All for accumulator #1. 10 test runs was performed for each setup. In Figure 11.1 the result for TESTRIG_1 is depicted. This test run contains 10 samples and the graph shows the measured pressure and temperature for all 10 samples plotted in the same graph.

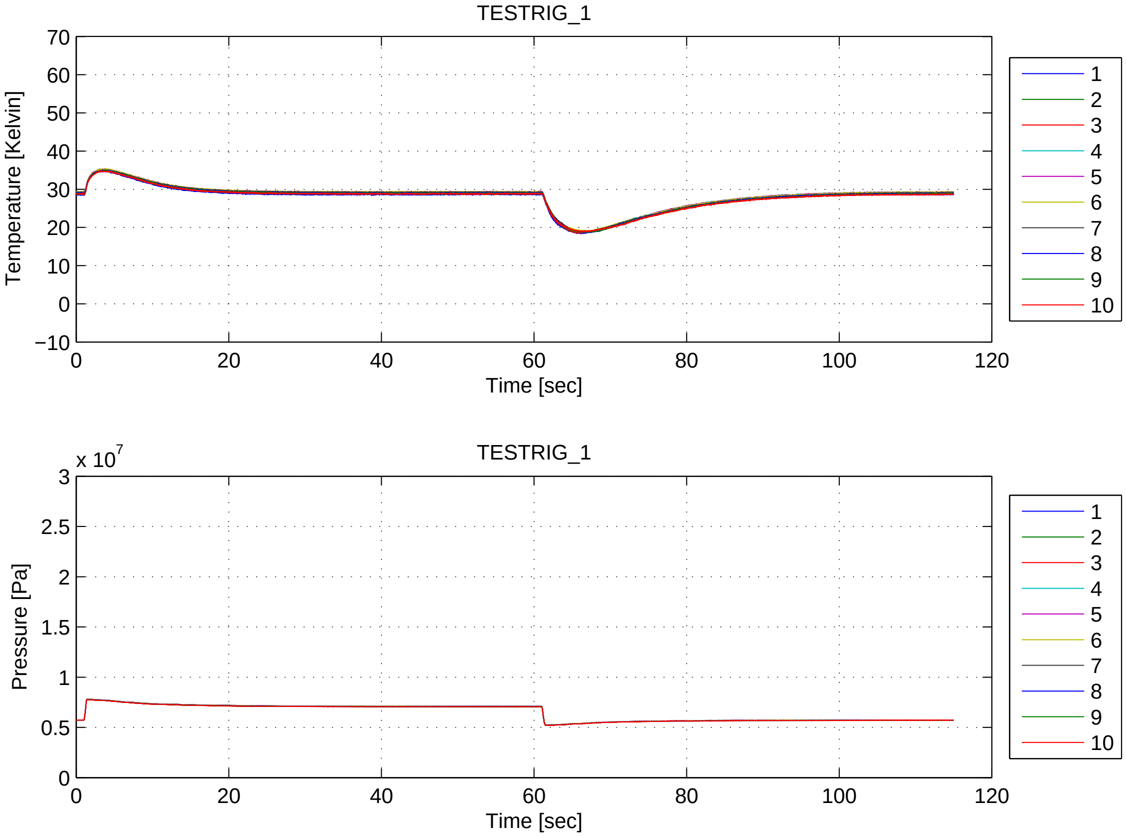

Figure 11.1: *Plot of test run TESTRIG_2 with 10 samples all with the same setup.*

The results shows very good consistency between the samples. To investigate this further the standard deviation between the 10 samples has been calculated for each time step. The result of this can be seen in Figure 11.2 and Figure 11.3 for the pressure and temperature respectively.

Graphs for the other three test runs can be seen in Appendix I.1. As seen from the figures the standard deviation is very small for both pressure and temperature for the test run. This is also the case for the the other three test runs. The standard deviation for the pressure never exceeds 0.5 bar and never 0.5 Kelvin for the temperature.

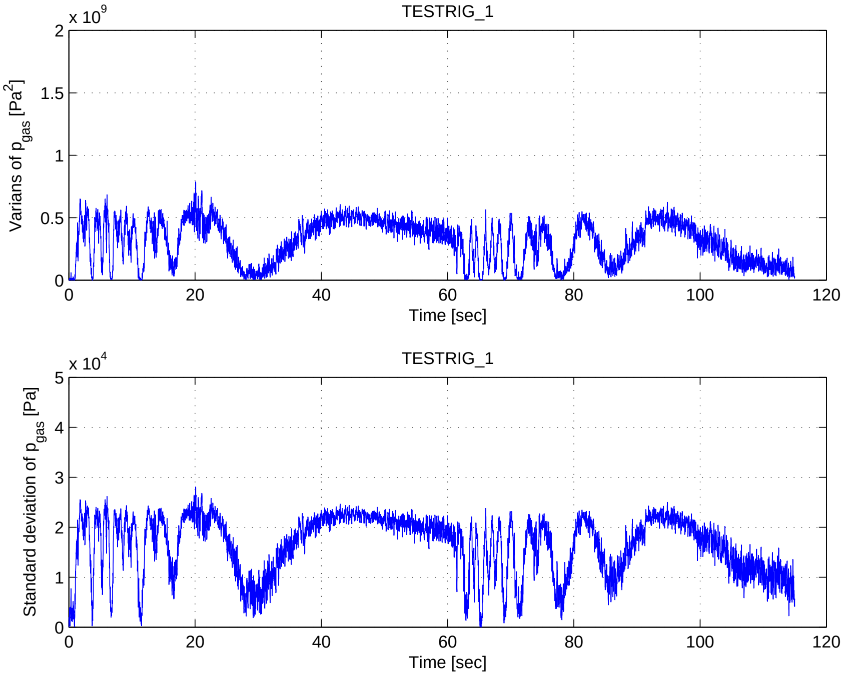

Figure 11.2: *Variance and standard deviation of the pressure calculated for all 10 samples for each time step.*

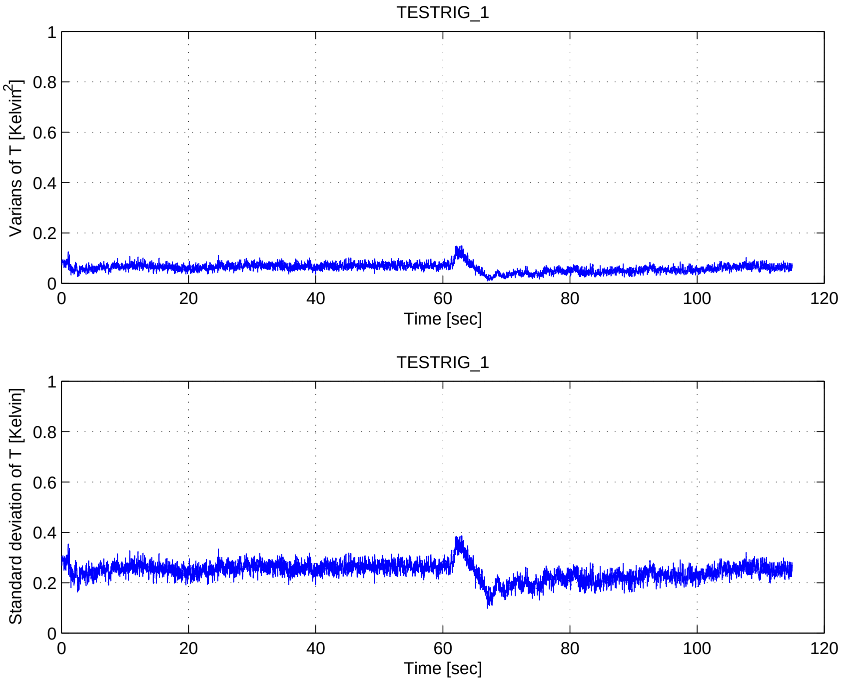

Figure 11.3: *Variance and standard deviation of the temperature calculated for all 10 samples for each time step.*

11.1 Conclusion

The deviation between the the 10 samples are so small, that it will not have any significant effect on the result of the following test runs. Therefore it is concluded that one sample per setup is sufficient. As seen later on in the report normally three samples will be made for each setup. This is to have some back-up data in case the first sample has any errors like defective transmitters.

Measuring the thermal time constant

12

This chapter will present the results from experiment performed to measure the thermal time constant. The aim of the experiment was to measure the thermal time constant to be used during the simulations of the test rig.

A report of this experiment can be found in Appendix G. The thermal time constant is a measure for how fast the pressure in the accumulator will drop by 63.5% when applied when a step change in the gas volume. The thermal time constant has been measured for accumulator #1 for all setups both before and after each test run. In Figure 12.1 is depicted the result when measuring the thermal time constant for GAS_2. The thermal time constant has been measured before and after the test run to validate the value.

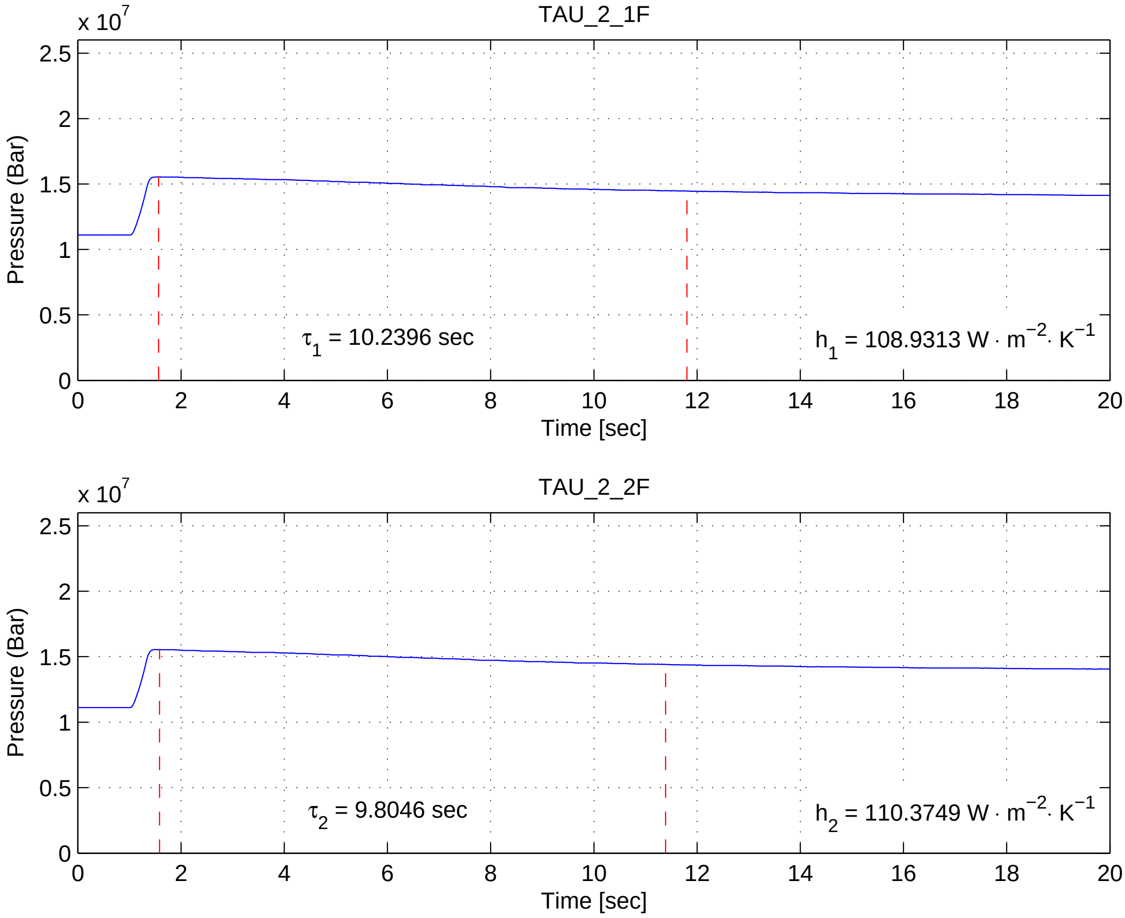

Figure 12.1: *Measured values of the thermal time constant for GAS_2. The top graph being before the testrun and the bottom one being after.*

The graph shows a difference between the two samples of approximately 0.4 seconds or 4.2%. In other test runs larger differences was experinced. To give an insight of how much the measured values varies, all masures thermal time constants are depicted in Figure 12.2 for accumulator #1. Graphs for all other test runs can be found in Appendix I.2

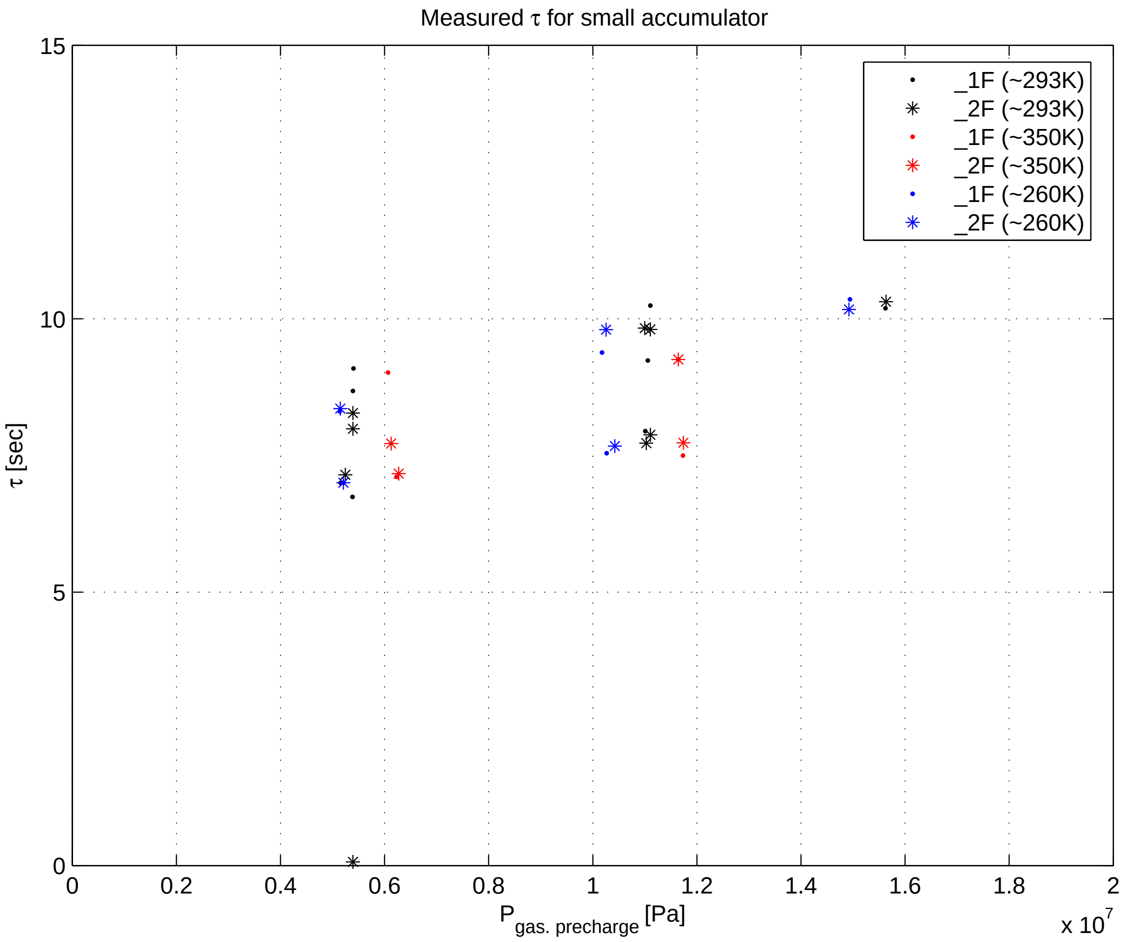

Figure 12.2: *Measured thermal time constants for accumulator #1.*

It can be seen that no single value for the thermal time constant is present. In fact large differences in the constant can be found within the same precharge pressure. The only conclusion to make is that the overall ambient temperature seems to have no influence on the value. But instead the precharge pressure has. Here it can be seen that the larger the precharge pressure, the larger the thermal time constant. The same conclusions can be made for accumulator #2. The latter is in good consistency with other conclusions[Rupprecht, 1988, Figure 4.8]. In Appendix I.2 the graphs for accumulator #2 can be found.

The reasons for the variation in the measured data can be many. But the circulation of the air in the laboratory i the many sources of error. If there is a large circulation of air the thermal time constant will drop because the amount of energy convected away from the accumulator is larger then without any air circulation.

12.1 Conclusions

Because of the large differences in the thermal time constant, it has been decided that the measured data will not be used in the simulations. In stead the thermal time constant will be measured using data from the test runs that are going to be validated (Data named GAS).

13

Validating gas pressure models

This chapter will present the results from the experiment in order to validate the gas pressure models. The aim of the experiment was to perform a number of test runs with different setups on two different accumulators. Simulations with the same setup was then performed with the different models and the result was compared with the measured data.

13.1 Collected data

A report of this experiment can be found in Appendix H. During each test run data as described in Appendix A is collected. The position of the piston will be used for the simulation together with the oil pressure. The data of this will not be presented in this chapter, only the gas pressure. In the next chapter the gas temperature will be presented and compared with the simulated data. In Figure 13.1 data for one test runs with three samples is depicted. Graphs for all other test runs can be found in Appendix I.3.

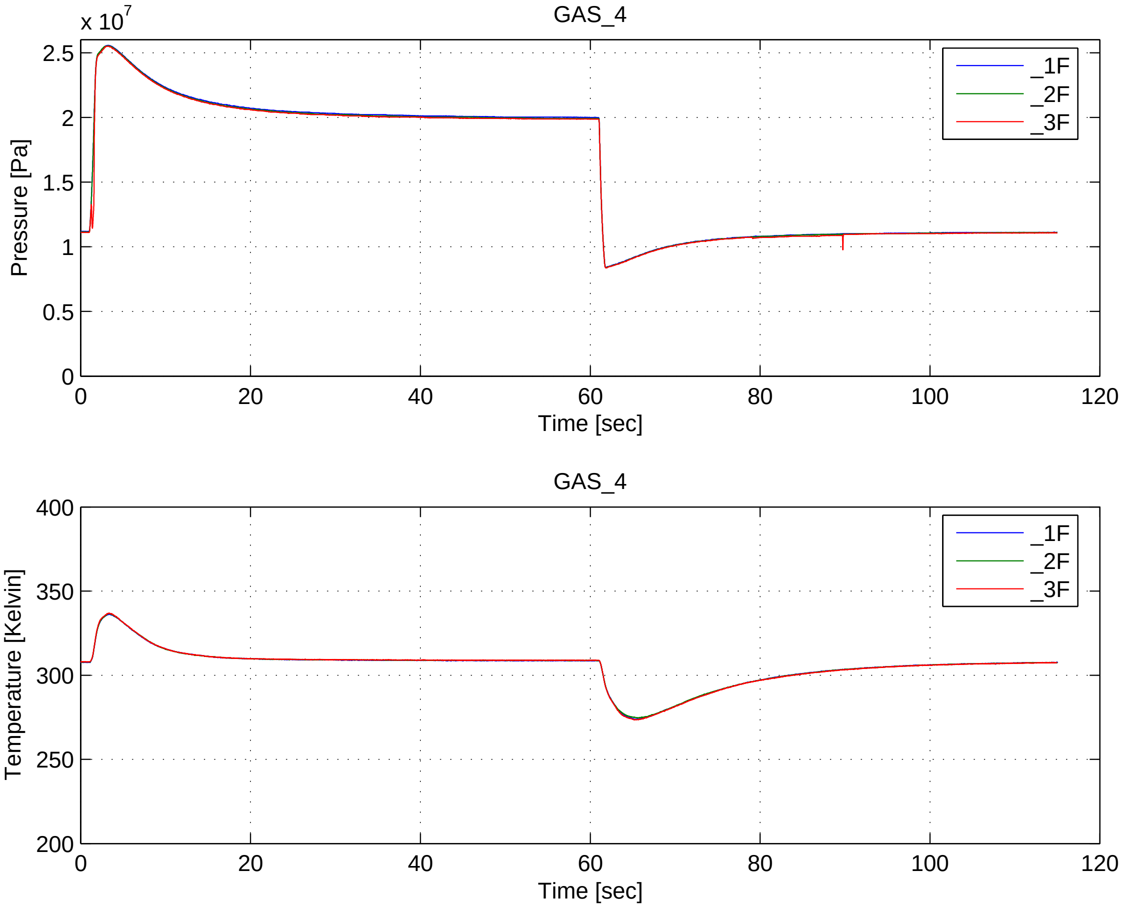

Figure 13.1: *Gas pressure and temperature for GAS_4.*

The graph shows an expected progress of the pressure and the temperature, namely that they increase during a compression and decrease during an expansion. The matching position and oil pressure have then been used to calculate the pressure and temperature using models as described in Chapter 7 and Chapter 8. For the above test run, namely GAS_4, the gas pressure has been calculated and compared with the measured data. This is depicted in Figure 13.2. Graphs for all other test runs can be found in Appendix I.4.

As explained in the experimental report in Appendix H the test run for accumulator #2 was performed using a simulated gas pressure as reference signal. Most likely there has been an error in the data used for the reference signal so the piston of the accumulator has not be where it was assumed to be. This is concluded as there are large differences between the measured and calculated data. Therefore all data for accumulator #2 must be considered unfit for use. In Figure 13.3 the measured and calculated data are shown for a test run with accumulator #2. The large difference appears clearly.

13.2 Comparison with models

To get an overview of the difference between the measured and the calculated data, the percentage-wise difference has been calculated and depicted as a function of the measured pressure in Figure 13.4. Graphs for all other test runs can be found in Appendix I.5.

As seen from Figure 13.4 each test run consists of four stages, namely two nonlinear and two approximate linear. The four stages are depicted separately in Figure 13.5 and are described in the following.

> Stage 1: The compression stage where the gas is compressed and the pressure and temperature therefore increases. The stage is approximately linear as the dominating variable here is the position and the position is the same in both the measured data and the calculated data.
>
> Stage 2: The first interaction stage, where the volume is kept constant. The gas interacts with the surrounding air and the temperature decreases reaching ambient temperature causing the pressure too decrease. The stage is not linear as the dominating variable is the thermal time constant. In the calculations the thermal time constant is assumed the same at all time. But this is in fact not the case since both the convection heat transfer coefficient and the effective wall area changes with time[Pourmovahed and Otis, 1990]. This difference is causing the nonlinear behavior.
>
> Stage 3: The expansion stage where the gas is expanded and the pressure and temperature therefore decreases. The stage is approximately linear because of the same reason as for stage 1.
>
> Stage 4: The second interaction stage, where the volume is kept constant. The gas interacts with the surrounding air and the temperature increases reaching ambient temperature causing the pressure to increase. The stage is nonlinear because of the same reason as for stage 3.

To give an overview off all test runs two values have been calculated for each model, namely the mean percentage value and the difference between the minimum percentage difference and the maximum percentage difference. The mean percentage value takes the mean value of all data points for each model. This value gives an indication of how precise the model is compared with the measured data. The value can only give an indication of how the model performs in average, i.e. does the model in average calculate a too low pressure or does it in average calculate a too high pressure. This value does anyhow not give an indication of how precise the model is in each data point, i.e. how far away from the average value the data points are. A model could have a difference of -20 % in one data point and 20 % in another data point. In average this gives a difference of 0 %, which is not a reliable and true result of that model. To give an indication of this the variance is calculated for each model. A large variance indicates that the data points are fare away from the average value. Vice versa a small variance indicates that the data points are close to the average. The latter is the most desirable.

The mean value and the variance have been calculated for all test runs both for accumulator #1 and accumulator #2. The result of this are depicted in Figure 13.6 and Figure 13.7. In Figure 13.6 the first five test runs are for normal ambient temperature, the next four are for warm ambient temperature and the last five are for cold ambient temperature. For Figure 13.7 the first four test runs are for cold ambient temperature and the last four are for ambient temperature.

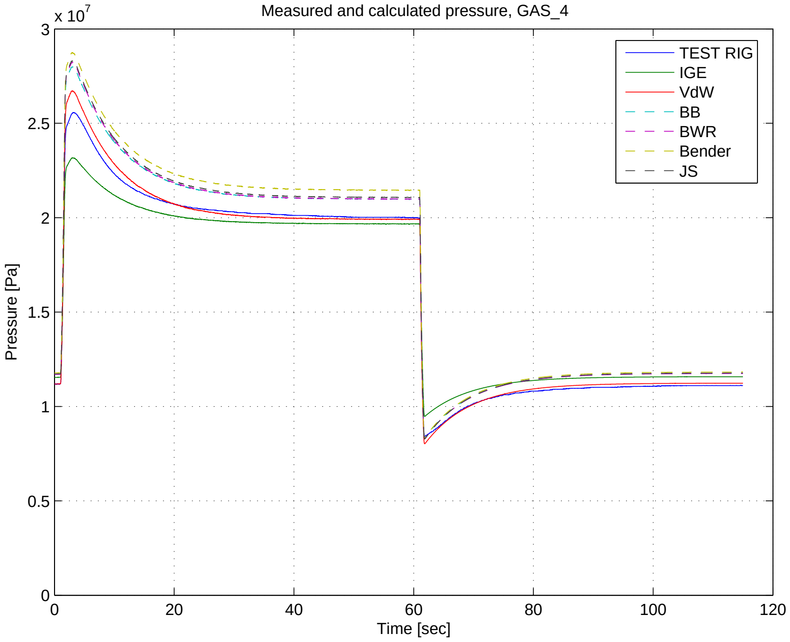

Figure 13.2: *Measured and calculated gas pressure using six equations of state for accumulator #1.*

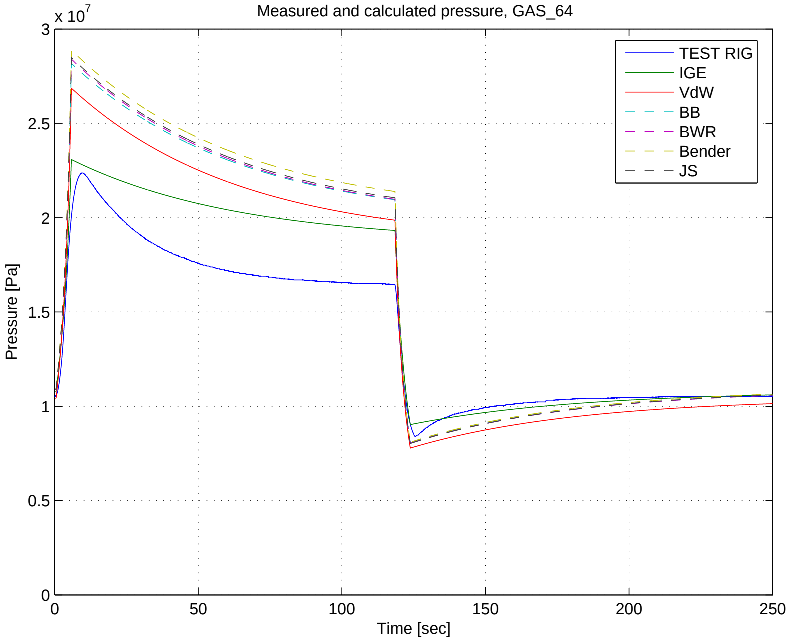

Figure 13.3: *Measured and calculated gas pressure using six equations of state for accumulator #2. Notice the large differences between measured an calculated.*

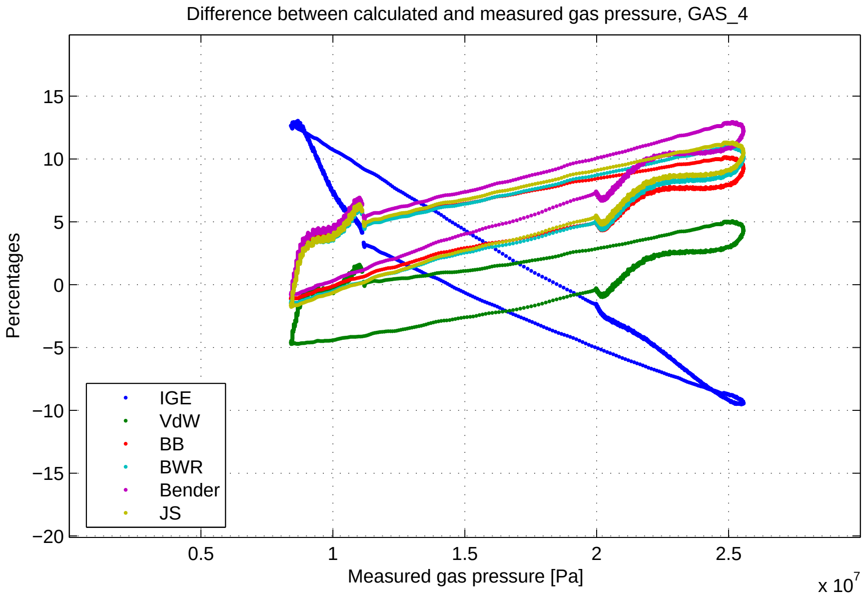

Figure 13.4: *Percentage-wise difference between measured an calculate gas pressure as a function of the measured pressure.*

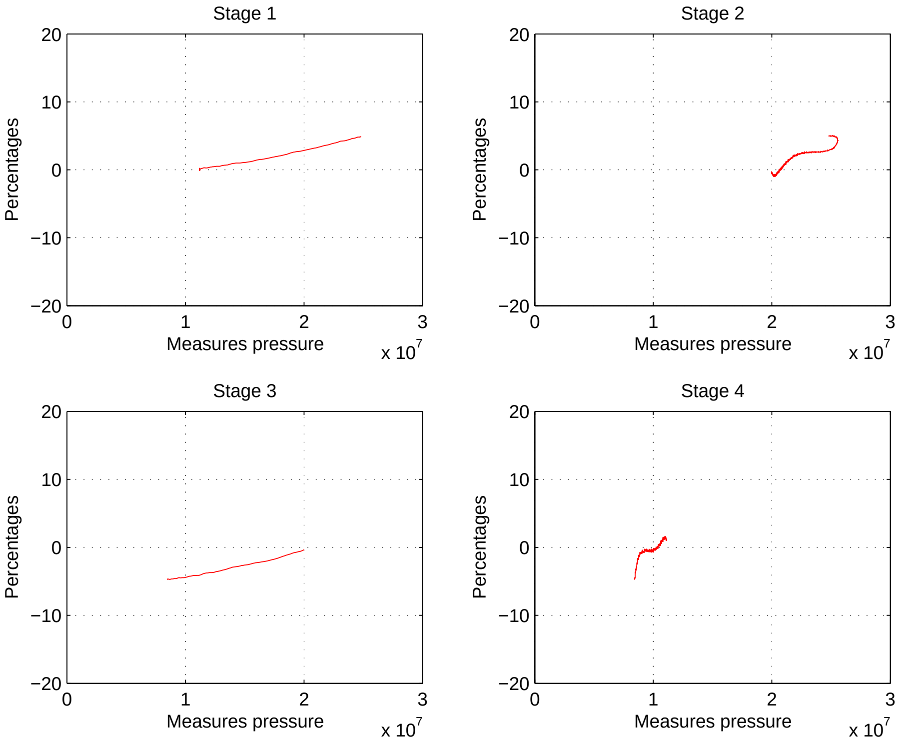

Figure 13.5: *The four stages in a test run, namely the compression, the first interaction, the expansion and the second interaction for accumulator #1.*

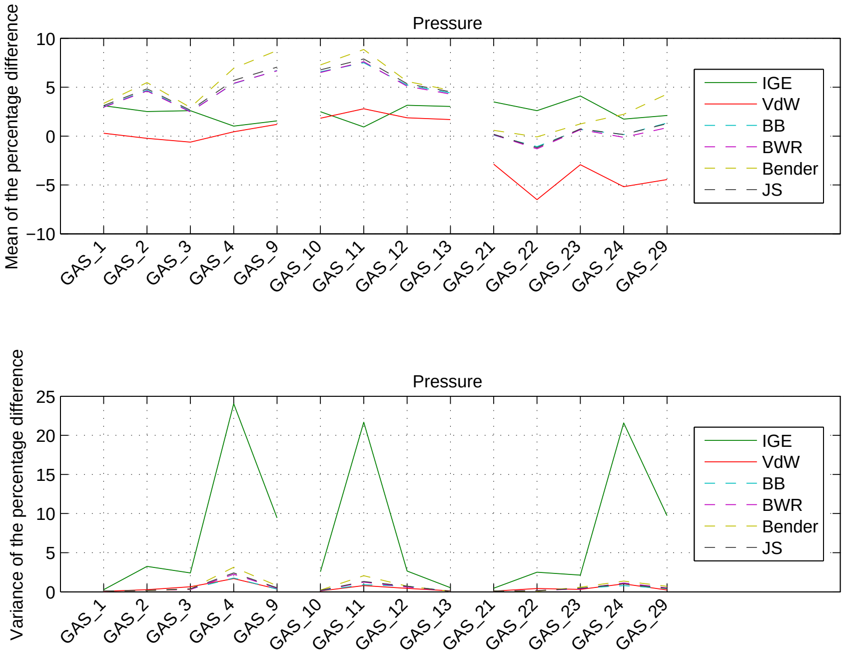

Figure 13.6: *Calculation of mean value and variance of all test runs for accumulator #1. The first five test runs are for normal ambient temperature, the next four are for warm ambient temperature and the last five are for cold ambient temperature*

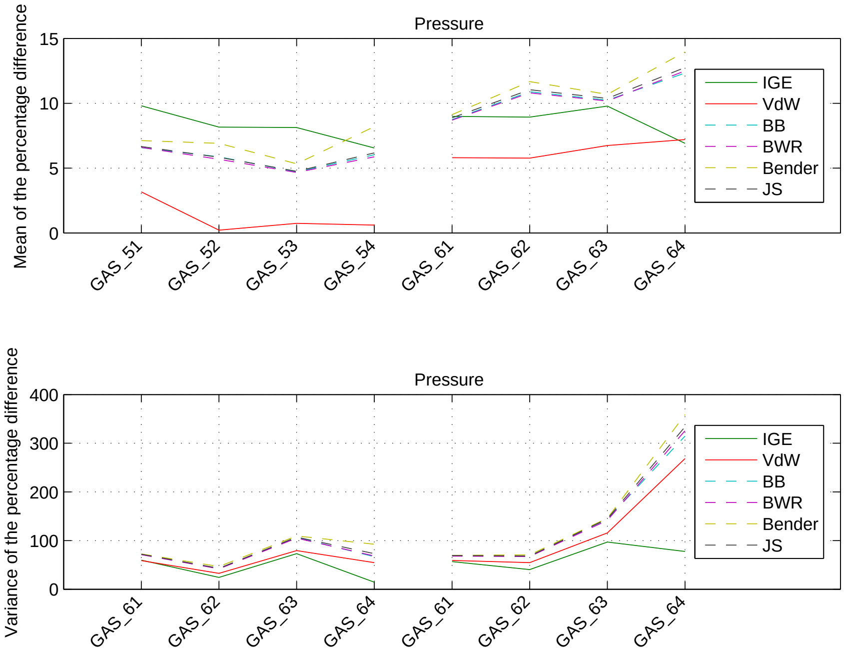

Figure 13.7: *Calculation of mean value and variance of all test runs for accumulator #2. The first four test runs are for cold ambient temperature and the last four are for normal ambient temperature.*

13.3 Conclusion

Based on the 14 test runs with accumulator #1 and the results depicted in Figure 13.6 some conclusions can be drawn for this accumulator and the six gas models:

- In general the ideal gas equation does seems to be very accurate for all three ambient temperatures and pressures. However when the results are studied further it is clear to see that this model has a large variance for large pressures. This is the case for both normal, warm and cold ambient temperature. As expected this model is not suitable for simulating hydraulic accumulators as described in this project.
- The next equation of state of interest is the Van der Waals equation of state. This provides precise results and has a low variance for both normal and warm ambient temperatures. This is as expected as this equation of state is known to be accurate for temperature above 250 Kelvin.
- For normal and warm ambient temperatures the four most complex equations of state proves to be more inaccurate then the less complex Van der Waals equation of state. Only for cold ambient temperatures it is reasonable to use the more complex equations of state. But still the difference between this four equations of state are so small, that it is recommended just to use Beattie-Bridgeman equation of state.

Regarding accumulator #2 no clear conclusions can be drawn. Although a tendency can be seen in the mean value, namely that a difference in accuracy between normal and cold ambient temperature of approximately 5 percentage point is observed, see Figure 13.7. This is also the case for accumulator #1. Assuming that the error in the data leads to a displacement of the result of approximately 5 percentage point the same conclusion as for accumulator #1 can be drawn, namely that for normal ambient temperature the Van der Waals equation of state is sufficiently and for cold ambient temperature Beattie-Bridgeman equation of state is sufficient.

Validating gas tempersture models

14

14.1 Collected data

A report of this experiment can be found in Appendix H. During each test run data as described in Appendix A is collected. The position of the piston will be used for the simulation together with the oil pressure. The data of this will not be presented in this chapter, only the gas pressure. In the next chapter the gas temperature will be presented and compared with the simulated data. In Figure 13.1 data for one test runs with three samples is depicted. Graphs for all other test runs can be found in Appendix I.3.

Figure 13.1 shows an expected progress of the pressure and the temperature, namely that they increase during a compression and decrease during an expansion. The matching position and oil pressure have then been used to calculate the pressure and temperature using models as described in Chapter 7 and Chapter 8. For the depicted test run, namely GAS_4, the gas temperature has been calculated and compared with the measured data. This is depicted in Figure 14.1 and Figure 14.2. Graphs for all other test runs can be found in Appendix I.6.

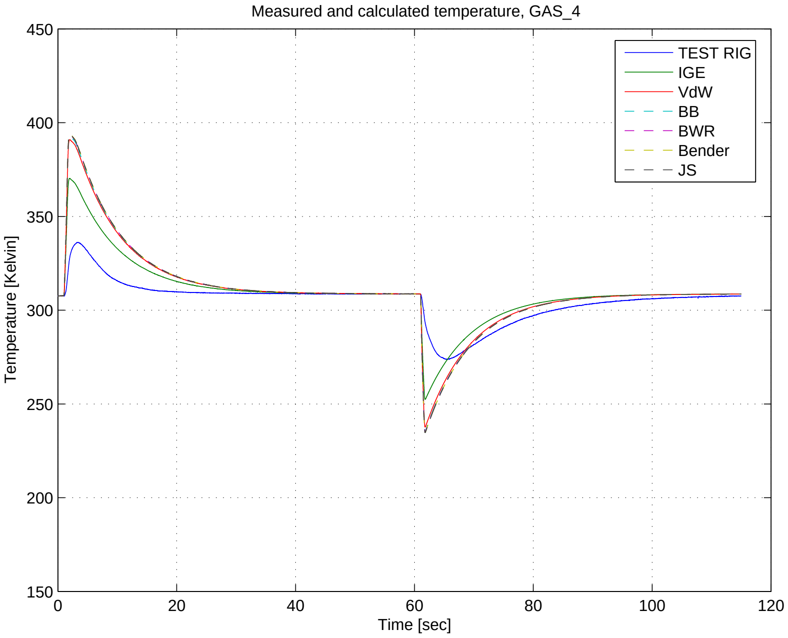

Figure 14.1: *Measured and calculated gas temperature using six equations of state for accumulator #1.*

As seen in the two figures, large differences are observed. Most distinct for accumulator #2. This may be explained with the same reason as mentioned in the experimental report in Appendix H, namely that the position of the piston has not been as expected leading to a lower pressure than expected during a compression. Regarding accumulator #1 large differences between calculated and measured data are also observed. The differences are not assumed to be from errors in the calculations but rather from errors in measuring the temperature. Actually measuring the temperature proved to be quite a challenge which is way Section 14.2 has been devoted to explaining the problems faced during this operation.

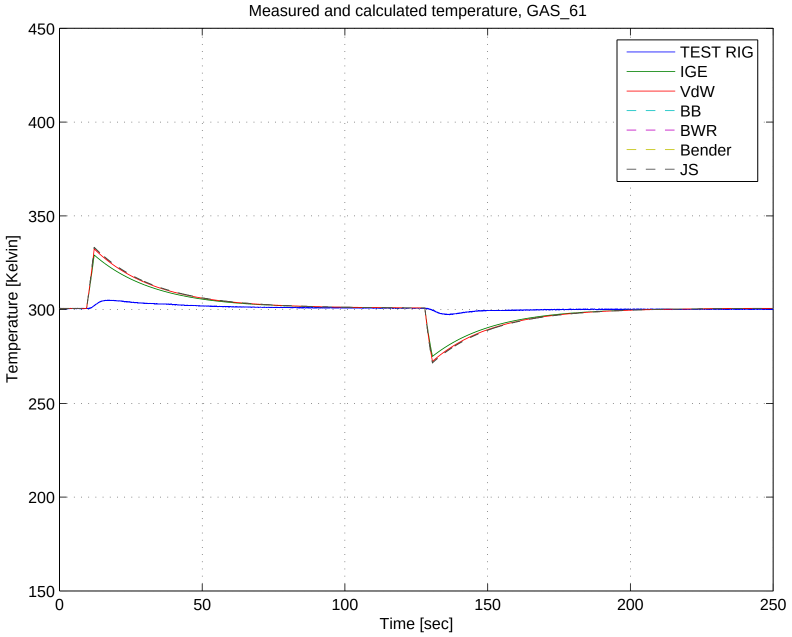

Figure 14.2: *Measured and calculated gas temperature using six equations of state for accumulator #2.*

14.2 Measuring the temperature

As seen in Figure 14.1 the measured temperature differs from the calculated. This was not expected as the pressure was quite accurate for the test run. And as the temperature calculations are based on the pressure models the same precision was expected. A conclusion could be that the approach was incorrect, but the formula presented in (8.16) has been validated by other sources. Therefore it is assumed that the method for measuring the temperature had some flaws. A study of this was therefore carried out. Two reasons for the errors in the measurement were found, both described in the following.

- The temperature probe is of the thermo coupler type (type T) made out of two different metals. The thermo coupler works in the way that when the metal gets colder or warmer it induces a small current. The current is measured by a temperature transmitter and amplified. The problem here is that the metal has to interact with the surroundings before it measures the temperature.
  In Figure 14.3 the thermo coupler used in the experiments are shown. The thermo coupler in question had a relatively large amount of metal touching each other which had to change temperature. It is assumed that there was not enough time to due this before the temperature of the surroundings had reached ambient temperature again. In Figure 14.1 it is seen that the peak temperature of more the 350 Kelvin only lasts for some few seconds. The optimal solution would be have a very small amount, e.g. the tip, touching.
- The second reason for not measuring the correct values should be found in the progress of heat or cooling the gas in the accumulator during an compression or expansion respectively. Rotthäuser has studied this and found that the temperature in the gas is not the same throughout the accumulator. An experiment has been performed showing that the temperature closes to the piston was the highest[Rotthäuser, 1993, Figure 6.2]. The result of the experiment is shown in Figure 14.4. The same conclusion has been reached during discussions with Peter Wind Rasmussen.

To verify the latter conclusion two test runs were performed where the accumulator was placed vertical with the thermo coupler up and down respectively. The measured temperature of the two test runs are depicted in Figure 14.5. The graph shows that a temperature difference along the accumulator must be present as

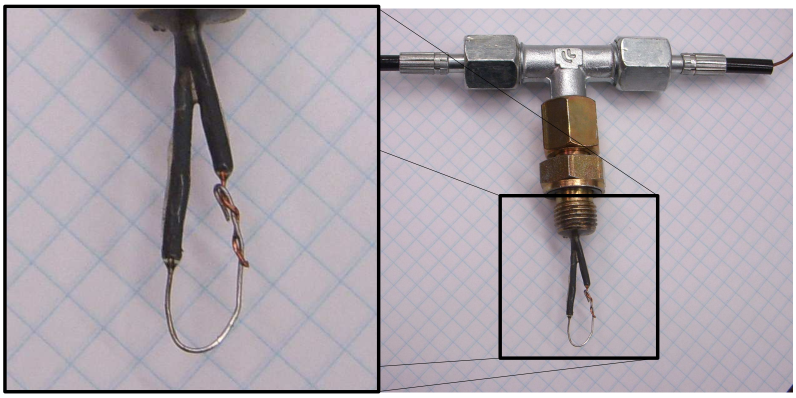

Figure 14.3: *Picture of the thermo coupler used to measure the gas temperature. Notice the large amount of metal that touches each other.*

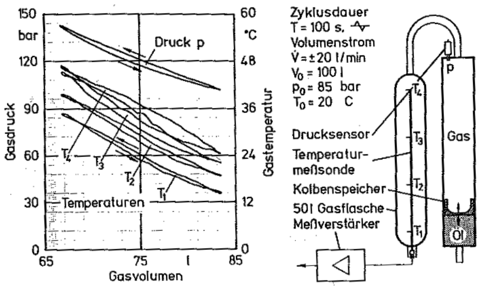

Figure 14.4: *Experiment performed to study the temperature in the gas during a cycle[Rotthäuser, 1993, Figure 6.2].*

the temperature raises more, when the thermo coupler is placed in the top. As the warm gas is raising it is expected to measure a higher temperature for the test run. The opposite is expected when the thermo coupler is placed in the bottom, namely that a lower temperature is measured. If the temperature was the same throughout the gas, the same temperature was to be measured.

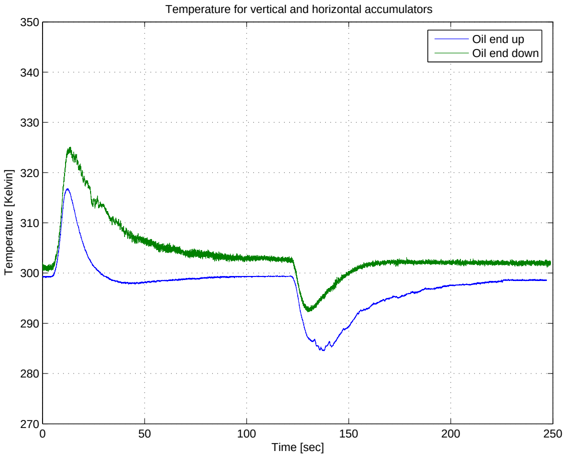

Figure 14.5: *Temperature measured when the accumulator was placed vertical with with the thermo coupler up and down respectively.*

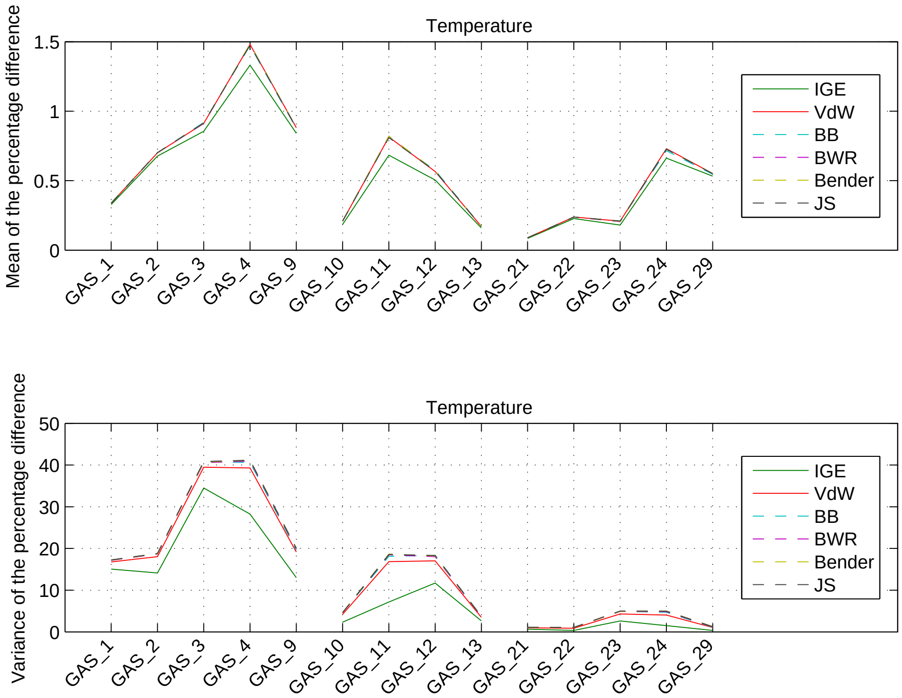

Figure 14.6: *Percentage-wise difference between measured an calculate gas temperature as a function of the measured temperature.*

14.3 Comparison with models

The difference between the measured and calculated temperature has been calculated in the same way as in Chapter 13. None of the results are to be found in the chapter but all graphs can be found in Appendix I.7. In figure 14.6 the results for accumulator #1 is depicted. The results show that no significant difference are to be found between the six models and that the most accurate results are obtained at the low ambient temperatures. This is assumed not to be correct based on two reasons:

- The equations for calculating the temperature are based on the pressure models. The pressure models has shown very accurate results.
- The formula used for calculating the temperature are used by other sources as well.

The findings must therefore be, that the results are not valid. This is backed up by simulations done by other sources with almost the same setup reaching approximately the same temperatures[Rupprecht, 1988, Figure 5.3]. It is therefore assumed that the simulations are correct. Since they are based on the pressure models, that the Van der Waals equation of state is valid for normal and warm ambient temperature and the Beattie-Bridgeman equation of state is valid for cold ambient temperatures.

14.4 Conclusion

To sum up the test runs the following conclusions can be drawn:

- No certain result are seen when comparing the measured temperature with the calculated. This is primarily because the test rig was not able to measure the correct temperature. Therefore no certain conclusions can be drawn regarding the accuracy of the six models.
- Since the formula used for calculating the temperature is used by other sources and since the calculations are based on the models for calculating the pressure, which have shown very accurate results. It is assume that the temperature models are showing equally accurate results.

As the same problems with accumulator #2 as presented in Chapter 13 are present, no conclusions will be drawn based on this data.

Conclusion

15

The objectives of the project have been to investigate the correlation between complexity and accuracy when calculating the gas pressure and temperature in a hydraulic accumulator for a number of real gas models.

To do so a literature review was carried out to identify any real gas models suitable for the project. In total five real gas models were identified together with the ideal gas equation. The five real gas models range in complexity from 4 to 32 constants.

To investigate the correlation, a non linear model of a test rig was developed. The non linear model consists of a mechanical model, a hydraulic model, a model to calculate the gas pressure and finally a model to calculate the gas temperature. The latter two were of primary interest of the project focus has therefore been on them. The first two models were not validated as they were considered relatively simple and not of high importance for the project.

The validation of the two gas models were done by performing a number of test runs on two different test rigs. The two test rigs varied in the size of the accumulator. All other equipment was kept the same. The first accumulator was the smallest and was named accumulator #1. This accumulator was made purpose-build and fitted with a position transducer. The largest accumulator, namely accumulator #2, was a standard off-the-shelf accumulator.

The test runs with the accumulator were performed under three different temperatures, namely normal ambient temperature (300 Kelvin), warm ambient temperature (350 Kelvin) (Only accumulator #1) and cold ambient temperature (260 Kelvin). The results were found by calculating the difference for each time step between the measured and calculated data. This was followed by finding the mean of the difference for each model. Furthermore the variance of the difference for each model was also determined.

During the experiments it was clear the measuring the gas temperature was more difficult than first assumed. Actually large differences were observed between the measured and calculated data with the measured data being of the lowest value. It is assumed that the differences are caused by unsuitable measuring equipment and not by inaccuracy in the models. Due to the differences in the data it has not been possible to draw clear conclusions for the gas temperature models, although nothing suggest that the models should differ from the gas pressure models.

During the experiments it was not possible to determine the position of the piston in accumulator #2. This is assumed to have caused some errors in the results for this accumulator. This means that no clear conclusions can be drawn for this accumulator. With this said, it should be mentioned that some clear tendencies in the results for accumulator #1 and accumulator #2 has been observed, namely the same difference in the accuracy of the models as function of the temperature. It is therefore assumed that the results for accumulator #1 are also valid for accumulator #2.

For accumulator #1 the following clear conclusions can be drawn:

- For normal and warm ambient temperature, the most accurate models are the ideal gas equation and the Van der Waals equation of state with the lowest mean value. But when studying the variance it is clear to see that the ideal gas equation has a variance many time larger the Van der Waals equation of state. This means that although the ideal gas equation in average might have the same accuracy as Van der Waals equation of state, it has significant large differences at some time steps. Therefore it must be concluded that for temperature ranging from some 300 Kelvin and to some 350 Kelvin the Van der Waals equation is the most accurate equation to use. As this is also the least complex equation of the five real gas models it makes sense to recommend to use this equation in future work.

- For cold ambient temperature the picture is slightly different. Here the ideal gas equation and the Van der Waals equation of state are the models with the highest mean differences. Instead the four most complex models are showing very accurate results with equal variance for all models. This leads to the conclusion that for cold ambient temperatures both Beattie-Bridgeman, Benedicte-Webb-Rubin, Jacobsen & Stewart and to some extend Bender equations of state are the most suitable. And with the Beattie-Bridgeman equation of state being the least complex it is recommended to use this equation in the future work.
- An interesting observation for all temperatures is that for the non-accurate models, the precharge pressure has a quite substantial effect of the accuracy. The accuracy drops with high precharge pressures. This goes for both Beattie-Bridgeman, Benedicte-Webb-Rubin, Jacobsen & Stewart and Bender equations of state at normal and warm ambient temperatures and for the ideal gas equation and the Van der Waals equation of state for cold ambient temperatures.

The project has therefore shown that it is not necessary to use very complex models to obtain accurate results when calculating the pressure in a hydraulic accumulator. The opposite has actually shown to be the case, namely that the least complexreal gas models resulted in the most accurate results. The above is valid for temperatures ranges from 260 Kelvin to 350 Kelvin, precharge pressures from 50 bar to 150 bar, maximum pressures of 250 bar and minimum pressures of 40 bar.

Bibliography

Henrik Alvarez. *Energi Teknik*. Studentlitteratur, 3. edition, 2006. ISBN: 91-44-04509-3.

Torben Ole Andersen and Michael Ryggard Hansen. *Fluid Power Systems*. 2. edition, March 2003. Institute of Energy Technology and Institute of Mechanical Engineering, Aalborg University.

James A. Beattie and Oscar C. Bridgeman. A new equation of state for fluids. ii. application to helium, neon, argon, hydrogen, nitrogen, oxygen, air and methane. *The Journal of the American Chemical Society*, 50 (2):3133–3138, 1928.

Yunus A. Cengel and Robert H. Turner. *Thermal-Fluid Sciences*. McGraw-Hill, international edition, 2001. ISBN: 0-07-118152-0.

James M. Gere. *Mechanics of Materials*. Nelson Thorness, 5. edition, 2001. ISBN: 0-7487-6675-8.

J. Ghazouani, O. Chouaieb, and A. Bellagi. Evaluation of the parameters of the bender equation of state for low acentric factor fluids and carbon dioxide. *Thermochimica Acta*, 432(1):10–19, 2005.

K. Ogata. *Modern Control Engineering*. Prentice Hall, 4. edition, 2001. ISBN: 0-13-043245-8.

D. R. Otis. New development in predicting and modifying performance of hydraulic accumulators. *Proceedings of the National Conference on Fluid Power*, 28:473–489, 1974.

A. Polt and G. Maurer. The bender equation of state for describing thermodynamic properties of krypton, neon, fluorine, sulfur dioxide and water over a wide range of state. *Fluid Phase Equilibria*, 73:27–38, 1992.

A. Pourmovahed. Sizing energy storage units for hydraulic hybrid vehicle applications. *American Society of Mechanical Engineers, Dynamic Systems and Control Division (Publication) DSC*, 52:231–246, 1993.

A. Pourmovahed and D. R. Otis. An algoritm for computing nonflow gas processes in gas springs and hydropneumatic accumulators. *Journal of Dynamic Systems, Measurement and Control*, 107:93–96, 1985.

A. Pourmovahed and D. R. Otis. An experimental thermal time-constant correlation for hydraulic accumulators. *Journal of Dynamic Systems, Measurement and Control*, 112:116–121, 1990.

Peter Windfeld Rasmussen, 2009. Systems Engineer, Fritz Schur Teknik. Interview carried out October 7th.

E. Dam Ravn. *Bogen om operationsforstærkere*. Clausen bøger, 1. edition, 1980. ISBN: 87-11-03783-0.

Siegfried Rotthäuser. *Verfahren zur Berechnung und Untersuchung hydropneumatischer Speicher*. PhD thesis, Rheinisch-Westfälischen Technischen Hochschule Aachen, January 1993. The reference is consider valid based as it is a Ph.D. thesis.

Karl-Rudolf Rupprecht. *Hydroospeicher - Experimentelle Und Analytische Untersuchungen zur Energispeicherung*. PhD thesis, Rheinisch-Westfälischen Technischen Hochschule Aachen, February 1988. The reference is consider valid based as it is a Ph.D. thesis.

R. Sandri. An empirical equation of state for gases. *The Canadian Journal of Chemical Engineering*, 51: 259–261, 1973.

R. B. Stewart and R. T. Jacobsen. The determination of equations of state for nitrogen and oxygen. *Cryogenics*, 13(9):526–534, 1973.

Torsten Thurén. *Videnskabsteori for begyndere*. Rosinante, 1. edition, 2006. ISBN-13: 978-87-7357-657-1.

Ronald E. Walpole, Raymond H. Myers, Sharon L. Myers, and Keying Ye. *Probability & Statistics for Engineers & Scientists*. Pearson Education International, 7. edition, 2002. ISBN: 0-13-098469-8.

Test rig

A

This chapter will present the test rig used in the project.

The test rig is built to test hydraulic accumulators of variable sizes. The test rig consists of two systems, namely:

- The hydraulic system
- The electrical system

The hydraulic system consists of all the hydraulic components as described in Section A.1 and the system is modeled in Chapter 5. The electrical system is used to feed the system with a signal, to control the system and to measure different variables in the system, all described in Section A.2. In Figure A.1 is shown a photo of the test rig. Please note that part of the system may be placed in other locations to obtain other temperature conditions. If so, this is explained in the experimental report.

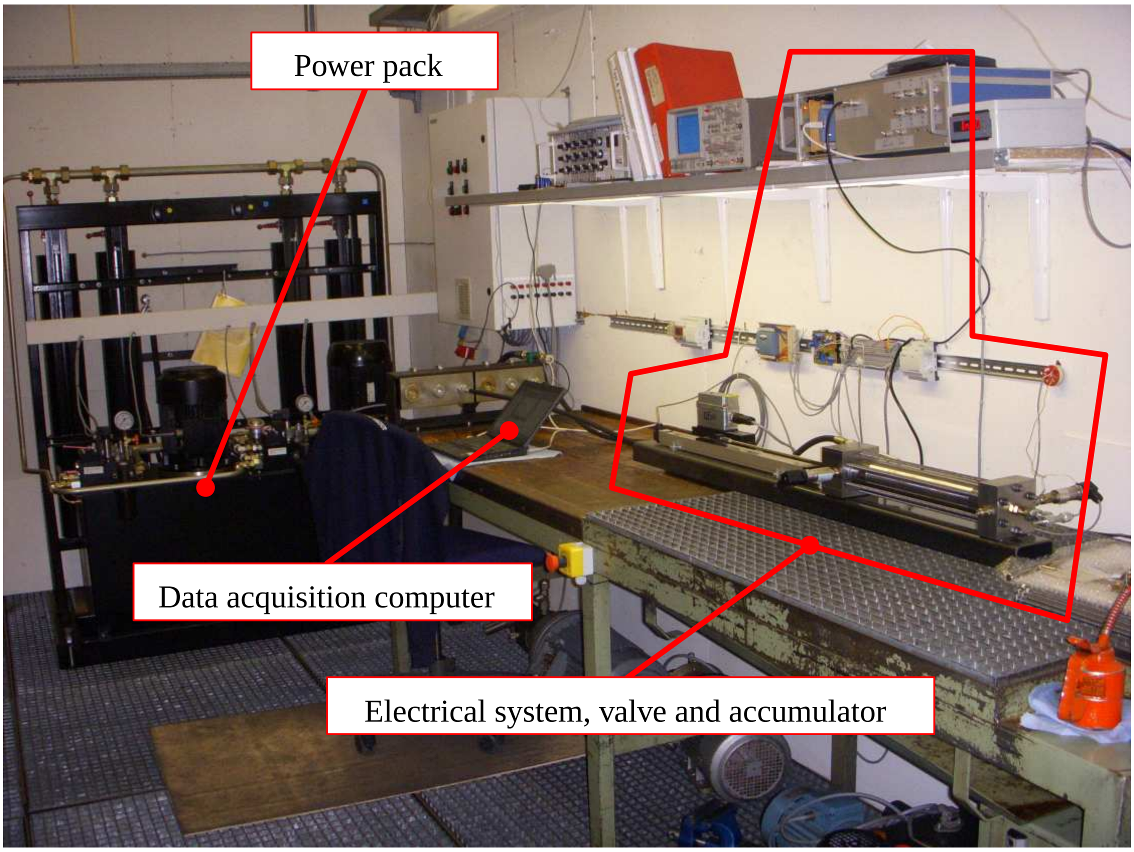

Figure A.1: *Photo of the test rig*

Pictures and video clips of the test rig and all components can be found on the attached CD.

A.1 Hydraulic system

In Figure A.2 the hydraulic diagram is shown for the system. The system consists of a number of components all presented in the following.

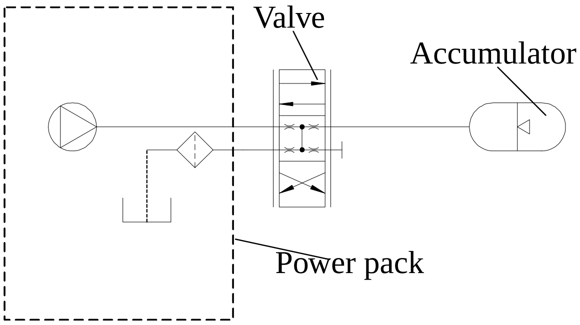

Figure A.2: *The hydraulic diagram showing the components of the system*

A.1.1 Valve

To control the flow volume and the direction of the flow, a valve is fitted in the system. The valve used is a direct operated proportional DC valve produced by Parker with Ordering Code D1FPE50HB9NB00 13. Data sheet is to be found in Appendix N.2. The valve has a nominal flow of Q_{nom} = 25 l/min = 416 $\cdot 10^{-6}$ m^3/sec, a nominal pressure of p_{nom} = 350 bar and a nominal signal voltage of U_{nom} = $\pm$10 V.

A.1.2 Accumulator

A number of different accumulators are used in the project. They will be presented in the following.

Accumulator #1

The first accumulator used is a piston type accumulator made of steel. Please refer to Appendix N.3 for data sheet of the accumulator. The accumulator has a volume of 0.6 liters. The piston is connected to a rod used for determining the position. In Figure A.3 a sketch of the setup is shown.

Accumulator #2

The second accumulator is also of the piston type made of steel. The accumulator is a HYDROLL HPS type-11 with a volume of 6 liters. The accumulator has no positioning system. Please refer to Appendix N.4 for data sheet of the accumulator.

A.1.3 Power pack

The power pack delivers the hydraulic oil to the system. The power pack is fitted with a pump and up to four accumulators. The pressure of the power pack can be adjusted via the PLC controlling the power pack.

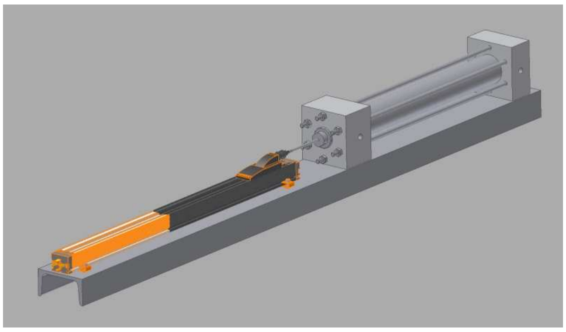

Figure A.3: *Drawing of the accumulator with the position transducer*

It can deliver a pressure of up to 250 bar. The power pack is also fitted with a tank to store the hydraulic oil. The pressure of the tank is p_{tank} = 1 atm as the tank is not sealed.

A.2 The electric system

As mentioned in the introduction, the purposes of the electrical system are to feed the system with a reference signal, to control the system and to measure different variables in the system. In Figure A.4 the electrical system is sketched. In the following all three purposes will be explained.

A.2.1 Reference signal system

The signal to the system is produced using a computer connected to an analog and digital I/O module via USB. The module is a USB-1208FS produced by Measurement Computing, please see Appendix N.1 for data sheet. The computer is using a software named VisSim produced by Visual Solutions. The software can communicate with the I/O module. In the software a digital signal is produced, e.g. a sinus curve, which is transferred to the I/O module via USB where the digital signal is converted to a analog signal and outputted via a specified output port. A program has been developed to produce the signal. The program code can be seen in Appendix J. The signal is sent to an amplifier where the signal is given an offset and amplified. The offset has been applied because the output of the position transducer is a $\pm$-signal and the reference signal therefore has to suit this. The amplifier has been fitted with a capacitor to reduce the noise in the reference signal. The capacitor has been fitted as sketched in Figure A.5.

The capacitor has been designed using[Ravn, 1980, page 45]

$$C2 = \frac{0.1125}{f \cdot R2} \tag{A.1}$$

where f is the cutoff frequency. Setting this to 100 Hz the equation yields $C2$ = 22.5 nF. A capacitor of 22 nF has been fitted. Please refer to Figure A.4 for wiring between the computer, the I/O module and the regulator.

A.2.2 Control system

As mentioned in Chapter 9 the valve will be controlled using a closed loop system measuring the position of the piston in the accumulator. To do this, a P-regulator has been fitted the system. The regulator is measuring

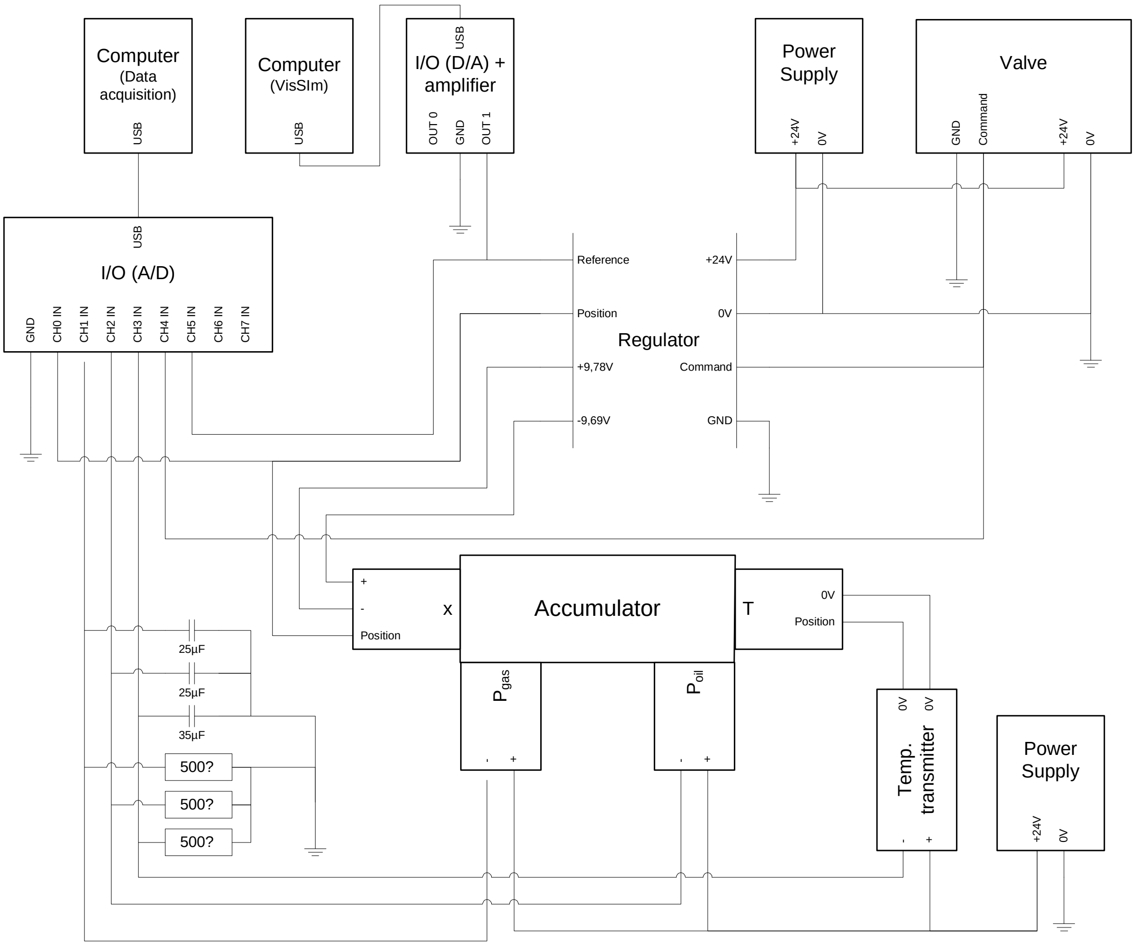

Figure A.4: *Sketch of the electrical system.*

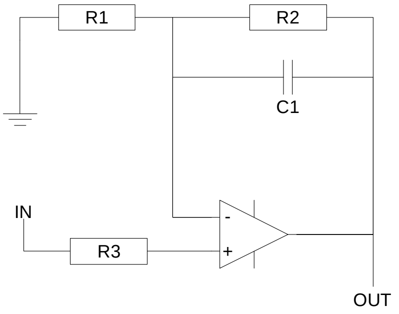

Figure A.5: *Sketch of placement of capasitor in reference signal amplifier*

the position of the piston and compares it with the reference signal from the computer. The error between the reference and the position is multiplied with a factor of 13.5 and the signal is then sent to the valve. In Figure A.6 the block diagram of this is shown. Please refer to Figure A.4 for wiring to the regulator. The regulator is equipped with a power supply producing +9.78V and -9.69V used for the position transducer.

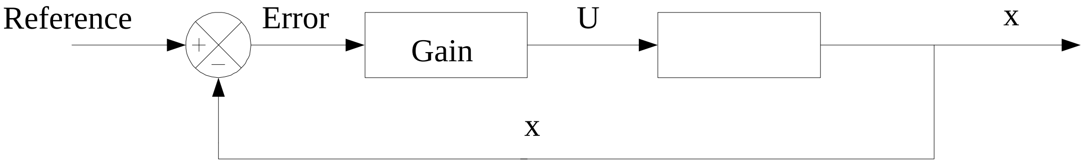

Figure A.6: *Block diagram of the closed loop system to control the valve*

A.2.3 Measuring system

In the following all hardware used to measure the data is described. To transfer the data from the measuring devises, an I/O module of the same type as mentioned in Section A.2.1 is used. The module converts the analog signal to a digital signal and transfers it via USB to a computer. The computer is using a software named MatLab produced by MathWorks to read the digital signals and convert them into data that can be read and stored. A program has been developed to do this. The program code can be seen in Appendix K. In the following it is explained how each variable is measured including any hardware used to do the measuring. Please refer to Figure A.4 for wiring between measuring equipment, the I/O module and other hardware.

Piston position, x

The position of the accumulator piston is measured using a position transducer connected to the piston via a ø5 mm rod. The transducer is a TLH500 made by NovoTechnik, please see Appendix N.5 for data sheet. The transducer is supplied by the regulator and the position signal is connected to CH0 IN in the I/O (A/D) module. Please note that this system is only installed on accumulator #1.

Gas pressure, P_{gas}

The gas pressure in the accumulator is measured using a pressure transducer connected to the gas side of the accumulator. The transducer is a 1600BGC4001G3UA made by GemsSensors, please see Appendix N.6 for data sheet. The transducer can measure from 0 bar to 400 bar. The transducer is supplied by a 24V power supply and the signal is connected to CH1 IN in the I/O (A/D) module. The signal output from the transducer is 4 - 20 mA. This is converted to 2 - 10 V with a 500Ω resistance. To reduce noise the signal has been fitted with a capacitor on 25μF as shown on Figure A.4.

Oil pressure, P_{oil}

The oil pressure in the accumulator is measured using a pressure transducer connected to the oil side of the accumulator. The transducer is a 1600BGC4001G3UA made by GemsSensors, please see Appendix N.6 for data sheet. The transducer can measure from $0bar$ to $400bar$. The transducer is supplied by a 24V power supply and the signal is connected to CH2 IN in the I/O (A/D) module. The signal output from the transducer is $4-20mA$. This is converted to $2-10V$ with a 500Ω resistance. To reduce noise the signal has been fitted with a capacitor on 25μF as shown on Figure A.4.

Gas temperature, T

The temperature of the gas is measured using a type T temperature probe. The signal is amplified using a TMRO temperature transmitter from Müller Industrie - Elektronik Gmbh. Please see Appendix N.7 for data sheet. The transmitter has been selected among many others based on its low response time ($\tilde{1}$ ms). Please refer to Section 14.2 for more details about how the temperature has been measured and any sources of error. The output of the amplifier is connected to CH3 IN in the I/O (A/D) module.

Command signal, U_c

The command signal to the valve is measured by connecting the wire to CH4 IN in the I/O (A/D) module.

Reference signal, Ref

The reference signal is measured by connecting the wire to CH5 IN in the I/O (A/D) module.

A.3 Temperature controlling

A number of test runs are to be made at different temperatures. In the following is will be explained how the different temperatures has been reached.

A.3.1 Normal ambient temperature

Normal ambient temperature has been reached by have the test rig placed in a room with approximately 300 Kelvin. See Figure A.7.

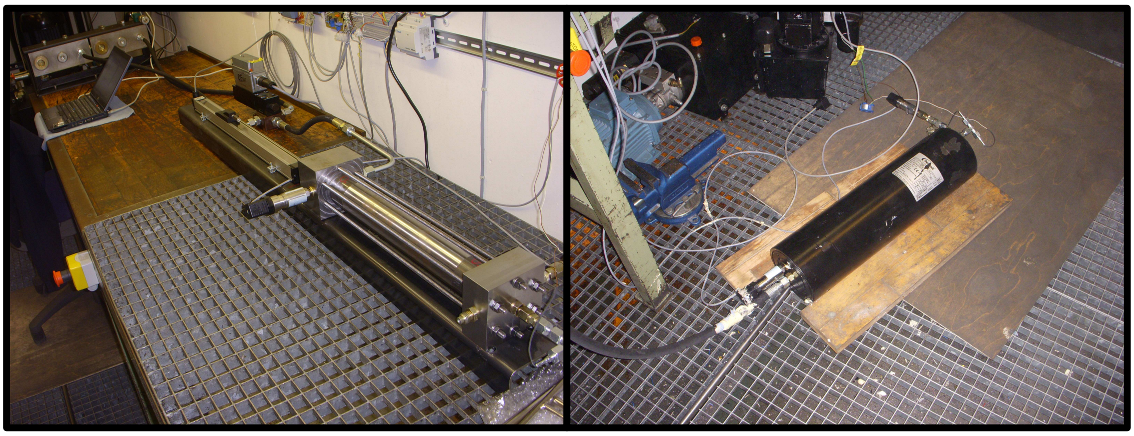

Figure A.7: *Picture of the two accumulators at normal ambient temperature. LEFT: Accumulator #1. RIGHT: Accumulator #2.*

A.3.2 Warm ambient temperature

Only accumulator #1 has been tested in warm ambient temperature. The warm temperature has been reached by heat the accumulator and the air around it with a hand held fan heater. The temperature has reached approximately 350 Kelvin.

A.3.3 Cold ambient temperature

both accumulators has been tested in cold ambient temperature. This has been done by placing the accumulator in a freezer with dry ice in the bottom. The reason for doing so, is that the majority of the electronic equipment still are in normal ambient temperature and are therefore not affected by the cold temperatures. The temperature has reached approximately 260 Kelvin. See figure Figure A.8.

Figure A.8: *Pictures of the two accumulators at cold ambient temperature with dry ice in the bottom of the freezer. LEFT: Accumulator #1. RIGHT: Accumulator #2.*

Implementing the non-linear model in SIMULINK

B

B.1 Hydraulic and mechanical models

B.1.1 Mechanical

In Figure B.1 the system is depicted as modeled in SIMULINK. The model is representing (6.2) added two additional blocks. The two blocks will be described shortly. In the model depicted is also implemented two integrators with initials conditions and saturation limits as listed in Table B.1

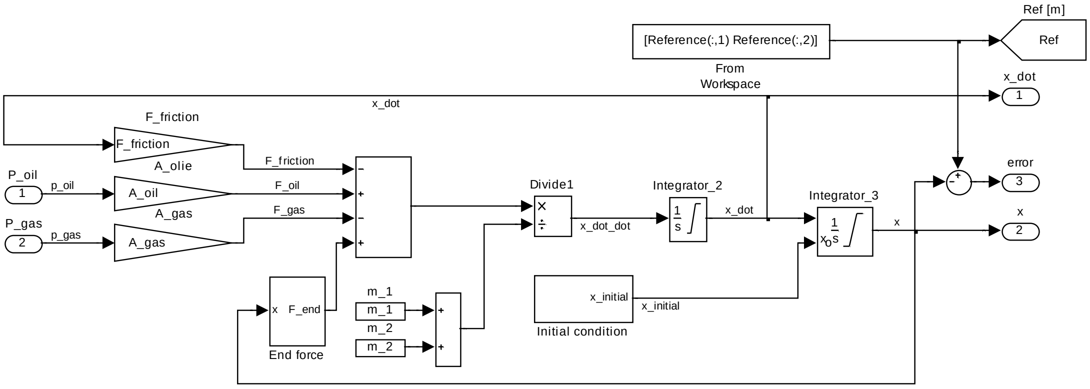

Figure B.1: *SIMULINK model of the mechanical part*

	Integrator 1	Integrator 2
Initial condition	0	$x_{initial}$
Upper saturation limit	∞	Cyl_{length}
Lower saturation limit	$-\infty$	0

Table B.1: *Initial conditions and saturation limits for Integrator 1 and Integrator 2.*

The first block is named *Initial Position* and calculates the initial position of the piston based on P_{oil} and P_{gas}. The block is depicted in Figure B.2. The block solves (6.2) equal zero with respect to x and outputs the result as $x_{initial}$.

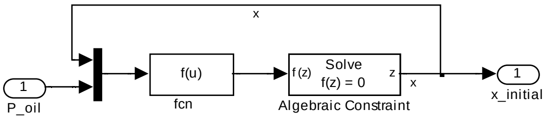

Figure B.2: *SIMULINK model of block to calculate the initial position of piston*

The second block named *End force* applies a force on the piston to make sure, that it does not move further back than $x = 0$, which is at the end of the accumulator. The force is applied by a spring with a large spring constant and is only applied over a short distance, in this case $0.2mm$. The force is calculated using[Gere, 2001, (2-1,a)]

$$F_{end} = k\delta \qquad\qquad 0[m] \leq x \leq 0.002[m] \tag{B.1}$$

where k is the spring constant and δ is the length, the spring is compressed. The spring constant is variable and is being calculated for each test run. The spring constant is a function of the precharge pressure, $P_{gas,precharge}$, as described in (B.2). Tests have gives that this correlation shown good results.

$$k = \frac{A_{gas} \cdot P_{gas,precharge}}{0.002[m]} \tag{B.2}$$

The End force block is depicted in Figure B.3.

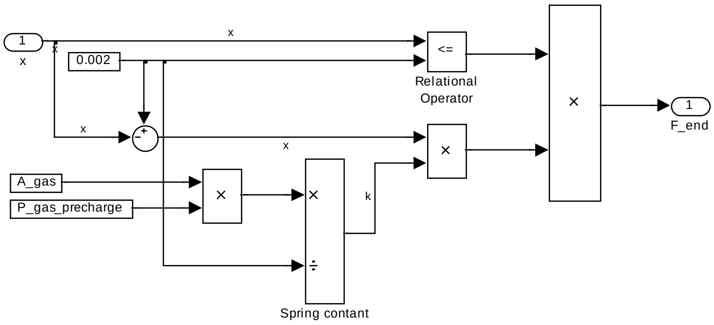

Figure B.3: *SIMULINK model of block to calculate the end wall force acting on the piston at* $P_{gas} > P_{oil}$ *and* $x = 0$.

B.1.2 Dynamic of the valve

The dynamic of the valve is implemented in the system using a Transfer Function Block which is multiplied with the signal voltage. The signal voltage equals x_{error}, when a closed loop system measuring the piston position, x, is used. (Please see Section 9.1 for explanation about why x is used). The following MATLAB code has been used in the block:

```
Omega_n        =   350*2*pi;                          %[rad/s]
Zeta           =   0.701;                             %[-]
num            =   [1];
den            =   [1/(Omega_n)^2 (2*Zeta)/Omega_n 1];
```

The output is feed to the next block calculating the flow, see section Section 6.1.3. The model can be seen in Figure B.4.

B.1.3 Flow through the valve

A number of things have been done to implement (6.12) in SIMULINK. Since the calculation of ΔP depends on whether the oil flows in or out of the accumulator, two logical operators have been used to

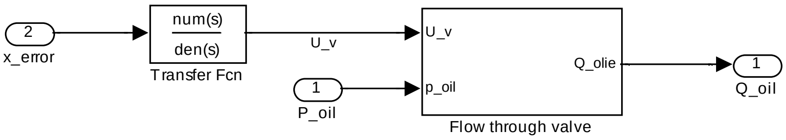

Figure B.4: *SIMULINK model of the valve dynamic*

	Logical operator 1	Logical operator 2
If	$U_v >= 0V$	$U_v < 0V$
Then	$\Delta P = P_s - P_{oil}$	$\Delta P = P_{oil} - P_{tank}$

Table B.2: *Rules of the logical operators.*

make sure that the correct calculation is performed. The logical operator is control by the voltage, U_v with a threshold of $0V$. The logical operators trigger the operations listed in Table B.2.

Calculating (6.14) has been done by implementing an Embedded MATLAB function with the following code

```
function K = fcn(p_nom,U_v)

p1              =   1.711e-008;
p2              =   -6.2408e-007;
p3              =   4.7339e-006;
p4              =   3.9433e-005;

U_1 = abs(U_v);

K = (p1*U_1^4 + p2*U_1^3 + p3*U_1^2 + p4*U_1)/(p_nom^0.5)*sign(U_v);
```

First the absolute value of input voltage is taken and used in the expression for K. K is then multiplied with the sign of the input voltage. This to make sure that K has the right sign.

In Figure B.5 the system is depicted as modeled in SIMULINK.

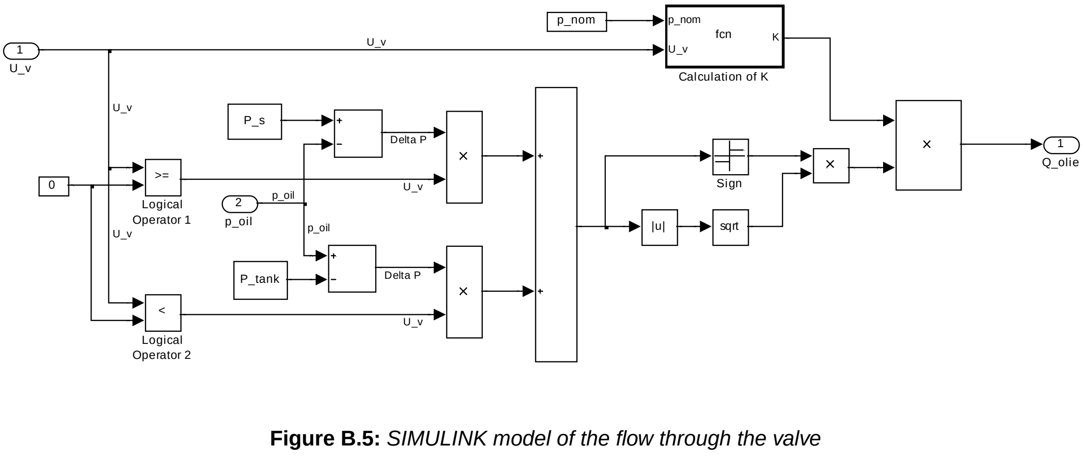

Figure B.5: *SIMULINK model of the flow through the valve*

B.1.4 Oil pressure

In Figure B.6 the system is depicted as modeled in SIMULINK. To do the integration a limit integrator has been used with settings as listed in Table B.3

	Integrator 1
Initial condition	$P_{oil,initial}$
Upper saturation limit	∞
Lower saturation limit	0

Table B.3: *Initial conditions and saturation limits for Integrator 3.*

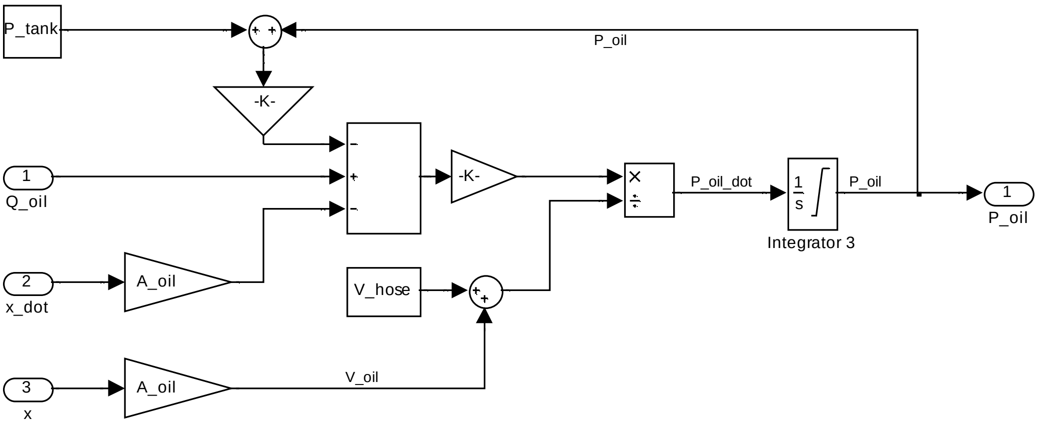

Figure B.6: *SIMULINK model of the hydraulic side of the accumulator*

B.2 Gas pressure model

B.2.1 Ideal gas equation

(7.1) is depicted in Figure B.7 as modeled in SIMULINK together with the derivative of P.

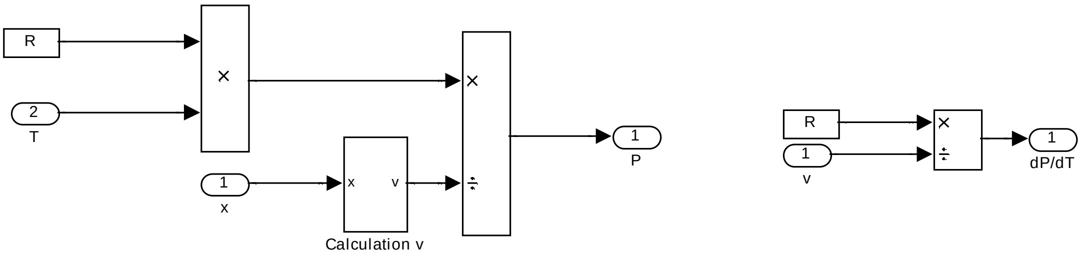

Figure B.7: *LEFT: SIMULINK model of the ideal gas equation of state. RIGHT: SIMULINK model of the derivative of ideal gas equation of state with respect to T.*

B.2.2 Ideal gas equation including compressibility factor (IGEcomp)

In Figure B.8 (7.6) is depicted as modeled in SIMULINK together with the derivative of P.

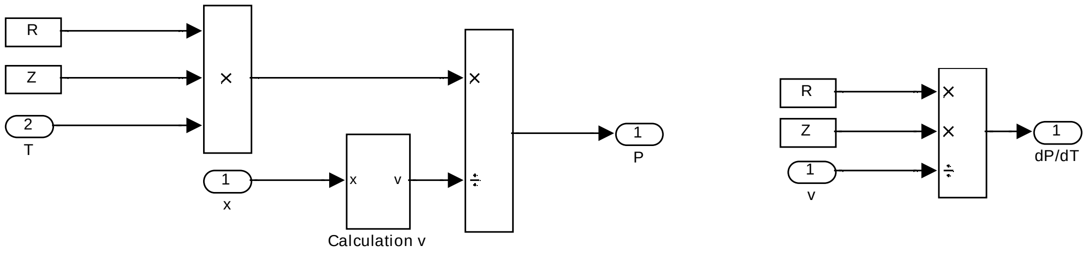

Figure B.8: *LEFT: SIMULINK model of the ideal gas equation of state with compressibility factor. RIGHT: SIMULINK model of the derivative of ideal gas equation of state with compressibility factor with respect to T.*

B.2.3 Van der Waals

(7.9) has been implemented using an embedded MATLAB function with the following code

```
function p = fcn(R,T,v)

T_cr    =   126.2;                      %[K]
P_cr    =   3.39e6;                     %[Pa]
a       =   27*R^2*T_cr^2/(64*P_cr);    %[Pa*m^6/kg^2]
b       =   R*T_cr/(8*P_cr);            %[m^3/kg]

p = (R*T)/(v-b) - (a/(v^2));
```

while the derivative of P has been implemented using the following code in an embedded MATLAB function.

```
function dp = fcn(v,R)

T_cr    =   126.2;              %[K]
P_cr    =   3.39e6;             %[Pa]
b       =   R*T_cr/(8*P_cr);    %[m^3/kg]

dp = R/(v-b);
```

B.2.4 Beattie-Bridgeman (BB)

(7.15) has been implemented using an embedded MATLAB function with the following code

```
function p = fcn(R_u,T,v)

a     =   0.02617;
b     =   -0.00691;
c     =   4.20e4;
A_0   =   136.2315;
B_0   =   0.05046;
```

```
A     =   A_0 * (1 - a/v);
B     =   B_0 * (1 - b/v);

P = ((R_u*T/v^2)*(1 - c/(T^3*v))*(v+B) - (A/(v^2)))*1000;
```

The result is multiplied with 1,000 to get the result in Pa. The derivative of P has been implemented using the following code in an embedded MATLAB function.

```
function dp = fcn(R_u,v,T)

b     =   -0.00691;
c     =   4.20e4;
B_0   =   0.05046;

B     =   B_0 * (1 - b/v);

dp = (R_u*(T^3*v + 2*c)*(v+B))/(T^3*v^3)*1000;
```

The result is multiplied with 1,000 to get the result in Pa.

B.2.5 Benedicte-Webb-Rubin (BWR)

(7.18) has been implemented using an embedded MATLAB function with the following code

```
function p = fcn(T,R_u,v)

a       =   2.54;
b       =   0.002328;
c       =   7.379e4;
A_0     =   106.73;
B_0     =   0.04074;
C_0     =   8.164e5;
alpha   =   1.272e-4;
gamme   =   0.0053;

p = (R_u*T/v + (B_0*R_u*T - A_0 - C_0/T^2)*1/v^2 + (b*R_u*T - a)/v^3
      + a*alpha/v^6 + c/(v^3*T^2)*(1 + gamma/v^2)*exp(-gamma/v^2))*1000;
```

The result is multiplied with 1,000 to get the result in Pa. The derivative of P has been implemented using the following code in an embedded MATLAB function.

```
function dp = fcn(v,T,R_u)

b       =   0.002328;
c       =   7.379e4;
A_0     =   106.73;
B_0     =   0.04074;
C_0     =   8.164e5;
gamma   =   0.0053;

dp = ((R_u/v) + ((B_0*R_u + 2*C_0/T^3)/v^2) + (b*R_u/v^3)
      - 2*c/(v^3)/(T^3)*(1 + gamma/(v^2))*exp(-gamma/(v^2)))*1000;
```

The result is multiplied with 1,000 to get the result in Pa.

B.2.6 Bender

(7.20) has been implemented using an embedded MATLAB function with the following code

```
function p_gas = fcn(R,T,v)

v_cr    =   0.003209;           %[m^3/kg]
T_cr    =   126.2;              %[Kelvin]

omega   =   v_cr/v;
tau     =   T_cr/T;
alpha   =   -0.9641;

B       =   [5.1564398e-1 -1.2350862 -3.3660701e-2 -4.3693391e-1 6.1598645e-2
             5.2599330e-2 2.0756488e-1 2.0273530e-1 2.3974975e-1 -4.7905077e-1
             -2.7239453e-2 1.2113829e-1 1.2924526e-1 -3.2495834e-1 5.3924336e-1
             -2.0692385e-1 -1.5625825e-1 5.2222667e-1 -3.8027769e-2];

Y       =   omega*[1 tau tau^2 tau^3 tau^4 omega omega*tau omega*tau^2 omega^2
             omega^2*tau omega^3 omega^3*tau omega^4*tau
             omega*tau^3*exp(alpha*omega^2) omega*tau^4*exp(alpha*omega^2)
             omega*tau^5*exp(alpha*omega^2) omega^3*tau^3*exp(alpha*omega^2)
             omega^3*tau^4*exp(alpha*omega^2) omega^3*tau^5*exp(alpha*omega^2)];

p       =   1:19;

for i=1:19;
P(i)    =   B(i)*Y(i);
i       =   i+1;
end;

p_gas = (R*T/v)*(1 + sum(P));
```

The derivative of P has been implemented using the following code in an embedded MATLAB function.

```
function dp = fcn(R,T,v)

v_cr    =   0.003209;           %[m^3/kg]
T_cr    =   126.2;              %[Kelvin]

omega   =   v_cr/v;
tau     =   T_cr/T;
alpha   =   -0.9641;

B       =   [5.1564398e-1 -1.2350862 -3.3660701e-2 -4.3693391e-1 6.1598645e-2
             5.2599330e-2 2.0756488e-1 2.0273530e-1 2.3974975e-1 -4.7905077e-1
             -2.7239453e-2 1.2113829e-1 1.2924526e-1 -3.2495834e-1 5.3924336e-1
             -2.0692385e-1 -1.5625825e-1 5.2222667e-1 -3.8027769e-2];

dp = -R/T^5*(-T^5 - B(1)*omega*T^5 - B(6)*omega^2*T^5 - B(9)*omega^3*T ^ 5
       - B(11)*omega^4*T^5 + 4*B(16)*omega^2*T_cr^5*exp(alpha*omega^2)
       + 4*B(19)*omega^4*T_cr^5*exp(alpha*omega^2) + B(3)*omega*T_cr^2*T^3
       + 2*B(4)*omega*T_cr^3*T^2 + 3*B(5)*omega*T_cr^4*T
       + B(8)*omega^2*T_cr^2*T^3
       + 2*B(14)*omega^2*T_cr^3*exp(alpha*omega^2)*T^2
       + 3*B(15)*omega^2*T_cr^4*exp(alpha*omega^2)*T
       + 2*B(17)*omega^4*T_cr^3*exp(alpha*omega^2)*T^2
       + 3*B(18)*omega^4*T_cr^4*exp(alpha*omega^2)*T)/v;
```

B.2.7 Jacobsen & Stewart (JS)

(7.27) has been implemented using an embedded MATLAB function with the following code

```
function p_gas = fcn(R,T,v)

v_cr    =   0.003209;           %[m^3/kg]
T_cr    =   126.2;              %[Kelvin]

omega   =   v_cr/v;
tau     =   T_cr/T;
alpha   =   -0.70371896;

N       =   [0.185927462121 1.30155934655 -2.64054394027 0.292709245322
             -0.287482987766 0.161225592835 -0.135129830972 0.0000137262707287
             13.6860808703 0.00128973300860 0.315240491447 -0.548670430729
             0.0744966916902 -0.151712926147 -0.728119881405 0.112790673192
             -0.0187922799332 0.0460360632178 -0.00251321896106 -12.5428246147
             -0.722843603762 -9.07779852949 0.333590008958 -2.10175282124
             -0.244752749620 -0.611651799016 -0.0244254052253 -0.0230295508018
             0.0157620487302 -0.0126428070667 -0.00146576723582 0.0000915063203408];

Y       =   omega*[1 tau^0.5 tau tau^2 tau^3 omega omega*tau omega*tau^2
             omega*tau^3 omega^2 omega^2*tau omega^2*tau^2 omega^3*tau
             omega^4*tau^2 omega^4*tau^3 omega^5*tau^2 omega^6*tau^2
             omega^6*tau^3 omega^7*tau^3 omega*tau^3*exp(alpha*omega^2)
             omega*tau^4*exp(alpha*omega^2) omega^3*tau^3*exp(alpha*omega^2)
             omega^3*tau^5*exp(alpha*omega^2) omega^5*tau^3*exp(alpha*omega^2)
             omega^5*tau^4*exp(alpha*omega^2) omega^7*tau^3*exp(alpha*omega^2)
             omega^7*tau^5*exp(alpha*omega^2) omega^9*tau^3*exp(alpha*omega^2)
             omega^9*tau^4*exp(alpha*omega^2) omega^11*tau^3*exp(alpha*omega^2)
             omega^11*tau^4*exp(alpha*omega^2) omega^11*tau^5*exp(alpha*omega^2)];

p       =   1:32;

for i=1:32;
P(i)    =   N(i)*Y(i);
i       =   i+1;
end;

p_gas = (R*T/v)*(1 + sum(P));
```

The derivative of P has been implemented using the following code in an embedded MATLAB function.

```
function dp = fcn(R,T,v)

v_cr    =   0.003209;           %[m^3/kg]
T_cr    =   126.2;              %[Kelvin]

omega   =   v_cr/v;
tau     =   T_cr/T;
alpha   =   -0.70371896;

N       =   [0.185927462121 1.30155934655 -2.64054394027 0.292709245322
             -0.287482987766 0.161225592835 -0.135129830972 0.0000137262707287
             13.6860808703 0.00128973300860 0.315240491447 -0.548670430729
             0.0744966916902 -0.151712926147 -0.728119881405 0.112790673192
             -0.0187922799332 0.0460360632178 -0.00251321896106 -12.5428246147
             -0.722843603762 -9.07779852949 0.333590008958 -2.10175282124
             -0.244752749620 -0.611651799016 -0.0244254052253 -0.0230295508018
             0.0157620487302 -0.0126428070667 -0.00146576723582 0.0000915063203408];

dp      =   -0.5*(-1*N(2)*omega*T_cr*T^4 + 2*N(14)*omega^5*T_cr^2*T^3*sqrt(T_cr/T)
             + 6*N(29)*omega^10*T_cr^4*exp(alpha*omega^2)*T*sqrt(T_cr/T)
             + 4*N(30)*omega^12*T_cr^3*exp(alpha*omega^2)*T^2*sqrt(T_cr/T)
             + 4*N(28)*omega^10*T_cr^3*exp(alpha*omega^2)*T^2*sqrt(T_cr/T)
             + 4*N(20)*omega^2*T_cr^3*exp(alpha*omega^2)*T^2*sqrt(T_cr/T)
             + 6*N(25)*omega^6*T_cr^4 *exp(alpha*omega^2)*T*sqrt(T_cr/T)
             + 4*N(22)*omega^4*T_cr^3*exp(alpha*omega^2)*T^2*sqrt(T_cr/T)
             + 6*N(21)*omega^2*T_cr^4*exp(alpha*omega^2)*T*sqrt(T_cr/T)
             + 6*N(31)*omega^12*T_cr^4*exp(alpha*omega^2)*T*sqrt(T_cr/T)
```

```
+ 4*N(26)*omega^8*T_cr^3*exp(alpha*omega^2)*T^2*sqrt(T_cr/T)
+ 2*N(17)*omega^7*T_cr^2*T^3*sqrt(T_cr/T)
+ 2*N(12)*omega^3*T_cr^2*T^3*sqrt(T_cr/T)
+ 8*N(32)*omega^12*T_cr^5*exp(alpha*omega^2)*sqrt(T_cr/T)
+ 8*N(23)*omega^4*T_cr^5*exp(alpha*omega^2)*sqrt(T_cr/T)
+ 8*N(27)*omega^8*T_cr^5*exp(alpha*omega^2)*sqrt(T_cr/T)
+ 4*N(5)*omega*T_cr^3*T^2*sqrt(T_cr/T)
+ 2*N(8)*omega^2*T_cr^2*T^3*sqrt(T_cr/T)
+ 4*N(24)*omega^6*T_cr^3*exp(alpha*omega^2)*T^2*sqrt(T_cr/T)
+ 4*N(15)*omega^5*T_cr^3*T^2*sqrt(T_cr/T)
+ 4*N(9)*omega^2*T_cr^3*T^2*sqrt(T_cr/T)
+ 2*N(4)*omega*T_cr^2*T^3*sqrt(T_cr/T)
+ 4*N(18)*omega^7*T_cr^3*T^2*sqrt(T_cr/T)
+ 2*N(16)*omega^6*T_cr^2*T^3*sqrt(T_cr/T)
+ 4*N(19)*omega^8*T_cr^3*T^2*sqrt(T_cr/T)
- 2*N(6)*omega^2*T^5*sqrt(T_cr/T) - 2*N(10)*omega^3*T^5*sqrt(T_cr/T)
- 2*N(1)*omega*T^5*sqrt(T_cr/T)
- 2*T^5*sqrt(T_cr/T))*R*(T_cr/T)^(-1/2)/T^5/v;
```

B.3 Gas temperature model

B.3.1 Temperature of gas side

In Figure B.9 the system is depicted as modeled in SIMULINK. This model uses a number of blocks to calculate the specific heat at constant volume, C_v, see Section B.3.2, the specific volume, v and the change in specific volume, $\dot{v}$, see Section B.3.3, the specific molar volume, $\bar{v}$, see Section B.3.4, the thermal time constant, τ, see Section B.3.5, the internal area exposed to gas in the accumulator, A_w, see Section B.3.6, the change in position, dx, see Section B.3.7 and the derivative of P_{gas} with respect to the temperature T, see Chapter 7.

The integrator in Figure B.9 is implemented with settings as listed in Table B.4.

	Integrator 1
Initial condition	$T_{gas,initial}$
Upper saturation limit	∞
Lower saturation limit	0

Table B.4: *Initial conditions and saturation limits for Integrator 4.*

B.3.2 Calculating C_v

C_v is calculated using the equation[Cengel and Turner, 2001, page 933]:

$$C_p = a + bT + cT^2 + dT^3 \tag{B.3}$$

where a, b, c and d for nitrogen is given by[Cengel and Turner, 2001, Table A-2]

$$a = 28.90 \qquad b = -0.1571 \cdot 10^{-2}$$
$$c = 0.8081 \cdot 10^{-5} \qquad d = -2.873 \cdot 10^{-9}$$

and C_v is calculated with[Cengel and Turner, 2001, (3-40)]

$$C_v = \frac{C_p}{k} \tag{B.4}$$

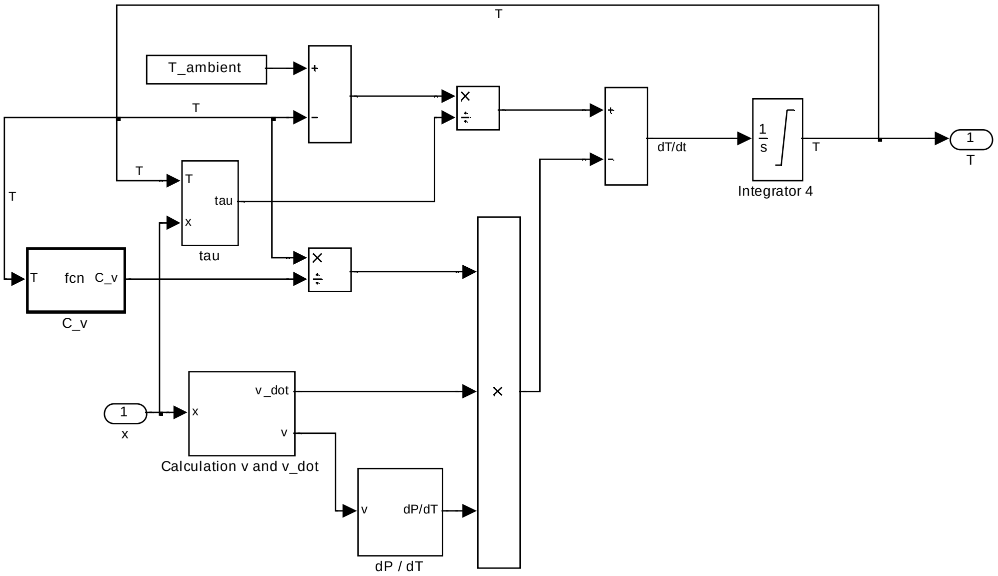

Figure B.9: *SIMULINK model of the block used to calculate the temperature in the gas side of the accumulator.*

where $k = 1.40$ for $T < 450K$[Cengel and Turner, 2001, Table A-2]. The calculations are implemented using a Embedded MATLAB function with the following code

```
function C_v = fcn(T)

a       =   28.90;
b       =   -0.1571e-2;
c       =   0.8081e-5;
d       =   -2.873e-9;
M       =   28.013e-3;          %[kg/mol]
k       =   1.4

C_p     =   a + b*T+c*T^2+d*T^3;

C_v = (C_p/M)/k;
```

B.3.3 Calculating v and $\dot{v}$

The specific volume, v, and the change in specific volume with respect to time, $\dot{v}$, are calculated using the equation[Cengel and Turner, 2001, (3-13)]

$$v = \frac{V}{m} \tag{B.5}$$

$$\dot{v} = \frac{dv}{dt} \tag{B.6}$$

The equations are implemented in SIMULINK as depicted in Figure B.10

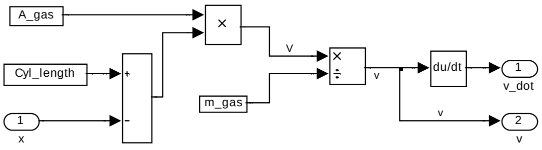

Figure B.10: *Implementation of specific volume, v, and change in specific volume with respect to time $\dot{v}$ in SIMULINK.*

B.3.4 Calculating $\bar{v}$

The specific molar mass, $\bar{v}$, is calculated using the equation[Cengel and Turner, 2001, (3-15)]

$$\bar{v} = \frac{V}{N} \tag{B.7}$$

The equations is implemented in SIMULINK as depicted in Figure B.11

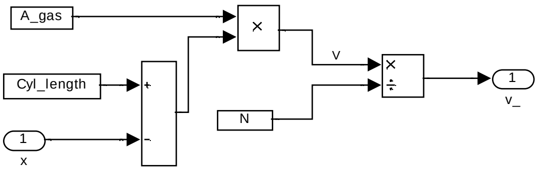

Figure B.11: *Implementation of the specific molar mass, $\bar{v}$, in SIMULINK.*

B.3.5 Calculating τ

The thermal time constant, τ, is calculated using (8.17) and equations are implemented in SIMULINK as depicted in Figure B.12

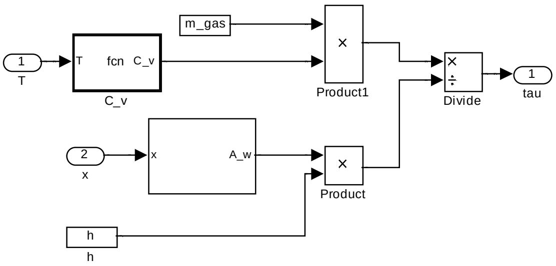

Figure B.12: *Implementation of the thermal time constant, τ, in SIMULINK.*

B.3.6 Calculating A_w

The internal area exposed to gas in the accumulator, A_w, is calculated using below equation.

$$A_w = (l_{cyl} - x)\, O_{cyl} \tag{B.8}$$

Please note that only the area of the cylinder wall is included. The area is used to calculate the energy leaving the accumulator and since both ends of the accumulator are many times thicker than the cylinder wall it is assumed that almost no energy are leaving through the ends hence they are not included in the calculation of the area. The equations are implemented in SIMULINK as depicted in Figure B.13

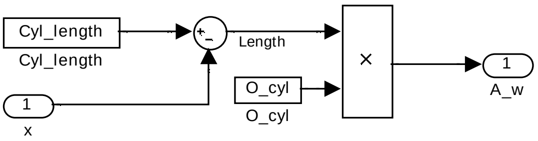

Figure B.13: *Implementation of the internal area exposed to gas in the accumulator, A_w, in SIMULINK.*

B.3.7 Calculating dx

The change in position, dx, is calculated by taking the present position minus the previous position as shown in below equation

$$dx = x(i) - x(i-1) \tag{B.9}$$

The equations are implemented in SIMULINK as depicted in Figure B.14

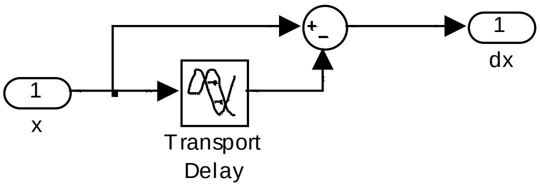

Figure B.14: *Implementation of change in position, dx, in SIMULINK.*

Coefficients for the Bender equation of state

C

The Bender equation of state can be written as[Rotthäuser, 1993, (4.25)]

$$p = \frac{RT}{v}\left[1 + \sum_{i=1}^{19} B_i Y_i\right] \tag{C.1}$$

and

$$\omega = \frac{v_{cr}}{v} = \frac{\rho}{\rho_{cr}} \qquad \tau = \frac{T_{cr}}{T} \tag{C.2}$$

The coefficients B_i and Y_i is listed in Table C.1[Rotthäuser, 1993, Table 4.5c and 4.5d]

i	B_i	Y_i
1	$5.1564398 \cdot 10^{-1}$	ω
2	$-1.2350862 \cdot 10^{0}$	$\omega\tau$
3	$-3.3660701 \cdot 10^{-2}$	$\omega\tau^2$
4	$-4.3693391 \cdot 10^{-1}$	$\omega\tau^3$
5	$6.1598645 \cdot 10^{-2}$	$\omega\tau^4$
6	$5.2599330 \cdot 10^{-2}$	ω^2
7	$2.0756488 \cdot 10^{-1}$	$\omega^2\tau$
8	$2.0273530 \cdot 10^{-1}$	$\omega^2\tau^2$
9	$2.3974975 \cdot 10^{-1}$	ω^3
10	$-4.7905077 \cdot 10^{-1}$	$\omega^3\tau$
11	$-2.7239453 \cdot 10^{-2}$	ω^4
12	$1.2113829 \cdot 10^{-1}$	$\omega^4\tau$
13	$1.2924526 \cdot 10^{-2}$	$\omega^5\tau$
14	$-3.2495834 \cdot 10^{-1}$	$\omega^2\tau^3 e^{\alpha\omega^2}$
15	$5.3924336 \cdot 10^{-1}$	$\omega^2\tau^4 e^{\alpha\omega^2}$
16	$-2.0692385 \cdot 10^{-1}$	$\omega^2\tau^5 e^{\alpha\omega^2}$
17	$-1.5625825 \cdot 10^{-1}$	$\omega^4\tau^3 e^{\alpha\omega^2}$
18	$5.2222667 \cdot 10^{-1}$	$\omega^4\tau^4 e^{\alpha\omega^2}$
19	$-3.8027769 \cdot 10^{-2}$	$\omega^4\tau^5 e^{\alpha\omega^2}$
α	-0.9641	

Table C.1: *B_i and Y_i coefficients in the Bender equation of state*

Coefficients for the Jacobsen & Stewart equation of state

D

The Jacobsen & Stewart equation of state can be written as[Rupprecht, 1988, (5.8)] and [Stewart and Jacobsen, 1973, (6)]

$$p = \frac{RT}{v}\left[1 + \sum_{i=1}^{32} N_i X_i\right] \tag{D.1}$$

and

$$\omega = \frac{\rho}{\rho_{cr}} \qquad \tau = \frac{T_{cr}}{T} \tag{D.2}$$

The coefficients N_i and Y_i is listed in Table D.1[Rupprecht, 1988, Table B and C]

i	N_i	X_i
1	0.185927462121	ω
2	1.30155934655	$\omega\tau^{0,5}$
3	-2.64054394027	$\omega\tau$
4	0.292709245322	$\omega\tau^2$
5	-0.287482987766	$\omega\tau^3$
6	0.161225592835	ω^2
7	-0.135129830972	$\omega^2\tau$
8	0.0000137262707287	$\omega^2\tau^2$
9	13.6860808703	$\omega^2\tau^3$
10	0.00128973300860	ω^3
11	0.315240491447	$\omega^3\tau$
12	-0.548670430729	$\omega^4\tau^2$
13	0.0744966916902	$\omega^4\tau$
14	-0.151712926147	$\omega^5\tau^2$
15	-0.728119881405	$\omega^5\tau^3$
16	0.112790673192	$\omega^6\tau^2$
17	-0.0187922799332	$\omega^7\tau^2$
18	0.0460360632178	$\omega^7\tau^3$
19	-0.00251321896106	$\omega^8\tau^3$
20	-12.5428246147	$\omega^2\tau^3e^{\alpha\omega^2}$
21	-0.722843603762	$\omega^2\tau^4e^{\alpha\omega^2}$
22	-9.07779852949	$\omega^4\tau^3e^{\alpha\omega^2}$
23	0.333590008958	$\omega^4\tau^5e^{\alpha\omega^2}$
24	-2.10175282124	$\omega^6\tau^3e^{\alpha\omega^2}$
25	-0.244752749620	$\omega^6\tau^4e^{\alpha\omega^2}$
26	-0.611651799016	$\omega^8\tau^3e^{\alpha\omega^2}$
27	-0.0244254052253	$\omega^8\tau^5e^{\alpha\omega^2}$
28	-0.0230295508018	$\omega^{10}\tau^3e^{\alpha\omega^2}$
29	0.0157620487302	$\omega^{10}\tau^4e^{\alpha\omega^2}$
30	-0.0126428070667	$\omega^{12}\tau^3e^{\alpha\omega^2}$
31	-0.00146576723582	$\omega^{12}\tau^4e^{\alpha\omega^2}$
32	0.0000915063203408	$\omega^{12}\tau^5e^{\alpha\omega^2}$
α	-0.70371896	

Table D.1: *N_i and X_i coefficients in the Jacobsen & Stewart equation of state*

E

Test run properties

In the following tables properties for all test runs are listed together with any measured data.

E.1 Accumulator #1

E.1.1 Normal ambient temperature

Name	GAS_1	GAS_2	GAS_3	GAS_4
Date	17/01/10			
Test run start	18:10	16:15	13:20	15:55
Test run end	18:30	16:35	13:40	16:15
Function	Ramp			
Supply pressure [Bar]	250			
Precharge pressure [Bar]	50	100	50	100
Initial position [m]	0.01			
Final position [m]	0.07		0.14	
Slope [m/s]	0.20			
Duration [sec]	120			
Samples	3			
Sample frequency [Hz]	200.008			
Ambient temperature [K]	305	307	299	308

Name	GAS_5	GAS_6	GAS_7	GAS_8	GAS_9
Date	17/01/10				
Test run start	17:30	16:35	17:20	17:00	14:55
Test run end	17:50	16:55	17:30	17:15	15:10
Function	Ramp				
Supply pressure [Bar]	250				
Precharge pressure [Bar]	50	100	50	100	150
Initial position [m]	0.01				
Final position [m]	0.07		0.14		0.07
Slope (Up) [m/s]	0.01		0.05		0.20
Duration [sec]	10		5.2		120
Samples	3				
Sample frequency [Hz]	200.008				
Ambient temperature [K]	305	305	305	306	302

E.1.2 Warm ambient temperature

Name	GAS_10	GAS_11	GAS_12	GAS_13
Date	18/01/10		19/01/10	
Test run start	16:40	16:45	15:10	15:20
Test run end	16:45	16:50	15:20	15:35
Function	Ramp			
Supply pressure [Bar]	250			
Precharge pressure [Bar]	100		50	
Initial position [m]	0.01			
Final position [m]	0.07	0.14		0.07
Slope [m/s]	0.20			
Duration [sec]	120			
Samples	1	2	3	
Sample frequency [Hz]	200.008			
Ambient temperature [K]	332	344	340	343

E.1.3 Cold ambient temperature

Name	GAS_21	GAS_22	GAS_23	GAS_24	GAS_29
Date	20/01/10				
Test run start	12:25	11:25	12:50	11:45	10:45
Test run end	12:50	11:40	13:20	12:05	11:10
Function	Ramp				
Supply pressure [Bar]	250				
Precharge pressure [Bar]	50	100	50	100	50
Initial position [m]	0.01				
Final position [m]	0.07		0.14		0.07
Slope [m/s]	0.20				
Duration [sec]	120				
Samples	3				
Sample frequency [Hz]	200.008				
Ambient temperature [K]	251	250	252	252	252

Notes

GAS_1: Due to defect pressure transducer only sample 1 can be used.

GAS_4: Due to defect pressure transducer only sample 1 and 2 can be used.

GAS_6: Due to defect pressure transducer only sample 1 and 2 can be used.

GAS_8: Due to defect pressure transducer only sample 2 can be used.

E.2 Accumulator #2

E.2.1 Cold ambient temperature

<table>
<tr><td>Name</td><td>GAS_51</td><td>GAS_52</td><td>GAS_53</td><td>GAS_54</td></tr>
<tr><td>Date</td><td colspan="4">22/01/10</td></tr>
<tr><td>Test run start</td><td>13:10</td><td>13:55</td><td>13:30</td><td>13:55</td></tr>
<tr><td>Test run end</td><td>13:30</td><td>14:20</td><td>13:45</td><td>14:25</td></tr>
<tr><td>Function</td><td colspan="4">Ramp</td></tr>
<tr><td>Supply pressure [Bar]</td><td colspan="4">250</td></tr>
<tr><td>Precharge pressure [Bar]</td><td>50</td><td>100</td><td>50</td><td>100</td></tr>
<tr><td>Initial position [m]</td><td colspan="4">0.01</td></tr>
<tr><td>Final position [m]</td><td colspan="2">0.09</td><td colspan="2">0.17</td></tr>
<tr><td>Slope [m/s]</td><td colspan="4">0.03</td></tr>
<tr><td>Duration [sec]</td><td colspan="4">250</td></tr>
<tr><td>Samples</td><td colspan="3">3</td><td>2</td></tr>
<tr><td>Sample frequency [Hz]</td><td colspan="4">200.008</td></tr>
<tr><td>Ambient temperature [K]</td><td>255</td><td>261</td><td>250</td><td>256</td></tr>
</table>

E.2.2 Normal ambient temperature

<table>
<tr><td>Name</td><td>GAS_61</td><td>GAS_62</td><td>GAS_63</td><td>GAS_64</td><td>GAS_65</td><td>GAS_66</td></tr>
<tr><td>Date</td><td colspan="6">22/01/10</td></tr>
<tr><td>Test run start</td><td>13:10</td><td>13:55</td><td>13:30</td><td>13:55</td><td>15:55</td><td>16:10</td></tr>
<tr><td>Test run end</td><td>13:30</td><td>14:20</td><td>13:45</td><td>14:25</td><td>16:00</td><td>16:15</td></tr>
<tr><td>Function</td><td colspan="6">Ramp</td></tr>
<tr><td>Supply pressure [Bar]</td><td colspan="6">250</td></tr>
<tr><td>Precharge pressure [Bar]</td><td>50</td><td>100</td><td>50</td><td colspan="3">100</td></tr>
<tr><td>Initial position [m]</td><td colspan="6">0.01</td></tr>
<tr><td>Final position [m]</td><td colspan="2">0.09</td><td colspan="4">0.17</td></tr>
<tr><td>Slope [m/s]</td><td colspan="6">0.03</td></tr>
<tr><td>Duration [sec]</td><td colspan="6">250</td></tr>
<tr><td>Samples</td><td colspan="3">3</td><td>2</td><td>2</td><td>1</td></tr>
<tr><td>Sample frequency [Hz]</td><td colspan="6">200.008</td></tr>
<tr><td>Ambient temperature [K]</td><td>300</td><td>304</td><td>302</td><td>304</td><td>300</td><td>301</td></tr>
</table>

Notes

GAS_53: Sample 3 not to be used, as the accumulator was leaking gas.

GAS_64: Sample 1 is not to be used.

GAS_65: Accumulator placed vertical with the oil end in the top. Sample 1 is not to be used.

GAS_66: Accumulator placed vertical with the oil end in the bottom.

Experiment report: Validating test rig

F

F.1 Participants

The experiment has been performed by the author.

F.2 Period of execution

Start: January 16th, 2010 @ 12:45

Ended: January 17th, 2010 @ 19:00

F.3 Abstract

The experiment was performed to investigate the variability in the test rig and to determine how many samples that should be acquired in the following test runs. The experiment showed that the test rig has a very low variability and that it therefore was necessary to take only one sample per test run.

F.4 Introduction

The aim of the experiment is to investigate the variability of the text rig, that is how similar the results was for the same setup. The result of the experiment will be used to decide how many samples that should be acquire for each test run.

F.5 Theory

The variance and standard deviation for each test run will be calculated and use the determine the variability of the test rig. The variance are calculated with[Walpole et al., 2002, Definition 1.1]

$$s^2 = \sum_{i=1}^{n} \frac{(x_i - \bar{x})^2}{n-1} \tag{F.1}$$

where $\bar{x}$ is the mean. The standard deviation can be calculated using[Walpole et al., 2002, Definition 1.1]

$$s = \sqrt{s^2} \tag{F.2}$$

F.6 Experimental apparatus and procedures

The apparatus used in the experiment are the test rig described in Appendix A. The experiment has been carried out by performing 10 samples for each test setup and then compared the data. Four test setup has been used all described in Table F.1.

Name	TESTRIG_1	TESTRIG_2	TESTRIG_3	TESTRIG_4
Date	16/01/10		17/01/10	
Test run start	12:45	16:30	18:30	15:25
Test run end	13:10	17:10	19:00	15:55
Function	Ramp	Ramp	Ramp	Ramp
Supply pressure [Bar]	250			
Precharge pressure [Bar]	50	100	50	100
Initial position [m]	0.01			
Final position [m]	0.07	0.07	0.14	0.14
Slope of ramp [m/s]	0.20	0.25	0.20	0.25
Duration [sec]	115	115	115	115
Samples	10			

Table F.1: *Properties for test runs used for validating the test rig.*

F.7 Data analysis, results and uncertainties

All measured data has been plotted on one plot per test setup. In Figure F.1 the data is shown for TESTRIG_1. Graphs for all other test runs can be found in Appendix I.1.

The variance and standard deviation has then been calculated using MATLAB. They have all been plotted. In Figure F.2 and Figure F.2 this is shown.

The main sources of error in this experiment has been the changing ambient temperature. Each test run has taken more the 30 minutes and the temperature can therefore have change considerably.

F.8 Discussion

Based on the acquired results the test rig is considered to have a low variability as the results was very similar. This means that when the rest of the test runs will be performed, it is only necessary to make one sample per test run.

F.9 Conclusion

It is concluded that the test rig has a low variability meaning that the following test runs one will need one sample.

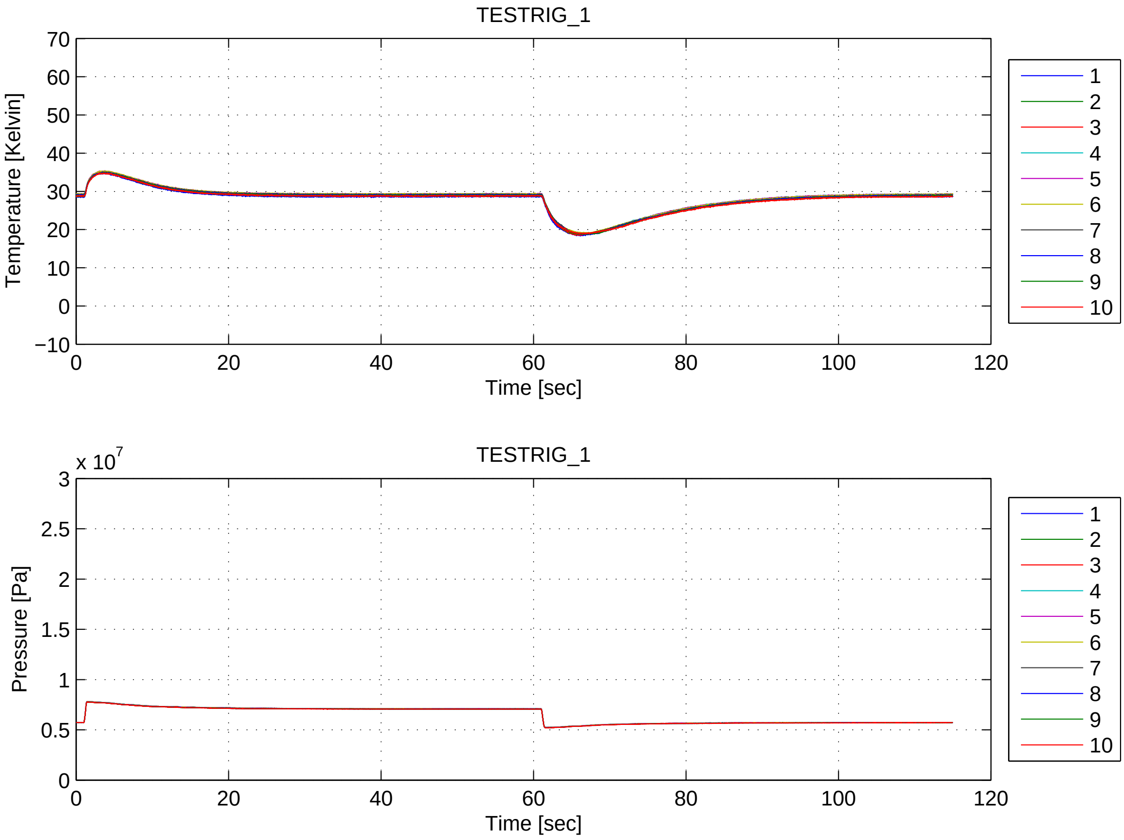

Figure F.1: *10 samples taken for TESTRIG_1*

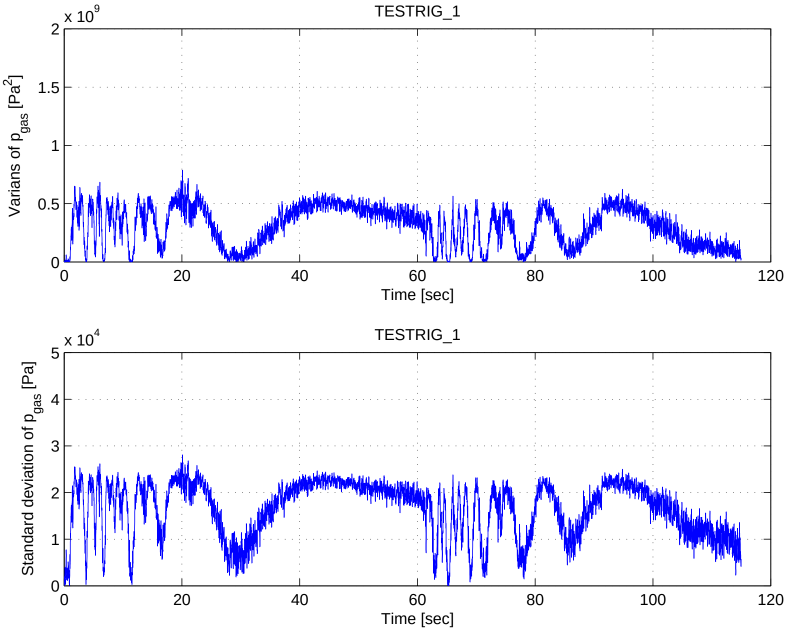

Figure F.2: *Variance and standard deviation of the pressure for TESTRIG_1*

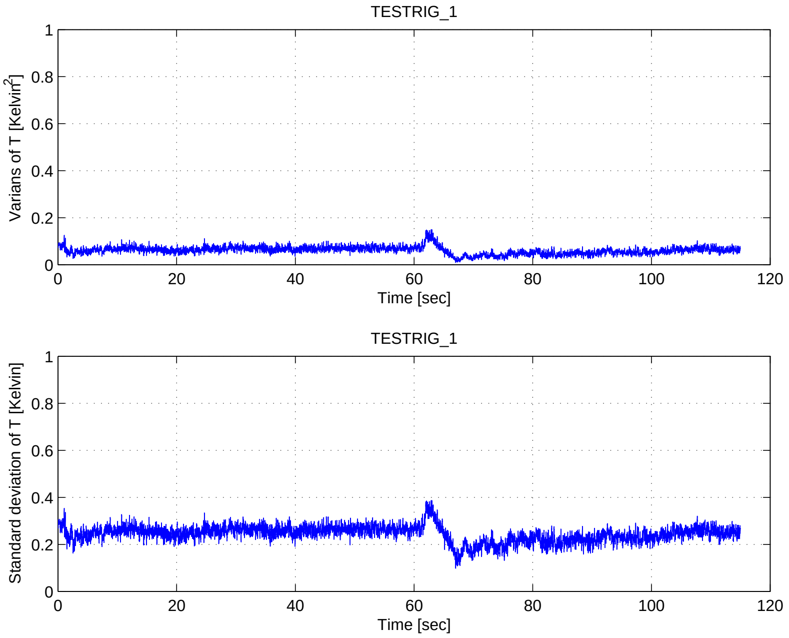

Figure F.3: *Variance and standard deviation of the temperature for TESTRIG_1*

Experiment report: Determining the thermal time constant

G

G.1 Participants

The experiment has been performed by the author.

G.2 Period of execution

Start: January 17th, 2010 @ 16:15
Ended: January 22nd, 2010 @ 15>00

G.3 Abstract

The experiment was perform to measure the thermal time constant. The conclusion from the experiment was that data had to large variations to be used in the simulations. Therefore it has been concluded that the thermal time constant will be calculated based on the actual test runs used for validation.

G.4 Introduction

In a hydraulic accumulator available energy is lost due to an irreversible heat transfer. When the pressure increases in the gas so does the temperature. But over time heat is transferred from the gas to the surrounding air causing the temperature to drop. To calculate the temperature an energy balance can be made for the gas side of the accumulator. In this energy balance the thermal time constant is introduced. The constant is a measure for how fast the pressure drops 62.5 % when exposed to a sted change in volume.

G.5 Theory

When the pressure of a gas increases, so does the temperature. If the pressure increase is taking place in a closed system e.g. a hydraulic accumulator the heat from the temperature will react with the ambient temperature transferring energy from the gas to the surroundings. The rate of heat being transferred through the wall of the accumulator is denoted the convection heat transfer coefficient, h. The convection heat transfer coefficient can be used to calculate the thermal time constant. The thermal time constant will in this project be measured. The thermal time-constant is measured in seconds a is the duration for how long time it takes the gas pressure to drop by 63.2% as shown in Figure G.1 By applying the system with a step change i volume and measure the gas pressure, the thermal time constant can be determined.

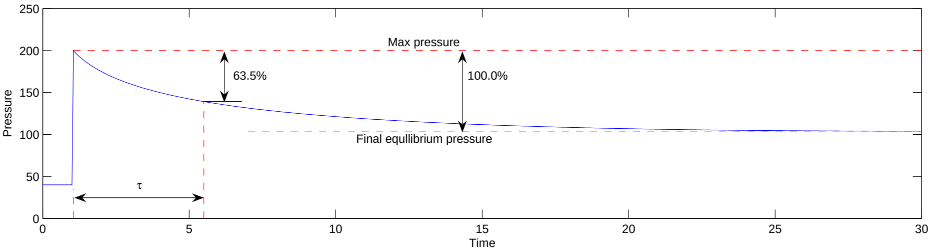

Figure G.1: *Definition of thermal time constant, τ*

G.6 Experimental apparatus and procedures

To perform the experiment the test rig as described in Chapter A is used. Furthermore a program has been developed to calculated τ based on the acquired data. The program is presented in Appendix M. The experiment was performed by applying the the accumulator with a reference signal that would yield a step change in the volume. To make sure, that the regulator was not saturating the reference signal was a ramp signal with a steep slope. The slope was varied depending on precharge pressure and how long the piston should move. The slope can be read off in Appendix E. A test run to measure the thermal time constant was performed before and after the test runs used to measure the gas pressure and temperature used for validating the models. The two test runs was made for each setup as described in Appendix M. Two test runs was made to validate the measurements.

G.7 Data analysis, results and uncertainties

For each setup the two test runs was measured and the thermal time constant was calculated. The result for one of the test runs is depicted in Figure G.2.

The graph shows a difference between the two samples of approximately 0.4 seconds or 4.2%. In other test runs larger differences was experinced. To give an insight of how much the measured values varies, all masures thermal time constants are depicted in Figure G.3 for accumulator #1. Graphs for all other test runs can be found in Appendix I.2

A number of sounds of errors er to be found in this experiment whereas the biggest must be the air flow around the accumulator is the largest. In the laboratory a heating fan was installed with a fairly large fan circulating the air around in the room. This may have had a large influence on the air flow around the accumulator.

G.8 Discussion

It can be seen that no single value for the thermal time constant is present. In fact large differences in the constant can be found within the same precharge pressure. The only conclusion to make is that the overall ambient temperature seems to have no influence on the value. But instead the precharge pressure has. Here it can be seen that the larger the precharge pressure, the larger the thermal time constant. The same conclusions can be made for accumulator #2. The latter is in good consistency with other conclusions[Rupprecht, 1988, Figure 4.8]. In Appendix I.2 the graphs for accumulator #2 can be found.

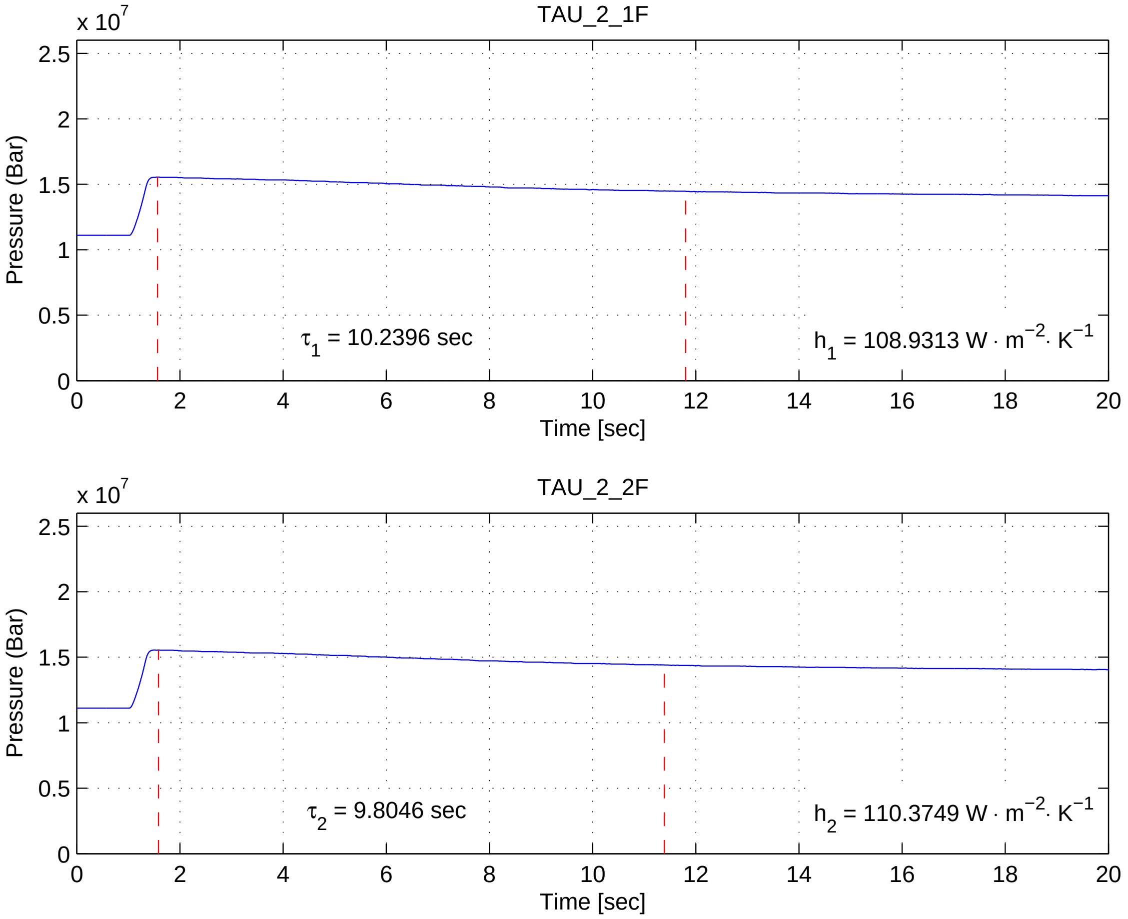

Figure G.2: *Measured values of the thermal time constant for GAS_2. The top graph being before the testrun and the bottom one being after.*

The reasons for the variation in the measured data can be many. But the circulation of the air in the laboratory i the many sources of error. If there is a large circulation of air the thermal time constant will drop because the amount of energy convected away from the accumulator is larger then without any air circulation.

With the large variations in the results it is concluded that the measured thermal time constants can not be used in the simulations. Therefore the constant will be calculated based on the actual test runs used for validation.

G.9 Conclusion

Some fairly large variations in the measured data was observed most probably because of variations in the air flow around the accumulator. The variations are to large so the measured data can not be used in the simulations. Therefore it has been concluded that the thermal time constant will be calculated based on the actual test runs used for validation.

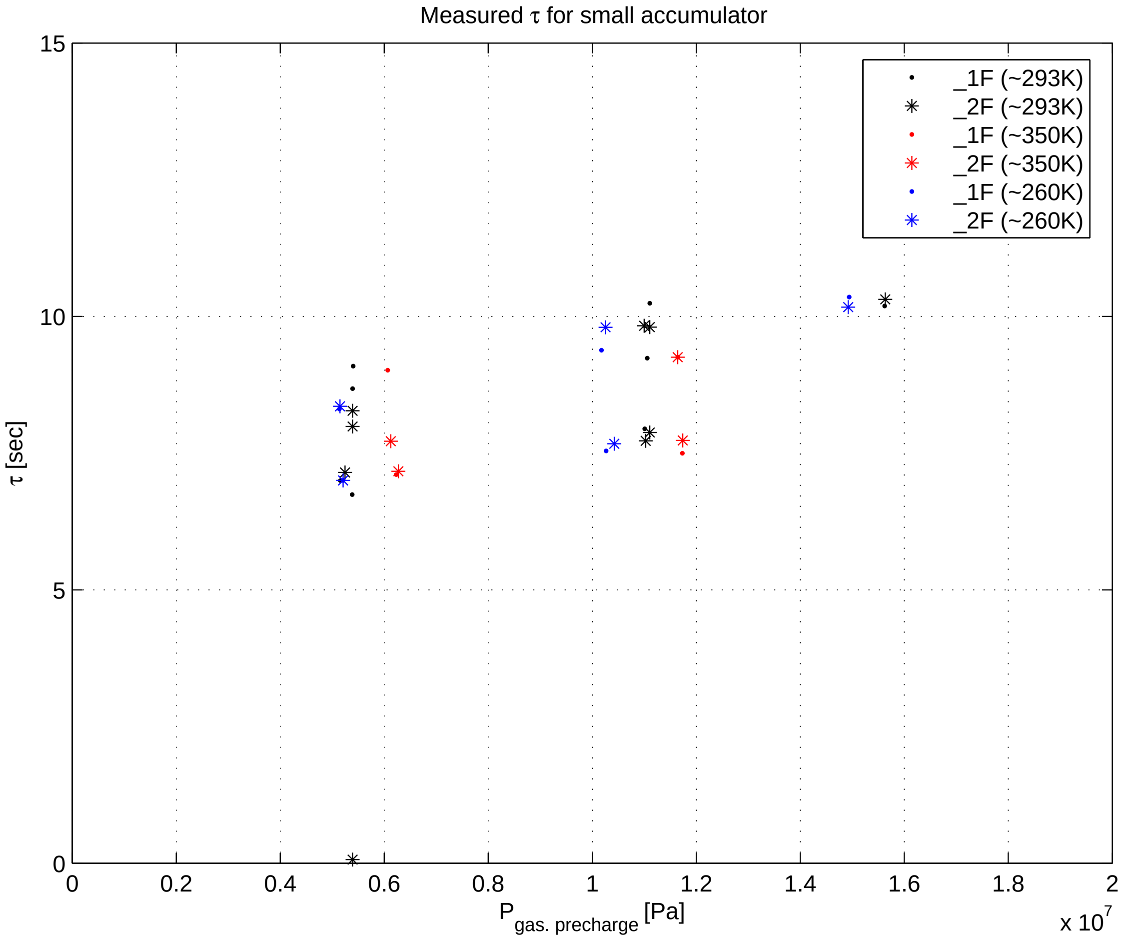

Figure G.3: *Measured thermal time constants for accumulator #1.*

Experiment report: Validation gas pressure and temperature model

H

H.1 Participants

The experiment has been performed by the author.

H.2 Period of execution

Start: January 17th, 2010 @ 16:15

Ended: January 22nd, 2010 @ 15>00

H.3 Abstract

H.4 Introduction

The experiment was carried out to validate six models to calculate the gas pressure and temperature in an accumulator. During the experiment the position of the piston was measured and used as input in the models. The out was the gas pressure and temperature. The objective if the experiment was to determine which model that gave the most correct result when taking complexity into account.

H.5 Theory

Six models for calculating the gas pressure has been presented in Chapter 7. They have all been used for calculating the gas temperature as described in Chapter 8. To compare the measured and calculated data the differences between them will be calculated for all time steps. This has been done using the following equation:

$$Difference = \frac{p_{measured} - p_{calculated}}{p_{measured}} \tag{H.1}$$

H.6 Experimental apparatus and procedures

To perform the experiment the test rig as described in Chapter A is used. The experiment was performed by applying accumulator #1 with a reference signal that would yield a step change in the volume as described in Chapter 10.2. To make sure, that the regulator was not saturating the reference signal was a ramp signal with a steep slope. The slope was varied depending on precharge pressure and how long the piston should move. The slop can be read off in Appendix E. For every setup three samples was measured and named with the date and a continuous number. In Section 10.2 the name of each rest run is presented.

Since accumulator #2 do not have a position transducer the hydraulic and mechanical model has been used firstly to calculate the gas pressure using a position as reference signal. The gas pressure has then been used as reference signal for accumulator #2.

For every sample the gas pressure and temperature was measured and plotted as a function of time. Then the gas pressure and temperature has been calculated and plotted as a function of time. After this the difference between the measured and calculated value has been determine as explained in the previous chapter and plotted as a function of the measured pressure. Finally the mean value of this together with the variance for all reulsts has been calculated and plotted in the same figure. In this way it is possible to get an overview over alle test runs.

H.7 Data analysis, results and uncertainties

In Figure H.1 is the data for one test run with three samples depicted. Graphs for all other test runs can be found in Appendix I.3.

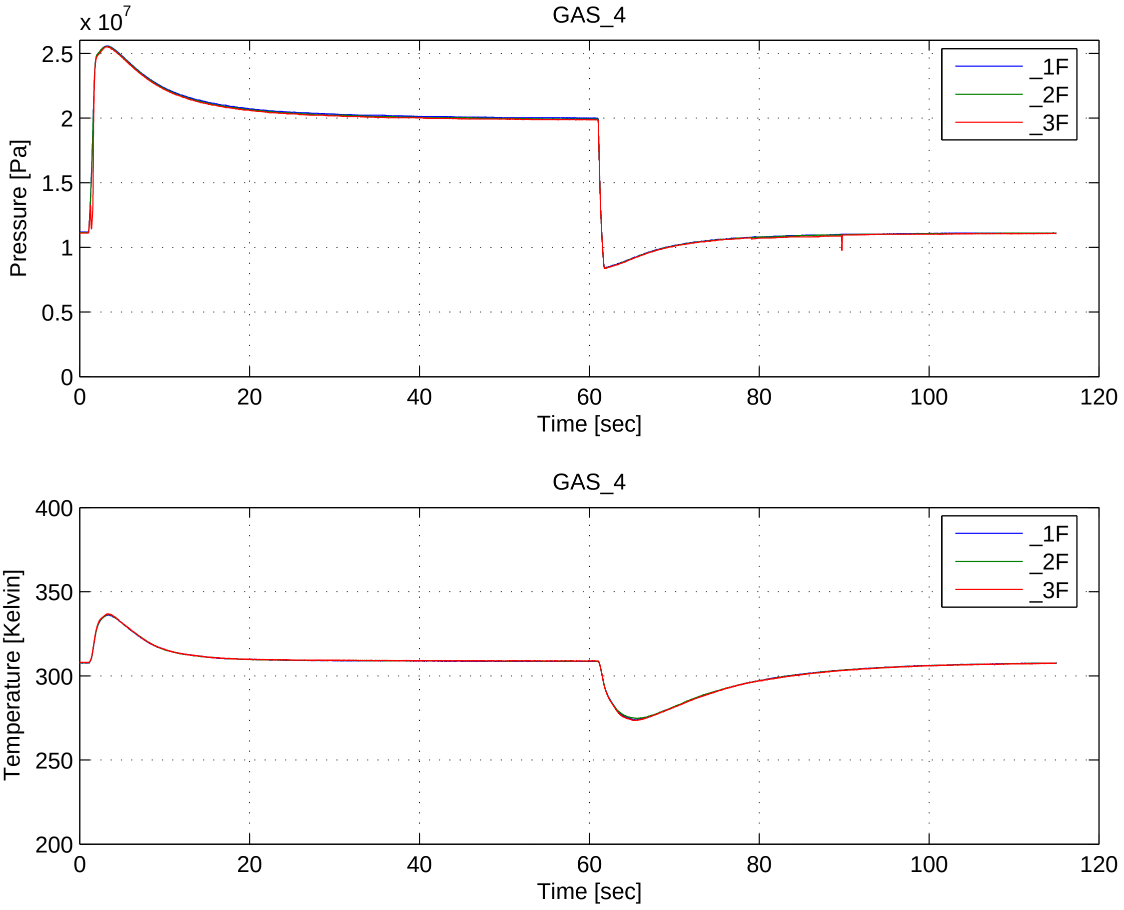

Figure H.1: *Gas pressure and temperature for GAS_4.*

The graph shows an expected progress of the pressure and the temperature, namely that they increase during a compression and decrease during an expansion. For the above test run, namely GAS_4, the gas pressure has been calculated and compared with the measured data. This is depicted in Figure H.2. The same calculations can be seen in Figure H.3 for a test run performed with accumulator #2. Graphs for all other test runs can be found in Appendix I.4.

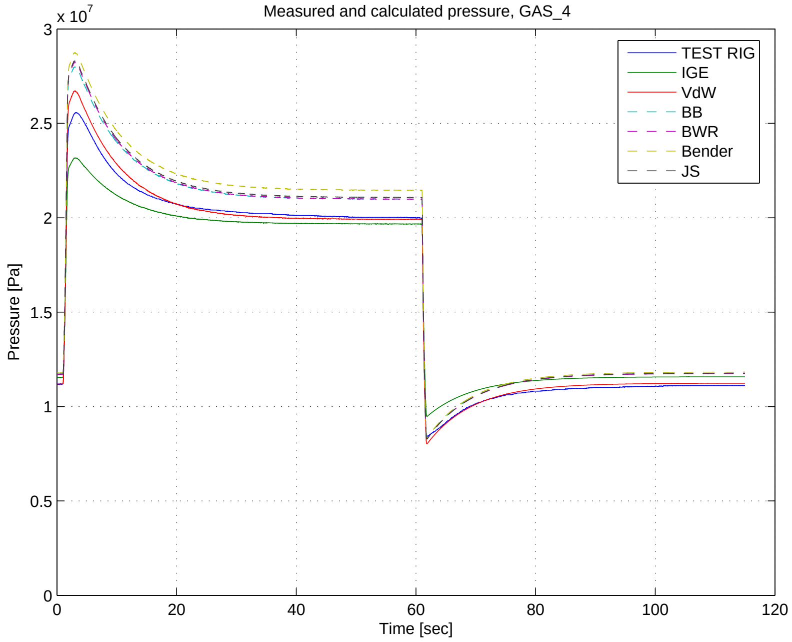

Figure H.2: *Measured and calculated gas pressure using six equations of state for accumulator #1.*

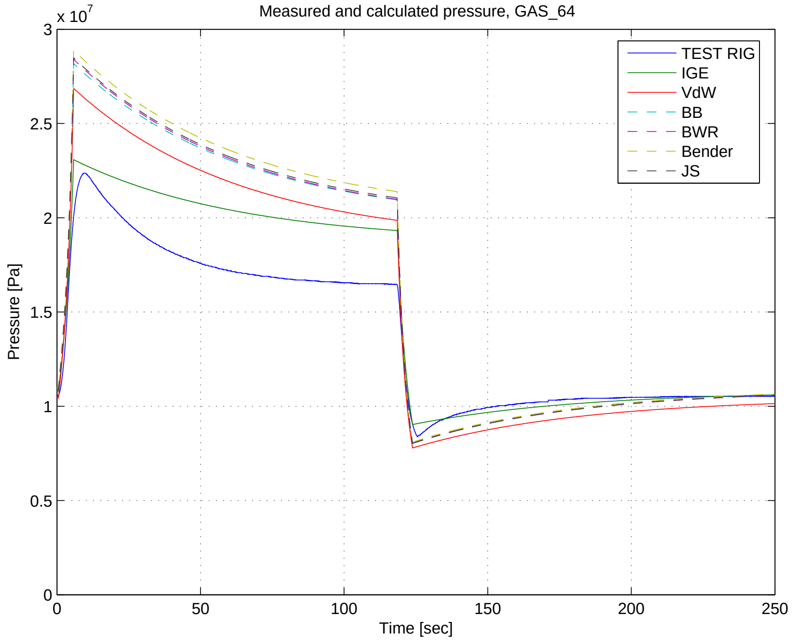

Figure H.3: *Measured and calculated gas pressure using six equations of state for accumulator #2. Notice the large differences between measured an calculated.*

To get an overview of the difference between the measured and the calculated data, the percentage-wise difference has been calculated and depicted as a function of the measured pressure in Figure H.4. Graphs for all other test runs can be found in Appendix I.5.

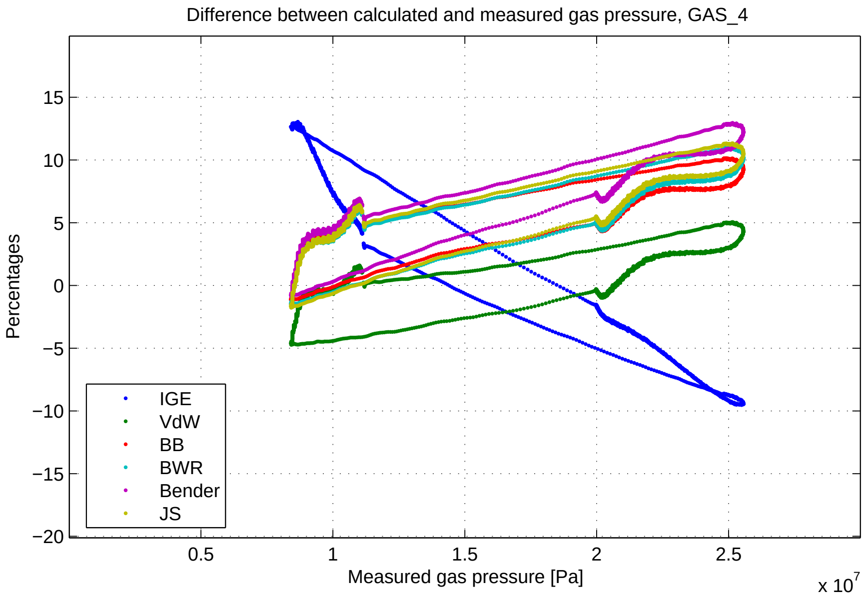

Figure H.4: *Percentage-wise difference between measured an calculate gas pressure as a function of the measured pressure.*

As seen from Figure H.4 each test run consists of four stages, namely two nonlinear and two approximate linear. The four stages are depicted separately in Figure H.5 and are described in the following.

> Stage 1: The compression stage where the gas is compressed and the pressure and temperature therefore increases. The stage is approximately linear as the dominating variable here is the position and the position is the same in both the measured data and the calculated data.
>
> Stage 2: The first interaction stage, where the volume is kept constant. The gas interacts with the surrounding air and the temperature decreases reaching ambient temperature causing the pressure to decrease. The stage is not linear as the dominating variable is the thermal time constant. In the calculations the thermal time constant is assumed the same at all time. But this is in fact not the case since both the convection heat transfer coefficient and the effective wall area changes with time[Pourmovahed and Otis, 1990]. This difference is causing the nonlinear behavior.
>
> Stage 3: The expansion stage where the gas is expanded and the pressure and temperature therefore decreases. The stage is approximately linear because of the same reason as for stage 1.
>
> Stage 4: The second interaction stage, where the volume is kept constant. The gas interacts with the surrounding air and the temperature increases reaching ambient temperature causing the pressure to increase. The stage is nonlinear because of the same reason as for stage 3.

To give an overview off all test runs two values has been calculated for each model, namely the mean percentage value and the difference between the minimum percentage difference and the maximum percentage difference. The mean percentage value takes the mean value of all data points for each model. This value gives an indication of how precise the model are compared with the measured data. the value can only give an indication of how the model in average performs, i.e. does the model in average calculate a to low pressure or does it in average calculate a to high pressure. This value does anyhow not give an indication of how precise the model are in each data point, i.e. how fare away from the average value the data points

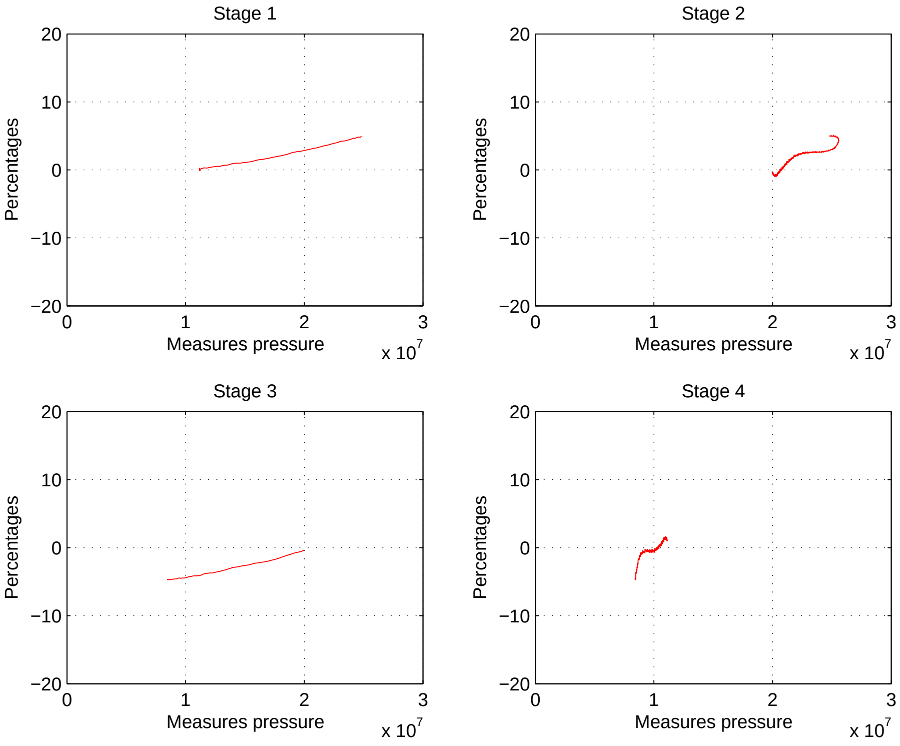

Figure H.5: *The four stages in a test run, namely the compression, the first interaction, the expansion and the second interaction for accumulator #1.*

are. A model could have a difference of -20 % in one data point an 20 % in another data point. In average this gives a difference of 0 %, which is not a clear and true result of that model. To give an indication of this the variance are calculated for each model. A large variance indicates that the data points are fare away from the average value. Vice versa a small variance indicates that the data points are close to the average. The latter is the most desirable.

The mean value and the variance has been calculated for all test runs both for accumulator #1 and accumulator #2. The result of this are depicted in Figure H.6 and Figure H.7. In Figure H.6 the first five test runs are for normal ambient temperature, the next four are for warm ambient temperature and the last five are for cold ambient temperature. For Figure H.7 the first four test runs are for cold ambient temperature and the last four are for ambient temperature.

For the depicted test run in Figure H.1, namely GAS_4, the gas temperature has been calculated and compared with the measured data. This is depicted in Figure H.8 and Figure H.9 for a test run preformed with accumulator #2. Graphs for all other test runs can be found in Appendix I.6.

As seen in the two figures large differences is observed. Most distinct for accumulator #2. This may be explained with the same reason as mentioned previous in this experimental report, namely that the position of the piston has not been as expected leading to a lower pressure then expected during a compression. Regarding accumulator #1 large differences between calculated and measured data are also observed. The differences is not assumed to be from errors in the calculations but rather from errors in measuring the temperature. Actually measuring the temperature proved to be quite a challenge which is why Section 14.2 has been devoted to explaining the problems faced during this operation.

The sources for uncertainties in this experiment are:

- An uncertainties that might be of influence to the result are fan heater placed in the laboratory. The fan heat has a quite large fan that circulates the air. This are influencing the thermal time constant.

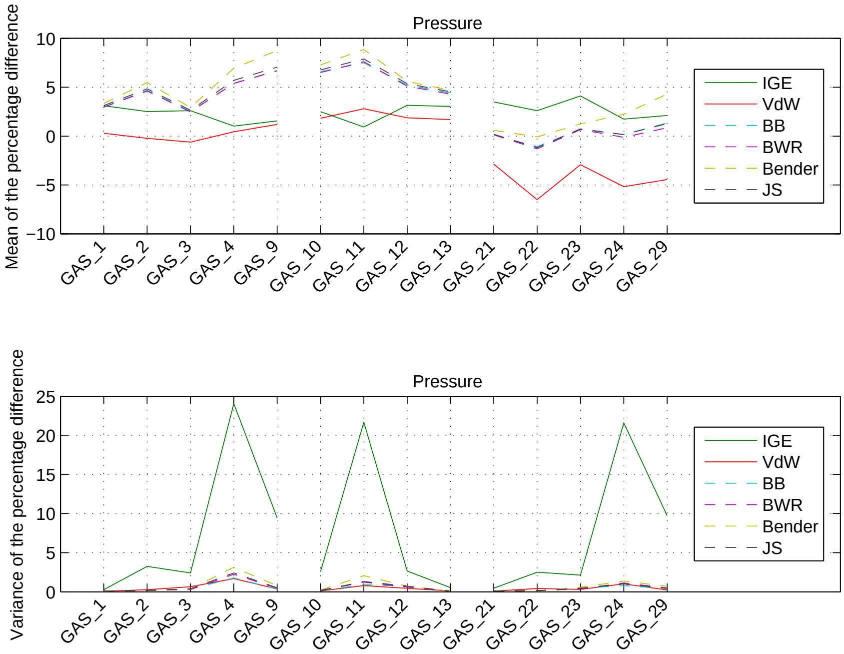

Figure H.6: *Calculation of mean value and variance of all test runs for accumulator #1. The first five test runs are for normal ambient temperature, the next four are for warm ambient temperature and the last five are for cold ambient temperature*

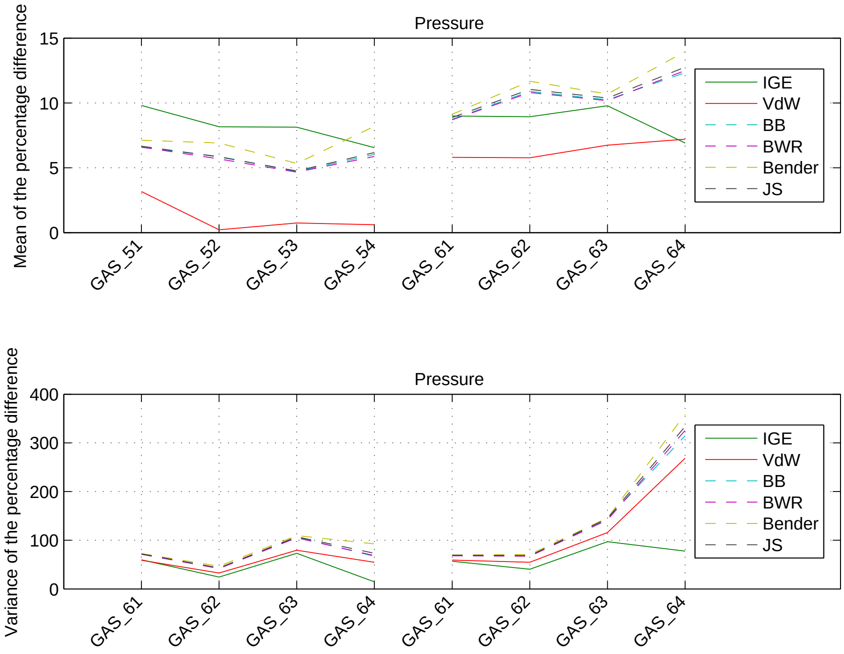

Figure H.7: *Calculation of mean value and variance of all test runs for accumulator #2. The first four test runs are for cold ambient temperature and the last four are for normal ambient temperature.*

If the circulation are changes during the test run so does the thermal time constant. But during the simulation a constant thermal time constant er used.

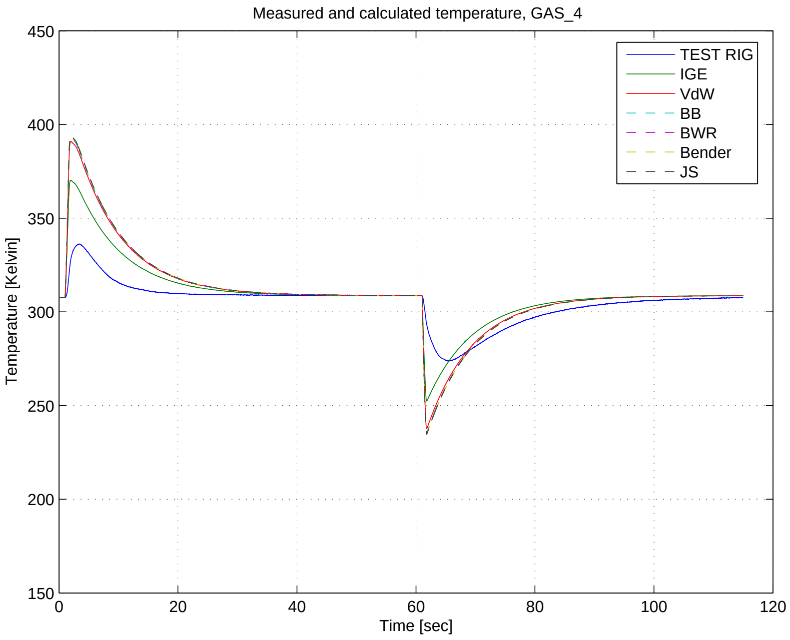

Figure H.8: *Measured and calculated gas temperature using six equations of state for accumulator #1.*

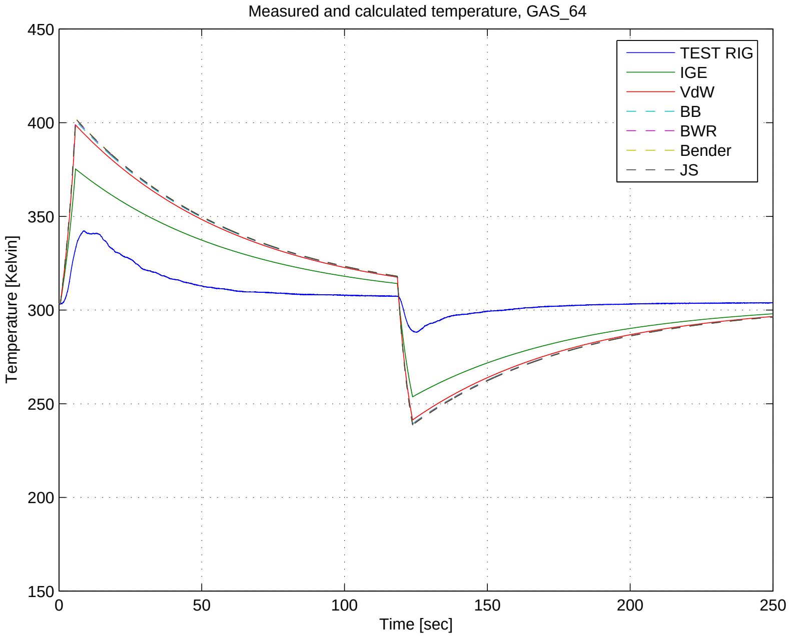

Figure H.9: *Measured and calculated gas temperature using six equations of state for accumulator #2.*

H.8 Discussion

The calculations for this experiment has been divided into two parts, namely the pressure and the temperature. Therefore the same will be done for this section.

H.8.1 Gas pressure

Based on the 14 test runs with accumulator #1 and the results depicted in Figure H.6 some conclusions can be drawn for this accumulator and the six gas models:

- In general the ideal gas equation does seems to be very accurate for all three ambient temperatures and pressures. But when the results are studies further it is clear to see that this model has a large variance for large pressures. This is the case for both normal, warm and cold ambient temperature. As expected this model is not suitable for simulating hydraulic accumulators as described in this project.
- The next equation of state of interest are the Van der Waals equation of state. This provides precise results and has a low variance for both normal and warm ambient temperatures. This is as expected as this equation of state are know be accurate for temperature above 250 Kelvin.
- For normal and warm ambient temperatures the four most complex equations of state proves to be more inaccurate then the less complex Van der Waals equation of state. Only for cold ambient temperatures it is reasonable to use the more complex equations of state. But still the difference between this four equations of state are so small, that it is recommended just to use Beattie-Bridgeman equation of state.

Regarding accumulator #2 no clear conclusions can be drawn. As explained in this experimental report the test run for accumulator #2 was performed using a simulated gas pressure as reference signal. Most likely there has been an error in the data used for the reference signal so the piston of the accumulator has not be where it was assumed to be. This is assumed as there are large differences between the measured and calculated data. Therefore all data for accumulator #2 must be considered wrong.

H.8.2 Temperature

In figure H.10 the result of this is depicted for accumulator #1. The results shows that no significant difference are to be found between the six models and that the most accurate results are obtained at the low ambient temperatures. This is assumed not to be correct based on two reasons:

- The equation for calculating the temperature are based on the pressure models. The pressure models has shown very accurate results.
- The formula used for calculating the temperature are used by other sources as well.

The findings must therefore be, that the results are not valid. This is back up by simulations done by other sources with almost the same setup reaching approximately the same temperatures[Rupprecht, 1988, Figure 5.3]. It is therefore assumes that the simulations are correct and, since they are based on the pressure models, that the Van der Waals equation of state are valid for normal and warm ambient temperature and that the Beattie-Bridgeman equation of state are valid for cold ambient temperatures.

H.9 Conclusion

H.9.1 Pressure

Based on the 14 test runs with accumulator #1 and the results depicted in Figure H.6 some conclusions can be drawn for this accumulator and the six gas pressure models:

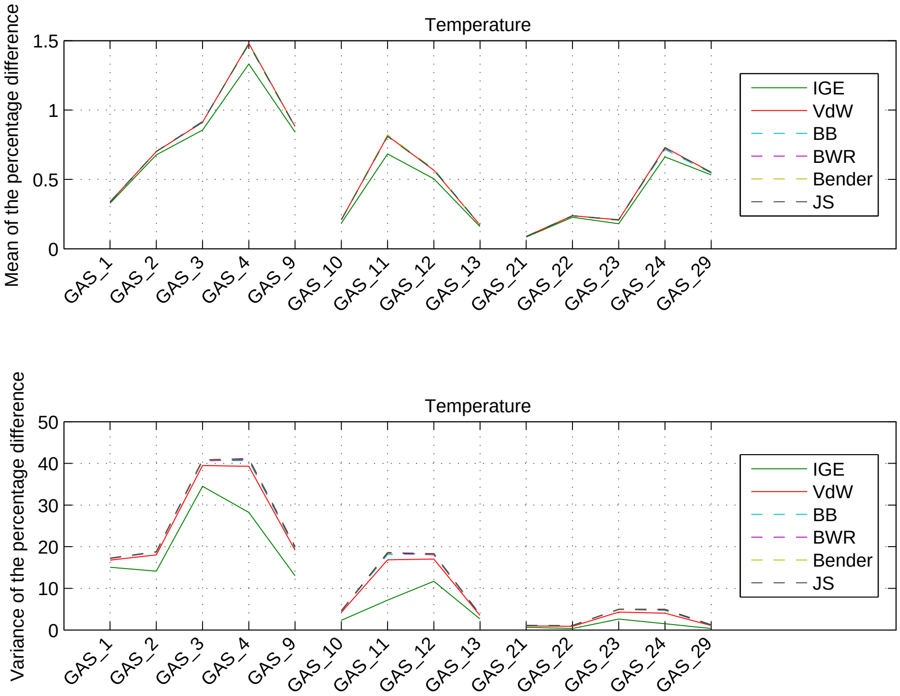

Figure H.10: *Percentage-wise difference between measured an calculate gas temperature as a function of the measured temperature.*

- In general the ideal gas equation does seems to be very accurate for all three ambient temperatures and pressures. But when the results are studies further it is clear to see that this model has a large variance for large pressures. This is the case for both normal, warm and cold ambient temperature. As expected this model is not suitable for simulating hydraulic accumulators as described in this project.
- The next equation of state of interest are the Van der Waals equation of state. This provides precise results and has a low variance for both normal and warm ambient temperatures. This is as expected as this equation of state are know be accurate for temperature above 250 Kelvin.
- For normal and warm ambient temperatures the four most complex equations of state proves to be more inaccurate then the less complex Van der Waals equation of state. Only for cold ambient temperatures it is reasonable to use the more complex equations of state. But still the difference between this four equations of state are so small, that it is recommended just to use Beattie-Bridgeman equation of state.

Regarding accumulator #2 no clear conclusions can be drawn. Although a tendency is to be seen in the mean value, namely that a difference in accuracy between normal and cold ambient temperature of approximately 5 percentage point is observed, see Figure H.7. This is also the case for accumulator #1. Assuming that the error in the data leads to a displacement of the result of approximately 5 percentage point the same conclusion as for accumulator #1 can be drawn, namely that for normal ambient temperature the Van der Waals equation of state are sufficiently and for cold ambient temperature Beattie-Bridgeman equation of state are sufficiently.

H.9.2 Temperature

To sum up the validation of the temperature models, the following conclusions can be drawn:

- No certain result are seen when comparing the measured temperature with the calculated. This is primarily because the test rig was not able to measure the correct temperature. Therefore no certain conclusions can be drawn regarding the accuracy of the six models.
- Since the formula used for calculating the temperature are used by other sources and since the calculations are based on the models for calculating the pressure, which have shown very accurate results, it is assume that the temperature models are showing equally accurate results.

As the same problems with accumulator #2 as presented in Chapter 13 are present no conclusions will be drawn based on this data.

Graphs

I

I.1 Validating test rig

On the attached CD all graphs can be found in .eps and .fig format.

I.2 Measuring the thermal time constant

On the attached CD all graphs can be found in .eps and .fig format.

I.3 Measured gas pressure and temperature

On the attached CD all graphs can be found in .eps and .fig format.

I.4 Comparing measured and calculated gas pressure

On the attached CD all graphs can be found in .eps and .fig format.

I.5 Procentage-wise difference between measured and calculated pressure

On the attached CD all graphs can be found in .eps and .fig format.

I.6 Comparing measured and calculated gas temperature

On the attached CD all graphs can be found in .eps and .fig format.

I.7 Procentage-wise difference between measured and calculated temperature

On the attached CD all graphs can be found in .eps and .fig format.

J

Program code for reference signal generation

This appendix will present the VisSim program made for generating the reference signal. The program can also be found on the appendix CD.

The program is made by adding blocks in the right order. Programs has been made for both accumulator #1 and accumulator #2. The input to the program is a signal generated by other blocks. The signal could be saw tooth, sinus, linear etc and should be given in mm.

J.1 Accumulator #1

The program first takes into account an offset of 95 mm between the position transducer and the accumulator. Then the signal is converted from mm to volt by multiplying with 1/26.458. Lastly the program takes into account the offset and amplification in the reference signal system as describing in Section A.2.1. The program can be seen in Figure J.1.

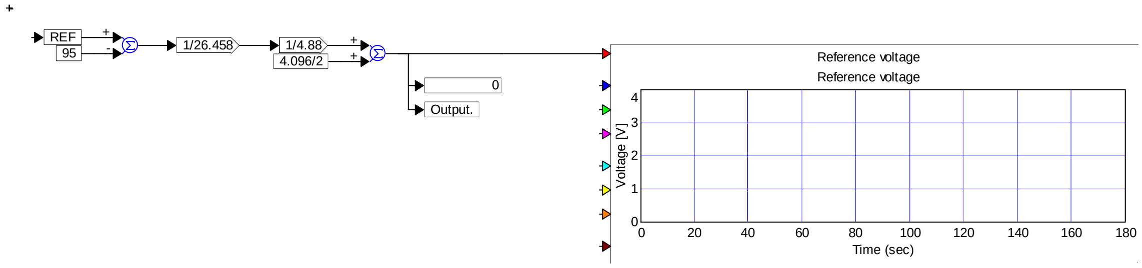

Figure J.1: *Screen dump of the VisSim program used for generation the reference signal for accumulator #1.*

J.2 Accumulator #1

The signal is converted from Pa to volt by multiplying with 10,000/244 and then added an offset. The program can be seen in Figure J.2.

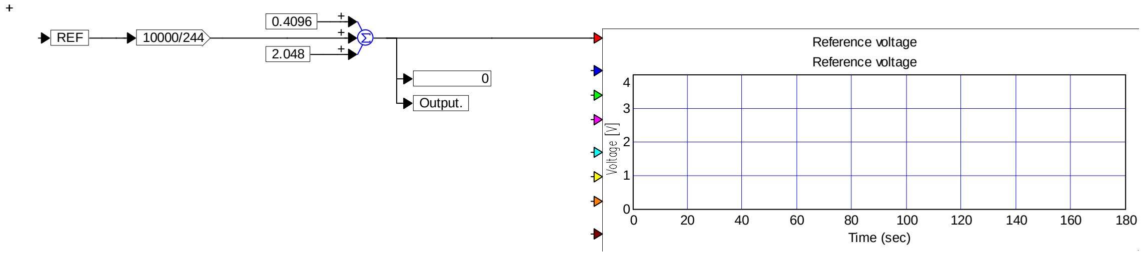

Figure J.2: *Screen dump of the VisSim program used for generation the reference signal for accumulator #2.*

Program code for data acquisition

K

This appendix will present the MATLAB program made for acquire data from the test rig. The program can also be found on the appendix CD.

A program has been developed to acquire the data measured at the test rig as described in Chapter A. The program has been made i MATLAB and used a add on toolbox called Data Acquisition Toolbox. The program is divided into four parts all explained in the following.

K.1 Setting up the program

In the first part of the program the setup is done. A number of parameters can be adjusted here. Firstly the I/O module is called and set to collect in the first six channels. Secondly the sample rate, `fs`, is set for 1,000 Hz followed by the length of the sample period, `duration`. The sampling can be triggered at a chosen value. In this case `trigger` is set for 0 mm. More about trigger will be explained in part three of the program. Finally a cutoff frequency, `Cutoff`, used for the filtering of the data is set. More about this in part four of the program.

```
ai        = analoginput('mcc');
ch        = addchannel(ai,0:5);
fs        = 1000;                                      %[Hz]
duration  = 30;                                        %[sec]
trigger   = 0;                                         %[mm]
Cutoff    = 15;                                        %[Hz]
```

After this the program will checks whether the variable 'number' exists. If it does, it adds 1 to the variable. If not it creates an variable and gives it the value 1. This ensures a continuous numbering of the data as explained below.

```
if exist('number')
    number = number+1;
else
    number = 1;
end
```

The third section of the first part is used for naming all acquired data. Every test run will create a variable called 'filetypeXXX', where XXX is a continuous number (The above makes sure that the number increases with 1 for each test run). All variables will be saved in a .mat-file named 'filetypedate.mat'. When the data is filtered a variable named 'filetypeXXXF' will be created and saved to a .mat-file name 'filetypedateF.mat'.

```
filetype    = 'TEST';
date        = 221209;
varname     = [filetype,num2str(number)];
filename    = [filetype,num2str(date),'.mat'];
varnameF    = [filetype,num2str(number),'F'];
filenameF   = [filetype,num2str(date),'F.mat'];
```

Finally some setup regarding the actual data acquisition is done. Firstly the I/O module is set to sample with the frequency `fs`. Since the module is not capable of sampling at all frequencies, it will select the nearest one possible and return it as `actualfs`. The actual sample rate is used for setting the

`SamplesPerTrigger`, which is the actual number of samples per run. The Data Acquisition Toolbox gives the option of starting the data acquisition by a trigger. To do so, it is necessary to set up what channel the trigger function should monitor. In this case `TriggerChannel` is channel 6, which is the reference signal. The `TriggerType` is set to software, meaning that the rules for the trigger function is set in the software. Other types could be Immediate, which execute the trigger function immediately after the starting the program. The `TriggerCondition` is set to Leaving, meaning that the program will trigger when the reference signal will leave the range specified in `TriggerConditionValue`. Other trigger conditions could be Falling, Rising and Entering. As described in the previous section, the trigger is set at 0 mm. The trigger condition value is then set to a range from 0 mm to 0 mm, meaning that the program will trigger when the reference signal has reached a value of 0 and changed to something else. It should be mentioned that `trigger` will be changed during the different test runs. This will be mentioned in the reports. The trigger value is converted from mm to a signal voltage. This will be explained in the next section. Finally the `TriggerDelay` is set for -1, meaning that as soon as the program has been triggered it will start collecting data from 1 second prior the trigger time and until it is stopped.

```
set(ai,’SampleRate’,fs);
actualfs=get(ai,’SampleRate’);
set(ai,’SamplesPerTrigger’,duration*actualfs);
set(ai,’TriggerChannel’,ch(6));
set(ai,’TriggerType’,’Software’);
set(ai,’TriggerCondition’,’Leaving’);
set(ai,’TriggerConditionValue’,[(trigger/-26.458)+3.5403;(trigger/-26.458)+3.5403]);
set(ai,’TriggerDelay’,-1);
```

K.2 Acquiring data

When all parameters has been setup, the program can be started by `start(ai)`. It will then have to wait for the data to be collected before moving further in the program. In this case, it has been set to wait the length of the sampling period plus five seconds. These five seconds has been added so the program has some initial time before triggering.

```
start(ai);
wait(ai,duration+5);
```

K.3 Save acquired data

Once the `wait` command has terminated, the program will move on to extract and save the data. The data is extracted with the `getdata` command and save in an array named ’data’.

```
data      =  getdata(ai);
```

The program then does two things. It makes a time array named ’time’ of the same length and spacing as the acquired data followed by extracting the individual data from ’data’ and creates six arrays where the data is save individually.

```
time      =  [0:1/actualfs:duration-1/actualfs];
```

Before it is saved, it is converted from signal voltage to mm, Pa or Kelvin. For the position x and the reference Ref, the signal is subtracted by 3.5387 to move the origin from the middle of the position transducer to the end of the accumulator. This value has been reached as it is measured, that when the position transducer is at its middle the piston is at a position $x = 93.5mm$. It is also measured, that $1V$ in the signal equals $26.422mm$. Dividing the two numbers would yield $3.5387V$. After subtracting, the signal is multiplied with $-26.422mm/V$ to convert the signal voltage to mm.

```
x         =   (data(:,1)-3.5387)*-26.422;
Ref       =   (data(:,6)-3.5387)*-26.422;
```

Regarding the pressure transducers it is known from the data sheet, that they have a range of $0 - 400bar$ and outputs $4 - 20mA$ which converted becomes $2 - 10V$. Therefore the signal is firstly subtracted by $2V$ to take into account that the signal starts at $2V$ then multiplied with $50bar/V$ and finally added an offset to get the signal in Bar. Lastly it is multiplied with $1 \cdot 10^5$ to get it in Pa.

```
p_gas     =  ((data(:,2)-2)*50+2.1978)*1e5;
p_oil     =  ((data(:,3)-2)*50+0.7326)*1e5;
```

When studying the data sheet for the temperature transmitter it is seen that the output is $4 - 20mA$ which converted becomes $2 - 10V$. The temperature range it set to $-50°$ to $100°C$. So firstly the signal is subtracted $2V$ and then multiplied with $19,75°C/V$ and then subtracted $50°C$ to take into account that the range starts at $-50°C$.

```
T         =  ((data(:,4)-2)*18.75)-50;
```

The last channel is measuring the signal voltage to the valve and is not converted to another unit.

```
U         =    data(:,5);
```

All the above offset values will continuously been monitored and adjusted if necessary. The time array and the six individual data sets are now saved in a new array named as described in Section K.1. Finally the program checks whether there is an .mat-file to store the array in. If there is, the array is added to the .mat-file. If not the .mat-file is created and the array is stored in the .mat-file.

```
eval([sprintf(varname) '=[time,x,p_gas,p_oil,T,U,Ref]']);

if exist(filename);
    save(filename,varname,'-append');
else
    save(filename,varname);
end
```

K.4 Filtering the data

The last section of the program is used for filtering the acquired data. Even though a lot of the noise has been removed from the data as described in Section A.2, some noise is still present as seen in Figure K.1. To filter the data a SIMULINK program has been developed as described in Appendix L. The data is run through this program. To do so, the array 'data' is overwritten with the converted data described in last section. To run the data through the filtering program, some setup for the program is made with the command `simset`. Firstly the step size is set as Fixed with a step size of $\frac{1}{actualfs}$. The solver chosen is ode4. The filtering program is then run with the command `sim`.

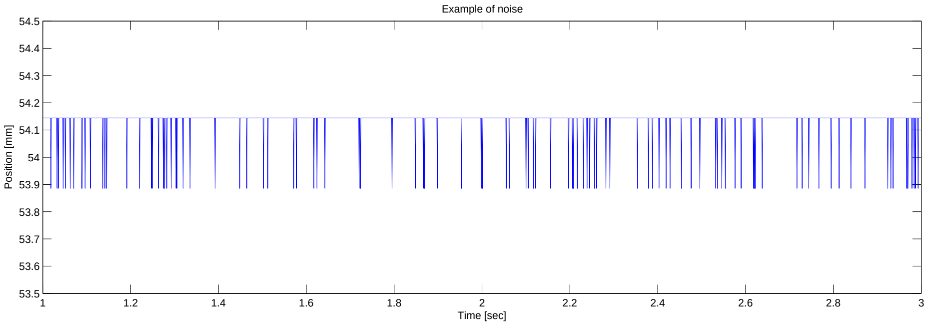

Figure K.1: *Example of noise in the signals*

```
data = [time,x,p_gas,p_oil,T,U,Ref];
options = simset(’FixedStep’,1/actualfs,’Solver’,’ode4’);
sim(’filtering.mdl’,data(end,1:1),options);
```

The filtering program outputs a new array named ’dataF’. The array is stored together with the time array in a new array named as described in in Section K.1. Finally the program checks whether there is an .mat-file to store the array in. If there is, the array is added to the .mat-file. If not the .mat-file is created and the array is stored in the .mat-file.

```
eval([sprintf(varnameF) ’=[time,dataF]’]);

if exist(filenameF);
    save(filenameF,varnameF,’-append’);
else
    save(filenameF,varnameF);
end
```

Program code for data filtering

L

This appendix will present the program developed to filter the acquired data. The data is filtered as there are some noise in it when stored on the data acquisition computer. The program is also to be found in the appendix CD.

Even though a lot of the noise has been removed from the data as described in Section A.2, some noise is still present in the acquired data as seen in Figure L.1.

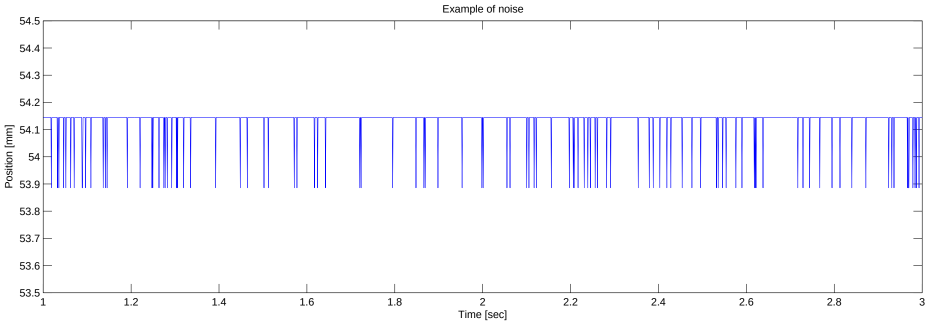

Figure L.1: *Example of noise in the signals*

The noise can be characterized as bit noise and can not be removed with capacitors. Therefore a program with filters has been developed. Good results have been observed when the signal has been feed through a number of first order transfer functions. In this case observations have shown that three transfer functions give good results[Rasmussen, 2009]. In Figure L.2 the program is shown as made in SIMULINK.

The program consists of three transfer functions for each signal that should be filtered. When the data is filtered it is collected in an array named 'dataF' and saved in the workspace. In Figure L.3 the transfer function is shown. It consists of a closed loop system with a gain and an integrator. The gain is the cut off frequency a described in Appendix K.1. The integrator is a standard integrator with settings as listed in Table L.1.

	Integrator 1
Initial condition	Mean value of the first five data points
Upper saturation limit	∞
Lower saturation limit	$-\infty$

Table L.1: *Initial conditions and saturation limits for the integrator.*

To investigate if the noise has a significant frequency that could be used as the cutoff frequency an FFT-analysis is performed.

The result is shown in Figure L.4. As it can be seen, the noise does not have a significant frequency. The cutoff frequency will therefore have to be decided by trial and error. When doing so, it is important to have in mind the consequences of adjusting a cutoff frequency, namely:[Ogata, 2001, Page 573]

- The lower the cutoff frequency the more noise is being removed from the signal. This implies that the lower the frequency the better.

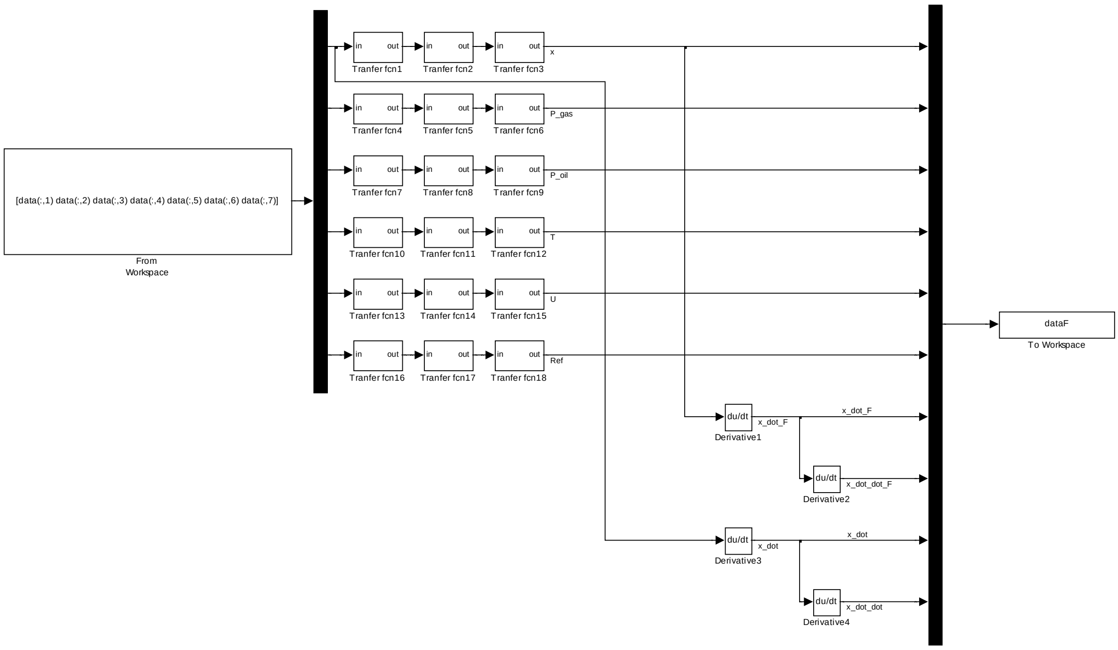

Figure L.2: *SIMULINK program to filter data*

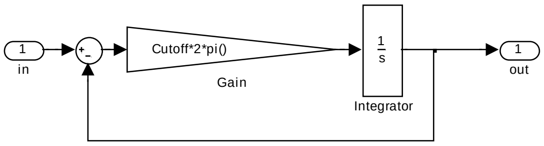

Figure L.3: *Transfer function in the filtering program.*

- The higher a cutoff frequency the faster response of the system. A high cutoff frequency is the same as a high bandwidth and it is general known that the bandwidth is proportional to the speed of the response. The speed of the response indicates how well the system will track an input sinusoid. This implies that the higher the frequency the better.

It is therefore necessary to make compromises. Test have shown that a cutoff frequency of $\omega_b = 15[Hz]$ is suitable. This removes the majority of the noise with a phase angle of approximately 0.033 seconds. In Figure L.5 a sinusoidal position signal is shown before and after filtering and in Figure L.6 the effect of filtering is shown on the velocity signal.

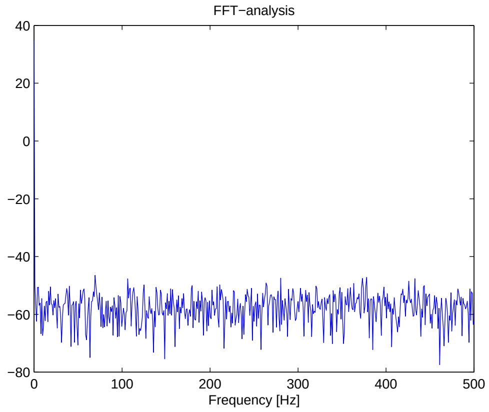

Figure L.4: *FFT-analyses using MATLAB Signal Processing Toolbox*

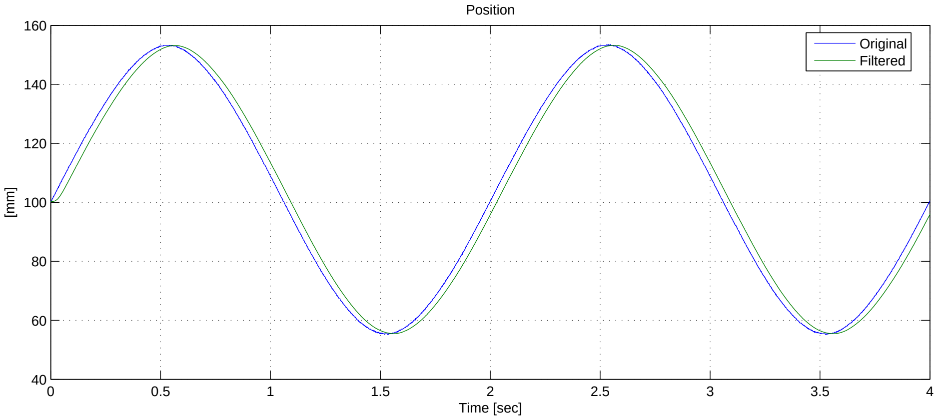

Figure L.5: *Sinusoidal position signal before and after filtering*

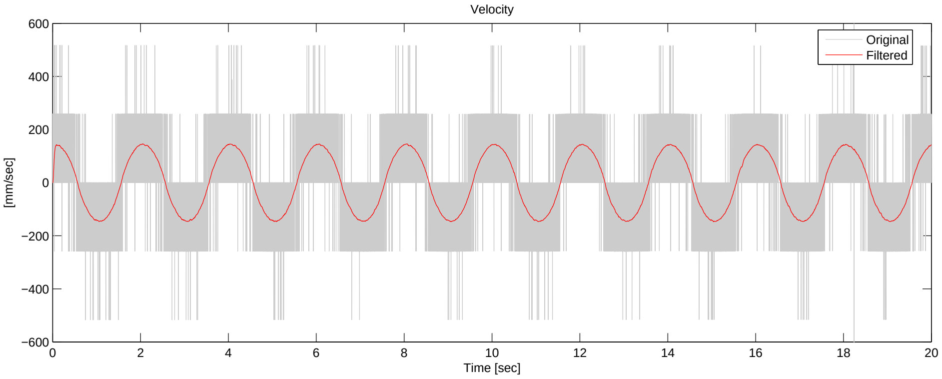

Figure L.6: *Velocity signal before and after filtering*

Program code for calculating the thermal time constant

M

This appendix will present the MATLAB program made for measuring the thermal time constant, τ. The program can also be found on the appendix CD.

The first part of the program calls the data that should be used for calculation h and saves it in an array names 'data'. From this array the program makes three arrays with the time, $time$, the position, x and the gas pressure, p_{gas}. Lastly it calculates the frequency of the data in question.

```
data        = DATA;

time        = data(:,1);
x           = data(:,2);
p_gas       = data(:,3);

fsactual    = time(2,:)-time(1,:);
```

Then the program finds the maximum pressure from which it calculate the pressure when it drops by 63,2% named `p_gas_632`.

```
[p_gas_max i_p_gas] = max(p_gas);
p_gas_632           = max(p_gas)-((max(p_gas)-p_gas(end,:))*0.632);
```

The program then starts a loop to find the time step at which the pressure is equal or smaller to the pressure `p_gas_632`. The program then returns the time step as the actual time. This is the thermal time constant, τ.

```
n = 0;
for i=time(i_p_gas):time(end);
    while p_gas(i_p_gas+n) >= p_gas_632
        n = n+1;
    end
end

tau = n*fsactual
```

Data sheets

N

N.1 Analog and digital I/O module

Please see attached CD for this data sheet.

N.2 Valve

Please see attached CD for this data sheet.

N.3 Accumulator #1

Please see attached CD for this data sheet.

N.4 Accumulator #2

Please see attached CD for this data sheet.

N.5 Position transducer

Please see attached CD for this data sheet.

N.6 Pressure transducer

Please see attached CD for this data sheet.

N.7 Temperature transmitter

Please see attached CD for this data sheet.